CHAPTER ONE

INTRODUCTION

1.1 Background to the Study

Geothermal energy originates from the formation of the earth and from decay of long lived isotopes of uranium, thorium and potassium found within the Precambrian basement rocks (Downing and Gray, 1986). The uprising of magma to the surface during the rifting often results in different geodynamic activities such as the surface expressions of tectonic lineaments and manifestation of geothermal resources (Komolafe, 2010). These lineaments such as faults and fractures play major roles in the study of the evolution and dynamism of the rift zones. Investigations into the tectonic lineaments and surface thermal structures are very crucial to the understanding of the geothermal activities and processes associated with the region. Continuous accumulation of tectonic strain helps to maintain faults and fractures as conduits for fluids flow thereby sustaining the geothermal systems (Komolafe, 2010).

In geothermal energy exploration, the potential fields of gravity and magnetic have been used to delineate bedrock valleys concealed by sediments or volcanic materials and mapping of permeable fractures during the early stages of investigation of Olkaria and Meningai fields, Kenya (Mariita, 2013). These measurement can significantly reduce the number of wells needed to characterize a prospect while improving the confidence of interpretations. In the same vein, Mariita (2013) noted that delineation of geothermal heat source is best carried out using gravity and magnetic measurements, while reservoir characteristics are best imaged by use of electric or electromagnetic techniques.

In Nigeria, the much dependence on oil and gas as the main source of energy has virtually collapsed her economy. It therefore becomes pertinent to find an alternative source of energy. So, the exploitation of possible geothermal resource areas in Nigeria could be a vital alternative to an industrializing nation like Nigeria (Obande *et al.*, 2013). The Wikki warm spring of Bauchi State and the Ikogosi warm spring of Ekiti State, the two main known geothermal resource areas in Nigeria are associated with circulation of water to great depths through faults in the Basement Complex rocks of the area (Obande *et al.,* 2013). The Ikogosi warm spring occurs some kilometers away from the northwestern flank of the study area.

As oil reserves decline, geothermal energy is becoming an attractive alternative, particularly in parts of western United States of America, such as the Salton Sea area of south California, where geothermal exploration and development have begun (Griscom and Muffler, 1971). The geothermal fields of Olkaria and Menengai in Kenya have equally witnessed intensive exploration and exploitation of geothermal energy in recent times (Mariita, 2013)

Geothermal energy comes from steam and hot water trapped within the crust (Downing and Gray, 1986). It is relatively non- polluting form of energy that is used as a source of heat and to generate electricity. Much of Earth's geologic activity such as earthquakes, volcanism, moving plates and the origin of mountains is caused by internal heat. In fact, the slow release of the heat from the Earth's interior is one major factor that makes it such a dynamic Earth (Rybach and Muffler, 1981).

One of the vital tools for investigating the thermal structure of the crust via aeromagnetic data is spectral analysis. Thermal structure of the crust determines the modes of deformation, depths of brittle and ductile deformation zones, regional heat flow variations, seismicity, subsidence/uplift patterns and maturity of organic matter in sedimentary basins (Dolmaz *et al.,* 2005). Adequate knowledge of the thermal structures of lithosphere is required for a wide variety of geodynamic investigations, including rock deformation, mineral phase boundaries and rates of chemical reactions, electrical conductivity, magnetic susceptibility, seismic velocity and mass density (Chapman and Furlong, 1992). Lithospheric thermal gradients are often estimated from near-surface heat flow measurements but high quality heat flow measurements are not available globally and are rarely distributed uniformly and are sometimes contaminated by local thermal anomalies. In places where heat flow information is inadequate, the depth to the Curie temperature may provide a proxy for temperature- at -depth.

In the last few decades, spectral analysis based on statistical models has been used in various geological applications like the estimation of average depth to the top of magnetic basement and the estimation of crustal thickness. The spectral method, pioneered by Spector and Grant (1970) has been used extensively in the interpretation of magnetic anomalies. It is based on the expression of the power spectrum for the total field magnetic anomaly produced by a uniformly magnetized rectangular prism (Bhattacharyya and Leu, 1975). Spector and Grant, (1970) assumed that a number of independent ensembles of rectangular prismatic blocks are responsible for generating anomalies in a magnetic map. Likewise, Spector and Grant (1970) defined Curie point depth (CPD) as the deepest level in the earth crust containing materials which create discernible signatures in a magnetic anomaly map. This definition can be restated as the depth at which the dominant mineral in the crust passes from a ferromagnetic state to a paramagnetic state under the effect of increasing temperature (Nagata, 1961). Similarly, the Curie point depth (CPD) can be defined as the depth at which the iron and titanium oxide minerals of the earth lose their ferromagnetic property (Nur *et al.*, 1999). For this purpose, the basal depth of a magnetic source from aeromagnetic data is considered to be the Curie point depth.

This study focuses on the interpretation of aeromagnetic data in parts of southwestern Nigeria in order to delineate geothermal energy and its associated attributes using spectral analysis. The result of this study will be a useful tool in determining the sedimentary thickness variations, depths to the Curie-temperature isotherm, heat flow values and regional thermal structure over parts of Southwestern Nigeria.

1.2 Statement of the Problem

In Nigeria, extensive geophysical investigations have been largely confined to sedimentary formations with proven natural resource potentials (Eletta and Udensi, 2012). The Niger Delta area of southern Nigeria has witnessed extensive gravity, magnetic and seismic surveys for oil and gas prospecting by oil companies operating in Nigeria. The other basins like the Chad Basin and the Anambra Basin have also attracted some attention in recent times because of the suspected propensity of the area for oil and gas deposits.

Nevertheless, geothermal investigations have not received enough attention across the Nigerian landscape as very few works have been documented. This was noted in the concluding statement of Nwankwo *et al.,* (2011) where they acknowledged the fact that there is a gap in crustal temperature information of the central Nigeria. Needless to say though, that there is no functional geothermal energy exploitation attempt in Nigeria and there is no record of any attempt at investigating, constructively, any previous area worthy of exploitation. There is therefore the need to find an alternative source of energy.

This study is therefore aimed at interpretation of aeromagnetic data over parts of southwestern Nigeria using spectral analysis. This research work will serve as a contribution to filling the gap in the crustal temperature information in the study area and also to deduce potential geothermal prospects zones for geothermal energy exploitation.

1.3 Location of the Study Area

The study area is bounded by longitudes $5^0 00^1 – 6^0 30^1$E and latitudes $6^0 00^1 – 7^0 30^1$N located at the Pre-Cambrian Basement of southwestern Nigeria to the north and sedimentary part of the Niger Delta to the southern part of the study area (Fig. 1.1). The area is covered by the aeromagnetic map sheet 264 (Akure), sheet 265 (Owo), sheet 266 (Auchi), sheet 283 (Siluko), sheet 284 (Ifon), sheet 285 (Ubiaja), sheet 297 (Okomu), sheet 298 (Benin City) and sheet 299 (Agbor) spanning an area of approximately 27, 225km^2. The study area is characterized by two distinct climatic conditions- the rainy season and the dry season. The rainy season lasts usually from April to October, while the dry season lasts usually from November to March, depending on the rainfall pattern for the particular year. The study area is within the Tropical Equatorial climate dominated by abundant rainfall and has a mean annual rainfall of about 2112 mm (Akujieze and Oteze, 2007). In terms of the occurrence of rain hours, the study area has a low probability values (less than 4%) for all times of the day between the late November and mid February and this interval can be classified as dry months in the study area. There is no probability maximum from June to September which indicates that occurrence is most probable (by over 28%) in the late afternoons during those months. The predominance of inland thunderstorms at the agency of rainfall is quite obvious. The mean annual temperature of the area is about 23^0C with the mean annual range not exceeding 27^0C. The relative humidity is about 80% (Balogun, 2003). The vegetation, which is predominantly of the rainforest type and grades into moist/dry woodland savanna type as one move northwards, is characterized by giant trees and few grasses (Duze and Ojo, 1977). The vegetation is fairly thick implying significant evapo-transpiration effect. The landscape mostly covered mostly with mosaic forest – shrubs and grasses. The soil cover in the area according to Duze and Ojo (1977) is mainly ferralitic red- yellow soils of humid tropical equatorial region.

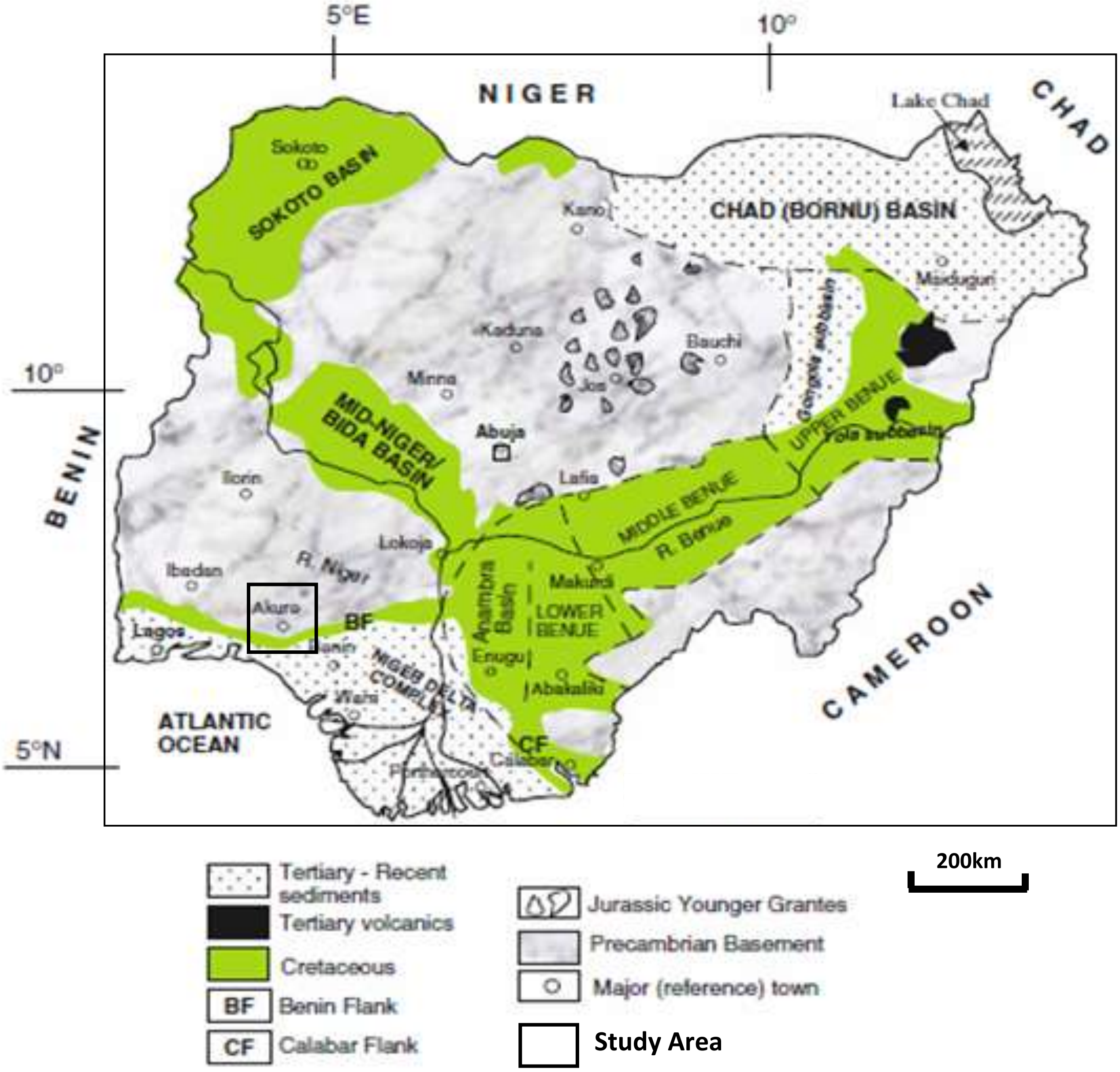

Fig. 1.1: Geological map of Nigeria showing the study area (After Obaje, *et al.*, 2004).

1.4 Aim and Objectives of the Study

The aim of this study is to carry out an interpretation of aeromagnetic data for delineation of geothermal energy and its attributes in parts of southwestern Nigeria. The specific objectives of this study include:

1. To produce the total magnetic intensity (TMI) and residual anomaly maps
2. To determine the sedimentary thickness variations in the area.
3. To determine the depths to the Curie temperature isotherm in the area
4. To determine the geothermal gradients and heat flow values in the area
5. To model the magnetic anomalies and the Curie isotherm in the area
6. To deduce the origin/source of warm (thermal) spring in the area
7. To delineate the structural pattern in the area.
8. To delineate area with geothermal energy potential.

1.5 Scope of the study

The study is limited to the use of spectral analysis method to interpret aeromagnetic data over parts of southwestern Nigeria in order to delineate geothermal energy (heat source) and its attributes.

1.6 Significance of the Study

This study will be a significant endeavour in the sense that it will bring to the fore several capabilities of the magnetic method that have not been adequately utilized.

1. This work will be beneficial to Nigerians as the exploitation of possible geothermal resource areas in Nigeria could be a vital alternative to an industrializing nation like Nigeria.
2. Moreover, the knowledge of Curie point depth offers a window for a better view of the thermal structure of the crust via the interpretation of aeromagnetic data.
3. The knowledge of the depth to the basement provides the thickness of the Sedimentary fill, which in turn is a key indicator in determining whether the deeper parts of the study area have been buried to sufficient depth to reach maturation window.
4. Importantly, an understanding of the variations in the bottom of the magnetically active layer of the lithosphere is an essential parameter during the structural interpretation for particular regions.

CHAPTER TWO

LITERATURE REVIEW

2.1 Spectral Analysis

2.1.1 Fundamental of Spectral Analysis

Several literatures have been written on the application of spectral analysis to the interpretation of aeromagnetic anomalies. Essentially spectral analysis pioneered by Spector and Grant (1970) has proved to be a powerful and convenient tool in the processing and interpretation of potential field geophysical data (Eletta and Udensi, 2012). The application of Spectral analysis to the interpretation of aeromagnetic anomalies has been discussed extensively by many authors like Bhattacharyya (1966); Spector and Grant (1970); Mishra and Naidu (1974); Hahn, *et al.,* (1976); Ofoegbu and Onuoha (1989); Onwuemesi (1997); Salem *et al.,* (2000); Nwankwo *et al.,* (2008); Anakwuba *et al.,* (2011); Chinwuko *et al.,* (2012); Obande *et al.,* (2013); Abraham *et al.,* (2014). These authors have successfully used the spectral method extensively to determine the sedimentary thickness variations, depths to the Curie-temperature isotherm and heat temperature measurements in different geologic settings around the world.

Various studies have shown correlations between Curie-temperature depths and average crustal temperature, leading to viable conclusions in a number of regions around the world (Anakwuba and Chinwuko, 2015). Smith, *et al.,* (1974), estimated an average Curie depth of 10 ± 3km at Yellow Stone National Park.

While Byerly and Stolt (1977) also estimated an average Curie depth of 20km for northern and central Arizona. Anakumba and Chinwuko (2015) estimated an average Curie isotherm depth that varies between 21.45km at Mafa-Bama area and 31.52km at Maiduguri-Gwoza area of eastern Chad Basin of Nigeria. Ofoegbu (1985) has subjected the aeromagnetic anomalies over the Benue trough and adjacent regions to a power spectral analysis in an effort to eliminate the anomaly component due to shallow sources. The resultant long wavelength anomalies were inverted in terms of a magnetized crustal layer whose bottom surfaces were made to coincide with the Curie isotherm in the area. The Curie isotherm underneath part of the trough analyzed was found to vary between 18 and 27km. Onwuemesi (1997), also estimated the Curie depth of the Anambra Basin and found out that it vary between 16 and 30km. Moreover, analysis have been published of Quseir area, northern Red Sea, Egypt (Salem *et al.*, 2000), Nupe Basin of Nigeria (Nwankwo *et al.,* 2009), Eastern sector of central Nigeria/Benue trough (Eletta and Udensi, 2012).

In the same vein, Curie isotherm (base of magnetized crust) of the Anambra Basin has been published by some authors. Onuoha and Ekine (1999), estimated the Curie isotherm of the basin to vary between 25±1 and 41±6^{0}C/km. These values compare favourably with analysis by Onwuemesi (1977) who estimated the Curie isotherm of the Anambra Basin to vary between 20 and 35^{0}C/km with an average of 29±5^{0}C/km.

Sheu *et al.,* (2004) carried out a spectral analysis of the magnetic residual anaomalies over the Upper Sokoto Basin, revealing an average maximum depth of 1.386km to the basement in the area. In the same vein, Adetona *et al.,* (2007) determined the depth to buried magnetic rocks under the lower Sokoto Basin using aeromagnetic data. The result revealed a variation of depth between 0.46km and 1.93km. Hence, the result revealed that the basin is generally shallow, with an average of 1.44km of thickness for sediments in the lower Sokoto Basin and this depth is considered very low for petroleum accumulation.

Kasidi and Nur (2012) estimated Curie depth isotherm deduced from spectral analysis of magnetic data over Sarti and environs of Northeastern Nigeria. They determined Curie depth which varies between 26 to 28km and the geothermal gradient varies between 21 and 23^0C/km, while the heat flow values range from 53 to 58mW/m^2. They also noted an inverse correlation between estimated Curie depth and heat-flow measurements. Abraham *et al.*, (2014) did a spectral analysis of aeromagnetic data for geothermal energy investigation of Ikogosi warm spring of Ekiti State, southwestern Nigeria. The result of his study revealed that the area is underlain by an average Curie depth of 15.1 ± 0.6 km and a heat flow of 91.2 ± 2.1 mW/m^2.

This research work focuses on the interpretation of aeromagnetic data for delineation of geothermal energy and its attributes in parts of southwestern Nigeria. The outcome of the analysis will help in estimating the sedimentary thickness variations, map the configurations of the Curie temperature isotherm, and the associated geothermal gradients and heat flow values in the study area.

2.1.2 Mathematical Background of Spectral Analysis

The mathematical method used in this study is the Discrete Fourier Transform Method (Fourier Series Expansion). The Discrete Fourier Transform is applied to regularly spaced data such as the aeromagnetic data. So, according to Onwuemesi (1997), for a residual magnetic anomaly profile of length L and digitized at equal intervals, the residual total intensity anomaly values can be expressed in a single Fourier Series expansion as:

$$Y_{i(x)} = \sum_{i=1}^{N}[\propto_n \, Cos\left(\frac{2\pi nxi}{L}\right) + \beta_n Sin(\frac{2\pi nxi}{L})] \qquad 2.1$$

Where:

$Y_{i(x)}$ = Reading at x_i position

L = Length of the cross section of the anomaly

n = Harmonic number of the partial wave; n = 1, 2 . . . Nyquist frequency $(\frac{N}{2})$

N = Number of digitized points on the profile Fourier amplitude

α_n = Real part of the amplitude spectrum

β_n = Imaginary part of the amplitude spectrum

Fourier amplitude

i = 0, 1, 2, 3, 4 . . . N;   x = 1, 2, 3 L

But,

$$\propto_n = \frac{2}{N}\sum_{i=1}^{N} Y_i Cos\frac{2\pi nxi}{L} \qquad 2.2$$

$$\beta_n = \frac{2}{N}\sum_{i=1}^{N} Y_i Sin\frac{2\pi nxi}{L} \qquad 2.3$$

Hence, the main amplitude spectrum (A_n) according to Davis, (1973) is given by the relation;

$$A_n = \sqrt{\propto_n^2 + \beta_n^2} \qquad 2.4$$

So, after calculating the values of A_n, a graph of natural logarithm of the amplitude (A_n) against frequency (n) is plotted. Linear segment from the low frequency portion of the spectrum, representing contributions from the deep – seated causative bodies was drawn from the graph. The gradient of the linear segment was evaluated and the depth to the basement was calculated using the equation according to Negi *et al.*, (1983), which is given as:

$$Z = - ML/2\pi \qquad 2.5$$

Where

Z = depth to the basement

M = gradient of the linear segment

L = width of the anomaly

According to Bhattacharyya and Leu (1975), the discrete Fourier transform has the ability to filter all the noise from the data. Generally, the Fourier transform methods are particularly useful in magnetic prospecting for the following purposes:

i. Resolution of specific anomalies by upward or downward continuation.
ii. Changing the effective field inclination (reduction to the pole) or conversion of total field data to vertical component data
iii. Calculation of derivatives

iv. General filtering, that is, separating anomalies caused by sources of differences in size and depth

v. Modeling of the anomalies.

It should be noted that the most important characteristics of transformations is that, information is not lost in the process and in many cases, operations are easier to perform in the transform domain (Telford *et al.*, 1990). Actually, most aeromagnetic datasets are dominated by the lower frequency Fourier components (that is magnetic intensity is smooth at airborne attitude). If they were not an aeromagnetic image, they could be composed of very rapid oscillations in the magnetic intensity that would make interpretations extremely difficult.

More so, it is possible to represent the data accurately by an analytical function using Fourier series (Onwuemesi, 1997). Most methods used involve Fourier Transformation of digitized aeromagnetic data to compute the power or amplitude spectrum. A plot of the logarithm of the amplitude versus frequency usually shows straight - line segments which decrease in slope with frequency and the slopes of the segments give estimates of the depth to the magnetic sources (Spector and Grant, 1970).

2.1.3 Curie Point Depth Determination from Aeromagnetic Data Analysis

Curie-point is defined as the temperature (above 580^0C) at which magnetic mineral loses its magnetic properties or susceptibility as a result of the high temperature (Stampolidis and Tsokas, 2002). This point is assumed to be the depth for the geothermal source (magnetic chamber) where most geothermal reservoirs tapped their heat from in a geothermal environment. Curie-point temperature depths provide general information on both regional and local temperature distribution as well as geothermal gradients. According to Dolmaz *et al.*, (2005), determination of Curie-point depth is one of the methods of examining the thermal structure of the crust using aeromagnetic data.

Curie depth determination concerns the delineation of Curie temperature isotherm for crustal rocks (Onwuemesi, 1997). At the Curie temperature, a substance loses its ferromagnetic magnetization, consequently, it may be possible to locate a point at the bottom of the polarized rock by spectra inversion of the magnetic data. If enough points/depths are determined an isothermal surface at the Curie temperature of the area can be defined.

The idea of using spectral analysis of geomagnetic data to estimate the thickness of the magnetized part of the lithosphere was widely used by geophysicists working in various regions around the world to examine the thermal structure of the crust (Dolmaz *et al.,* 2005). One of the most profound methods of Curie point depths (CPD) determinations are based on spectral analysis of geomagnetic data.

Computation of the CPD is one of the difficult problems in potential field inversion (Blakely, 1995). Two fundamental methods serve as a basis of all subsequent analysis. The first method provided by Spector and Grant (1970), is used in estimating the average depths to the top of magnetized bodies from the slope of the log power spectrum and second method by Bhattacharyya and Leu (1975, 1977) is used for obtaining the depth to the centroid of the causative body. Following Bhattacharrya and Leu (1975, 1977) estimation of the bottom depths could be approached in two steps:

i. First find the centroid depth (Z_0)

ii. Second determine the depth to the top (Z_t)

Briefly, CPD (Z_b) is estimated in two steps suggested by Bhattacharyya and Leu (1975) and Okubo *et al.*, (1985). The first is the depth to the centroid (Z_0) of the magnetic source from the slope of the longest wavelength part of the spectrum,

$$l_n \left[\frac{P(s)^{\frac{1}{2}}}{|s|} \right] = l_n\, A - 2\pi/s/Z_0 \qquad 2.6$$

Where P(s) is the radially averaged power of the anomaly, /s/ is the wavelength and A is a constant. The second step is the estimation of the depth to the top boundary (Z_t) of that distribution from the slope of the second longest wavelength spectral segment (Okubo *et al.*, 1985).

$$l_n \left[P(s)^{\frac{1}{2}} \right] = l_n\, B - 2\pi/s/Z_t \qquad 2.7$$

Where B is a sum of constant independent of /s/

Then the basal depth (Z_b) of the magnetic sources is calculated from the equation:

$$Z_b = 2Z_0 - Z_t \qquad 2.8$$

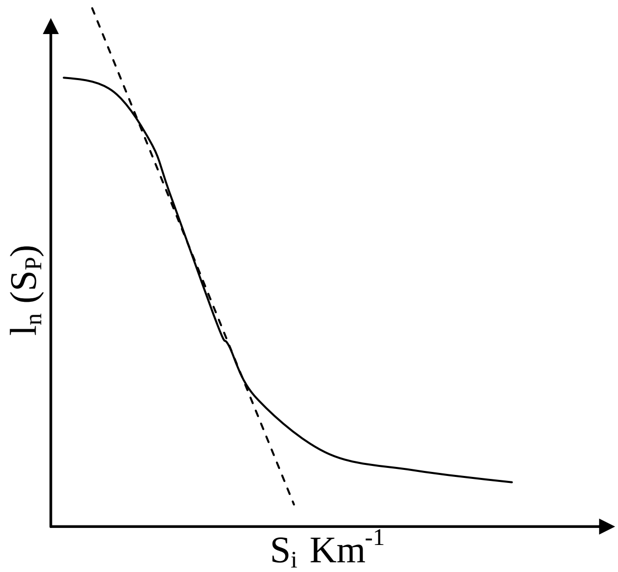

Fig 2.1: Scheme of radially average log power spectrum diagram for Z_0 estimation and calculation of depth to the bottom of the magnetic earth crust Z_b (After Trifonova *et al.*, 2006).

Bottom depth (Z_b) of magnetic sources can only be estimated if centroid (Z_0) can be accurately determined. The obtained basal depth of a magnetic source is assumed to be the CPD. According to Dolmaz *et al*., (2005), the CPD estimate involves three stages as follows:

1. Division into cross section of the anomaly
2. Calculation of the radially averaged log power spectrum for each cross section
3. Estimation of the CPD from the centroid and the top depth estimated from the magnetic source for each cross section.

The centroid depth Z_0 can be obtained from the slope of a straight line by the least square fitting as shown in Fig. 2.1, while Fig. 2.2 (a and b) shows an example of power spectrum estimation of the CPD using the two dimensional magnetic anomaly data for the centroid and top boundary using the gradient of spectra.

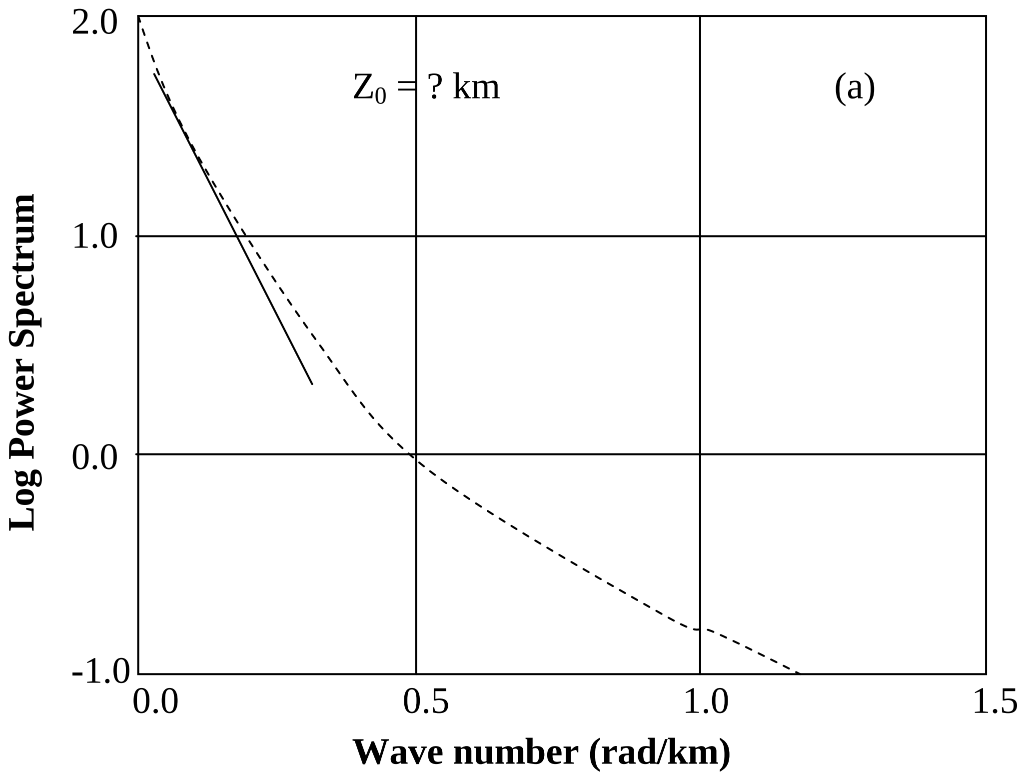

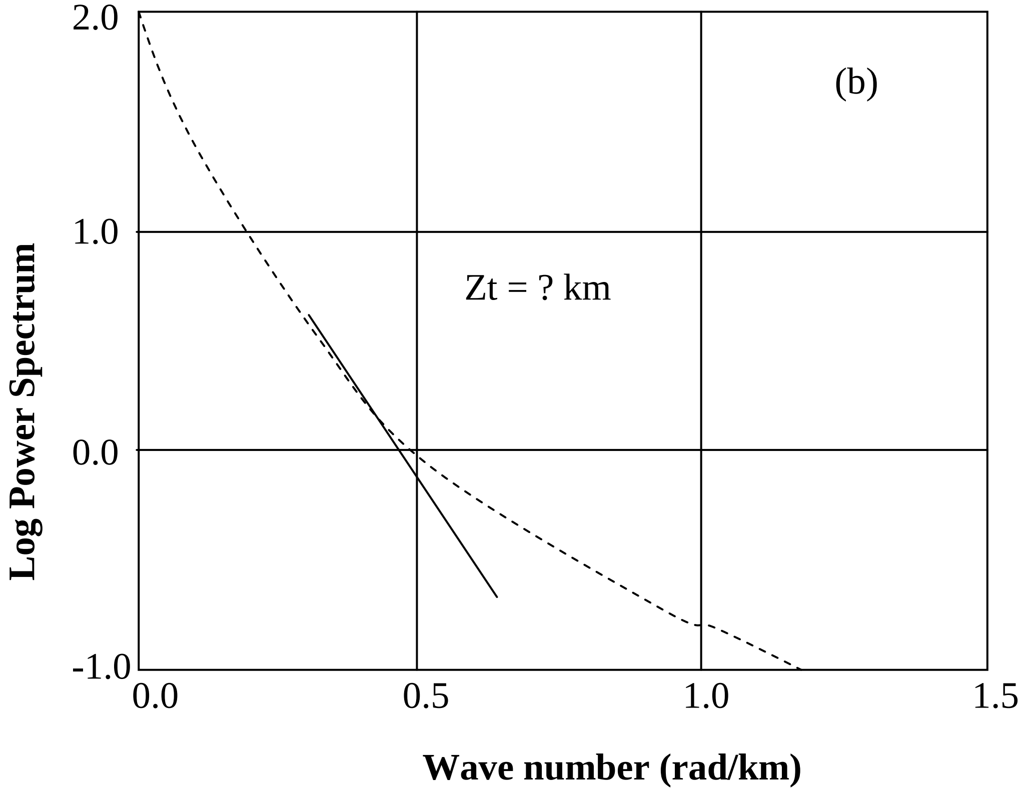

Fig. 2.2: Example of power spectrum for estimation of the CDP using the two – dimensional magnetic anomaly data for the (a) centroid and (b) top boundary using the gradient of spectra (After Dolmaz *et al.*, 2005).

2.2 Geothermal Gradients Estimation from Magnetic Data Analysis

For the purpose of computing the geothermal gradients, it was assumed that the temperature changes within the earth are linear and of the form:

$$T_h = mh + T_0 \qquad 2.9$$

(From Onwuemesi, 1997)

$$\text{Hence, } m = \frac{T_h + T_0}{h} \qquad 2.10$$

Where,

T_h = temperature in ^{0}C at depth h

m = geothermal gradient

h = depth of interest

T_0 = surface temperature

It was further assumed that the surface temperature was 27^{0}C while the Curie temperature was 580^{0}C (Onwuemesi, 1997). From the values of the Curie depths obtained, the geothermal gradients can be estimated from equation (2.9) by solving for the unknown m (geothermal gradient).

2.3 Calculation of heat flux

The basic relation for conductive heat transport is Fourier's law (Nwankwo *et al.*, 2011). In one – dimensional case under assumptions that the direction of temperature variation is vertical and the temperature gradients ($^{dT}/_{dZ}$) is constant.

Fourier law takes the form

$q_z = K\,(\frac{dT}{dz})$ 2.11

Where;

q_z = heat flow

K = coefficient of thermal conductivity

$dT/_{dz}$ = geothermal gradient

A Curie point temperature of 580^0C and temperature conductivity of 2.5 $wm^{-1}\ {}^0C^{-1}$ as average for igneous rocks is used as standard (Stacey, 1977) in the study.

Tanaka *et al.*, (1999) also noted an inverse relationship between estimated Curie depths and heat flow measurements; especially Curie depths calculated from magnetic anomalies generally agreed with Curie depths derived from the one- dimensional heat conductive transport model. The one- dimensional heat conductive transport equation;

$D_c = K\left[\frac{\theta}{q}\right]$ 2.12

Tanaka *et al.*, (1999) showed that a given depth to a thermal isotherm is inversely related to heat flow,

Where

D_c = depth to the isotherm

K = coefficient of thermal conductivity

θ = isotherm temperature

q = heat flux

This equation implies that regions of high heat flow are associated with shallow isotherms, whereas regions of lower heat flow are associated with deeper isotherms.

2.4 Regional Geologic Setting

2.4.1 Basement Complex

About one third of the study area is underlain by the Precambrian Basement Complex while two third of the entire study area is underlain by sedimentary rocks (Fig. 1.1 and 2.3). The study area is a square block situated at the Southwestern Nigeria. The crystalline rocks in the study area are made up of Precambrian Basement Complex and the Phanerozoic rocks. These crystalline basement rocks have been subjected to deformation of different intensities throughout geological period. As a result of the deformation, N – S, NE – SW, NW – SE, NNW – SSW, NNW – SSE and to a less extent, E – W fractures developed (Oluyide and Udoh, 1989). The Precambrian basement rocks consist of the migmatitie-gneiss-quartzite complex dated Archean to Early Proterozoic (2,700 to 2,000 Ma). Other units include the NE-SW trending Schist belts mostly developed in the western half of the country and the granitoid plutons of the Older Granite Suite dated Late Proterozoic to Early Phanerozoic (750 to 450 Ma). The main lithologies of the southwestern Nigerian basement complex include the amphibolites, migmatite gneisses, granite and pegmatites. Others are the schists made up of biotite, quartzite, talc-tromolite and the muscovite. The crystalline rocks intruded into these schistose rocks and the basement complex are in places intruded and interspersed also by the Older Granites which originated during the Pan-African orogeny (Rahaman, 1989). The basement complex rocks in the study area have been subjected to deformation of different intensities throughout the geological period, leading to the development of fractures.

Generally, the rocks are known as the basement complex and they are Precambrian in age. The rocks were formed as a result of metamorphism and igneous activities on a regional scale (Rahaman, 1989). Basement complex rocks are subdivided into migmatite-gneiss complexes, the older metasediments, the younger metasediments, the older granites and the younger granite alkaline ring complexes and the volcanic rocks.

The Ikogosi warm spring, which is about 10km away from the northwestern part of the study area, issues with a temperature of 38^0C near the eastern slope of the north-south trending ridge from a thin quartzite unit within a belt of quartzite which includes quartz-mica schist and granulitic migmatite, east of Ilesha (Abraham *et al.*, 2014). The Okemesi Quartzite Member is characterized by a North-South trending ridge called the Effon ridge (Elueze 1988).

The quartzitic rocks are composed of dominant quartz with muscovite, chlorite and sericite occurring in minor proportions (Adegbuyi and Abimbola

1977). Rogers *et al.*, (1969) suggested that the source of springs in the Effon Psammite Formation is associated with a faulted and fractured quartzite band, sandwiched between schists.

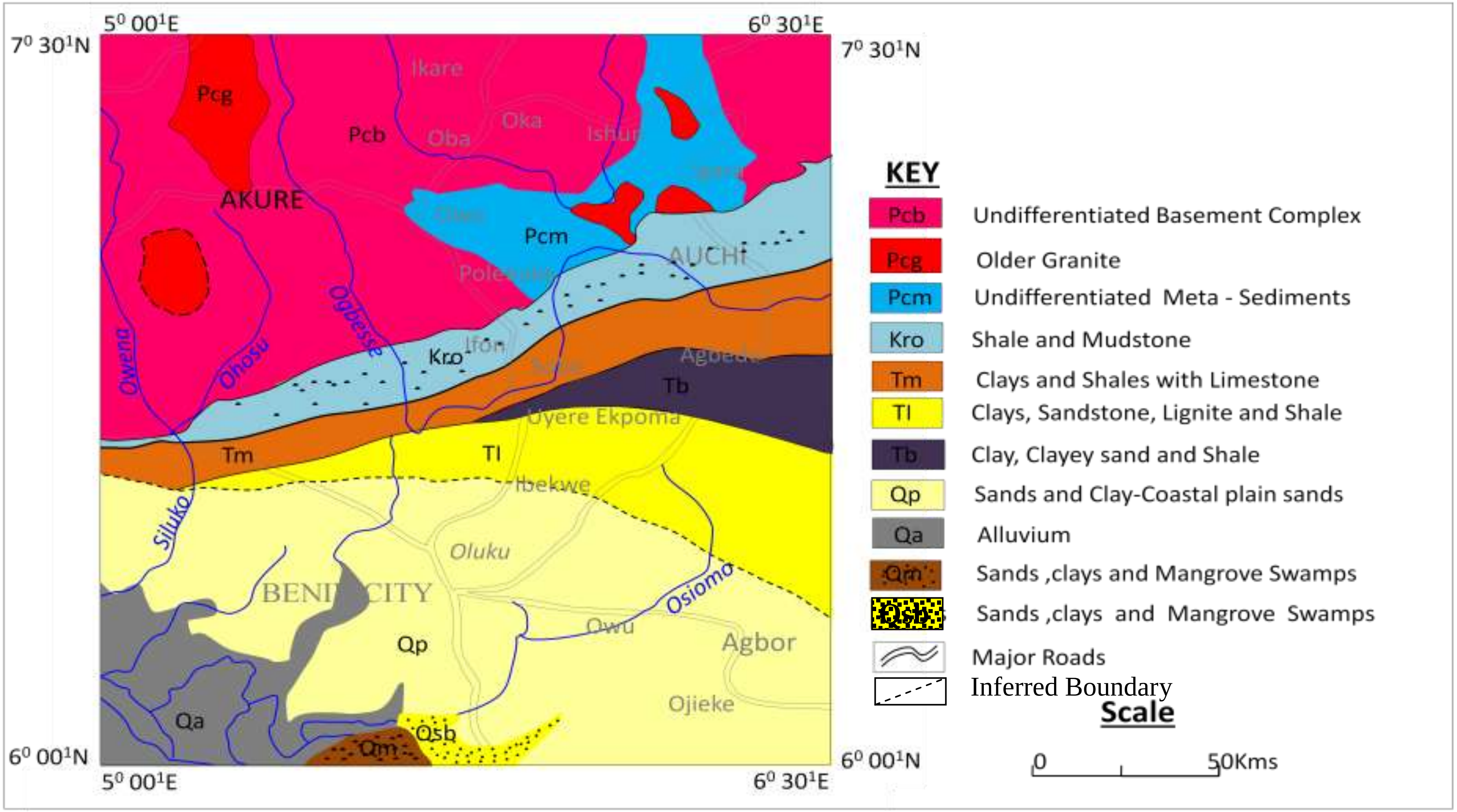

Fig. 2.3: Geologic map of the study area (Adapted from Geological Survey of Nigeria, 1974)

Olade and Elueze (1979) and Elueze (1988) reported that the chemical data of the quartzite of Ilesha area is composed largely of metamorphosed sandstones containing minor arkosic intercalations. On the basis of petrology, a medium pressure Barrovian and low-medium pressure types of a metamorphism had been suggested for the Precambrian basement rocks in southwestern Nigeria. Chuku-Ike and Norman (1977) and Mbonu (1990) noted that the intersections of the NNE – SSW epeirogenic belts with the NW-SE fracture trends in Nigeria coincide with the centres of warm springs like the Wikki spring of Bauchi and Ikogosi spring of Ekiti State. Rogers *et al.*, (1969) remarked that the issue of the springs is controlled by permeability developed within the quartzite as a result of intergranular pore spaces coupled with fracturing of the relatively competent quartzite.

Generally, Nigeria is not situated on any known seismic belt, yet between 1933 and 2000, Nigeria experienced fifteen seismic events, three of which occurred within a year (Abraham *et al.*, 2014). The intensities of these events ranged from III to VI based on the modified Mercalli Intensity Scale. Three of the events, the 1984 seismicity at Ijebu – Ode, the 1990 at Ibadan and 2000 at Jushi – Kwari were instrumentally recorded. They had body wave magnitudes ranging from 4.3 to 4.5, local magnitude ranging from 4.3 to 4.5, local magnitudes between 3.7 and 4.2 and surface wave magnitudes between 3.7 and 4.2 and surface wave magnitudes between 3.7 and 3.9 (Ajakaiye *et al.*, 1987). Out of these three seismic events, it is only the Ibadan and the Ijebu-Ode events that are located several kilometers away from the northwestern part of the study area. Some important fault systems in Nigeria include the Ifewara, Zungeru, Anka and Kalangai fault systems and they are interpreted to have resulted from transcurrent movements (Garba, 2003). The Ifewara fault is the only fault that is located some kilometers away from the northwestern part of the study area. Adepelumi *et al.*, (2008) revealed the existence of Ifewara shear zone formed by shearing activities during the Late Precambrian times using Multi-Spectral Scanner (MSS) and side-looking airborne radar (SLAR) images. They identified a NNE – SSW trending Ifewara fault system in the area and showed that the 250km long NE – SW trending Ifewara fault zone could be linked with Atlantic fracture system. Burke *et al.,* (1977) and Hubbard (1975) remarked that the pronounced age difference on both sides of the fault zone suggests that the zone may indeed be a suture of Kibaran age. Also, Burke (1969) noted possible relationship between the epicenters of some of the West African earthquakes and continental extensions of ocean fractures into the landmass. He noted that stresses built up around plate boundaries could travel towards the centre of the plate triggering intra-plate seismicity especially in pre-existing faults. Oluyide and Udo (1989) noted that the coastal areas of Nigeria lie in close proximity to the boundary between the African plate and South American Plate and that some of the seismic activities that occurred in the coastal areas of Nigeria have been possibly initiated by this process.

2.4.2 Sedimentary Formations

The southern part of the study area lies within the northern flank of the Niger Delta Basin in Nigeria. It falls within the localities where the lithofacies of the Niger Delta grade gradually into the lithofacies of the Anambra Basin. This part of the study area (southern part) is thus underlain from the earth's surface by the Nkporo Shale of Cretaceous age and this is composed mainly of shale and mudstone. This can be seen around Auchi area. The area is further underlain by the Imo Shale of Tertiary age, around Agbede area. This formation consists of clays and shales with limestone. The Imo Shale is underlain by the Bende-Ameki Formation of the Tertiary age and the lithology consists of clay, clayey sand and shale. The Imo Shale is underlain by the lignite series around Ekpoma area and it consists of clays, sandstone, lignite and shale, the age is Tertiary. The area around Benin-City and environ is underlain by the coastal plain sands, consisting of sands and clay. This formation is of Quartenary age. The southern flank of Okomu (southwestern part of the study area) is filled with alluvium, mangrove swamps and Sombrerio-Warri Deltaic Plain of more Recent age. Sands and clays of riverine Alluvium occur in the valley of the Okomu.

In summary, the geology of the Niger Delta has been described in detail by various authors (Allen, 1965; Reyment, 1965; Short and Stauble, 1967; Burke *et al.*,1972; Ekweozor and Daukoru 1984; Doust and Omatshola 1990) and they delineated basically three diachronous stratigraphic units viz: the Akata Formation, Agbada Formation and Benin Formation respectively.

2.4.2.1 Akata Formation

This is an open marine facies unit dominated by under pressured shale of 2000 to 4000m in thickness (Doust and Omasola, 1990). It is the oldest Formation and the age ranges from Paleocene to Eocene. It is a sequence of planktonic foraminefera rich under compacted transgressive marine shale, clays and silts. The Akata Shales are typically under compacted and frequently move either downward or laterally along the continental shelf or in an upward diapiric motion along faults, in response to the lithostatic pressure of over lying sediments (Ekweozor and Daukoru, 1984). The Akata Formation is overlain by the Agbada Formation.

2.4.2.2 Agbada Formation

The Agbada Formation consists of parallic sequence of alternating Lower Eocene to Pleistocene Sandstones and sand bodies with shale intercalations (Doust and Omotsola, 1990). The Agbada Formation is the major petroleum bearing unit in the Niger Delta. The thickness of the formation is over 3700m (Doust and Omotsola, 1990). The formation is highly faulted with assays of roll-over extensions induced growth faults, compensations listric fault and high grade thrust fault depending on the belt of the Niger Delta. The Agbada Formation is in turn overlain by the Benin Formation.

2.4.2.3 Benin Formation

This formation is dominantly a fluvial facies unit of 90% sand/sandstone and clay intercalations that ranges from Miocene to Recent (Doust and Omotsola, 1990). It consists of Late Eocene to Recent massive porous and unconsolidated freshwater bearing continental deposits including alluvial and upper coastal plain deposits.

Table 2.1: Outcropping lithostratiphic units of Tertiary Niger Delta (After Reyment, 1965)

Age	Lithostratigraphic Unit	Characteristics
Oligocene – Recent	Benin Formation	Known also as coastal plain sand. It consists of cross bedded coarse pebbly continental sand with clay lenses and lignite.
Oligocene – Miocene	Ogwashi-Asaba Formation (Lignite Series)	Clay, silts and sands with lignite seams up to 2m thick.
Eocene – Oligocene	Ameki/Nanka Formation	Calcareous clays and silts with thin shelly limestone rich in foraminifera
Eocene	Nanka Formation	Mainly sand, minor silts and clay
Paleocene – Eocene	Imo Formation	Blue-grey shales with sand lenses, marls and limestone, shales with Ostracods.

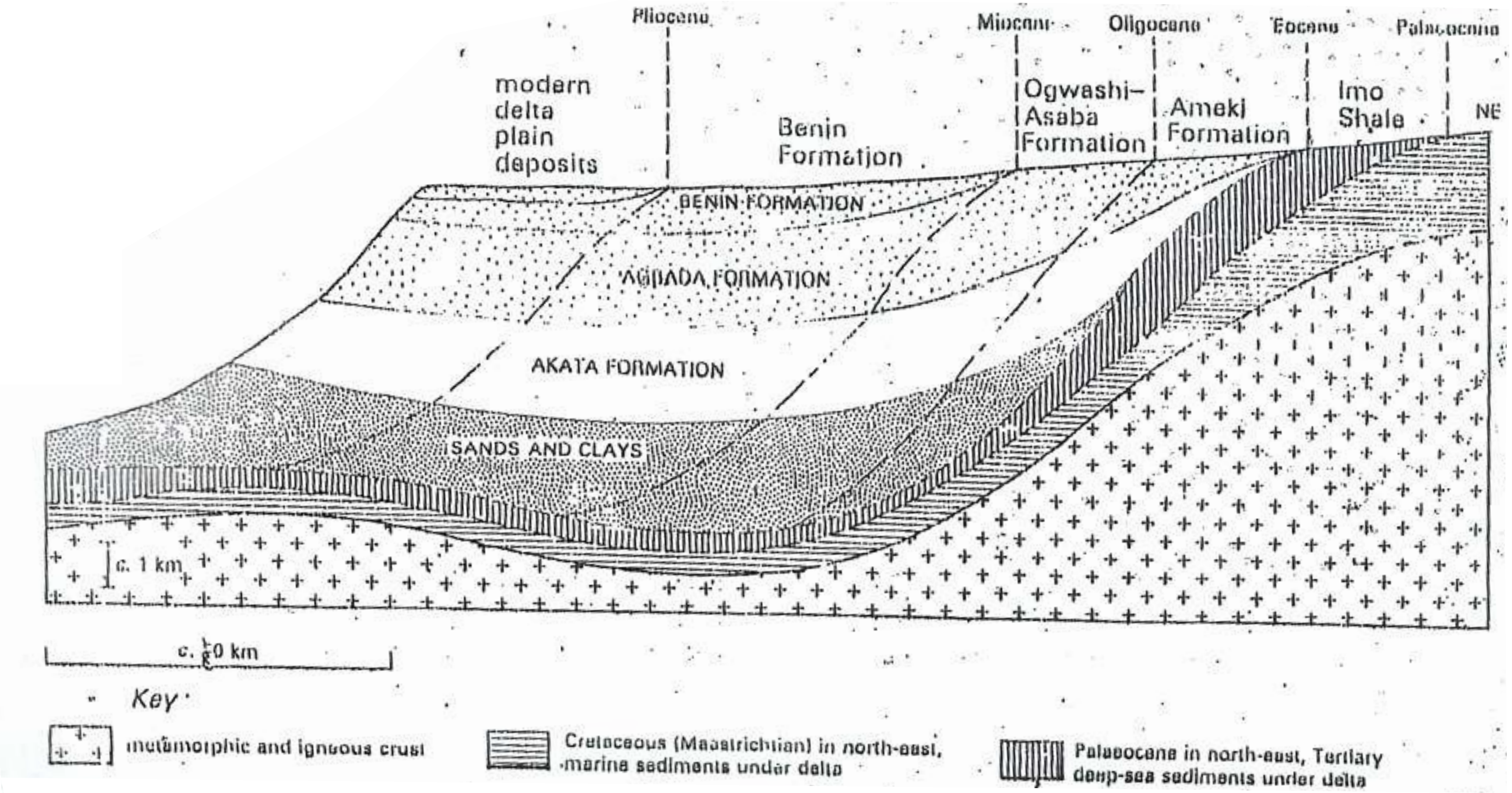

Fig. 2.4: Schematic diagram of lithostratigraphic unit of the Tertiary Niger Delta (After Reyment, 1965)

2.5 Principle of Magnetism of Rocks and Minerals

The Earth has a natural magnetic field caused by the motion of materials deep within the core (Lowrie, 1997). The magnetic field has been known and used by navigators since the Vikings used “lodestone” as simple compasses to find north. Today, detailed mapping of the Earth’s magnetic field is continually updated to assist navigation.

Importantly, when the Earth’s magnetic field interacts with a magnetic mineral contained in rock, the rock becomes magnetic. This is called induced magnetism (Fig. 2.5). The same thing occurs when an iron nail is placed near a magnet; the magnet’s magnetic field will induce a magnetic field in the nail. The induced field is often strong enough that one can pick up another smaller nail with the first nail. Nevertheless, the induced magnetic field ceases when the magnet is moved away from the nail. A rock therefore, would be magnetic if at least one of the minerals it is composed of is magnetic. The strength of the rock’s magnetism is related not only to the amount of magnetic minerals they contain, but also to the physical properties such as grain sizes of those minerals (Dobrin and Savit, 1988).

All substances are magnetic at an atomic scale. The phenomenon in which a material acquires a magnetization when placed within a magnetic field but loses it when removed from the field is termed induced magnetization or magnetic polarization. It results from the alignment of the elementary dipoles within the material parallel to the direction of the external field, but of opposite polarity (Telford *et al.*, 1990). The intensity of induced polarization (I), is proportional to the strength of the external field (H) hence,

$$I = XH \qquad 2.13$$

Where, X is a dimensionless proportionality constant for the particular magnetic material termed susceptibility. The magnetic susceptibilities of a single rock type can be very variable (Table 2.2). These ranges reflect the different amounts of magnetic minerals present in different samples of the same rock type. There are different types of magnetic materials classified according to the extent to which they can be magnetized when exposed to the external field (depending on the values of their magnetic susceptibility). According to Telford *et al.*, (1990) ,these materials include;

i. Diamagnetic materials
ii. Paramagnetic materials
iii. Ferromagnetic materials and
iv. Ferrimagnetic materials

i. Diamagnetic Materials

There are materials which has a low and negative magnetic susceptibility. This means that the intensity of induced magnetization in the material is in opposite direction to the inducing or external magnetic field. This situation is characteristic of atoms with closed electron shells.

Many elements and compounds exhibit diamagnetism. The most common diamagnetic earth materials are graphite, gypsum, marble, quartz and salt (Telford *et al.,* 1990).

ii. Paramagnetic Materials

These are materials that have low and positive magnetic susceptibility, with each atom or molecule in the paramagnetic substance having a net magnetic moment in zero external fields. This is characteristic of substances whose sub-shells are not filled to the maximum. Examples are iron, cobalt and nickel. The paramagnetic effect decreases with increase in temperature (Telford *et al.,* 1990).

iii. Ferromagnetic Materials

They have high and positive magnetic susceptibility, hundreds of times higher than that of paramagnetic and diamagnetic materials. Ferromagnetism also decreases with temperature and disappears completely at Curie temperature. Ferromagnetic materials apparently do not exist in nature (Telford *et al.,* 1990).

iv. Ferrimagnetic Materials

These are materials whose magnetic domain are subdivided into regions which may be aligned in opposition to one another but whose net moment is not zero when the external field is zero. Practically, all magnetic minerals are ferrimagnetic. Examples are magnetite, titanomagnetite and ilmenite (Telford *et al.*, 1990).

It should be noted that it is possible to locate minerals with negative magnetic susceptibility although the negative volumes are very small with detailed magnetic survey (Telford *et al.*,1990). If a rock containing thousands of ferromagnetic mineral grains is placed in a strong magnetic field, the individual magnetic moments become aligned with the applied magnetic field. If the magnetizing field is reduced to zero, a ferrimagnetic material retains part of the induced magnetization. This residual magnetization is termed remanence or isothemal remanence magnetization. When the ferrimagnetic material is heated, its spontaneous magnetization disappears at the ferromagnetic Curie temperature or Curie point. On cooling down below the Curie point, spontaneous magnetization reappears.

Table 2.2: Ranges and averages of magnetic susceptibility of some common rock types (Telford *et al.*, 1990)

Rocks	Susceptibility ($x10^6$ emu) range	
Sediments and Sedimentary Rocks		
Sandstone		
Shale	All very low (<1)	
Limestone		
Gypsum		
Coal		
Oil		
Igneous Rocks	**Range**	**Average**
Granite	0 – 400	200
Basalt	20 – 14, 500	6,000
Gabbro	80 – 7,200	6,000
Peridotite	7,600 – 15, 600	13,000
Metamorphic Rocks	**Range**	**Average**
Quartzite	-	350
Schist	25 – 240	120
Slate	0 – 300	50
Gneiss	10 – 2000	-

The main magnetic mineral is magnetite (Fe_3O_4), which is a common mineral found disseminated through most rocks in differing concentrations. Once an aeromagnetic data has been collected, the data is then processed to remove the Earth's natural magnetic field and any diurnal field changes (night to day variations) in order to reveal the variations in magnetization due to the underlying geology (Dobrin and Savit, 1988). Thus, individual magnetic anomalies which are magnetic signatures different from the background consist of a high and low (dipole) compared to the average field. In the southern hemisphere, the high is located to the north and the low to the south of the magnetic body, while the reverse is the case in the northern hemisphere. So, the position and size of the anomaly depend on the position of the magnetic body. A change in latitude will also affect the positioning of anomalies over magnetic body.

This situation allows the geophysicist to interpret the position of the body which has caused the anomalies reading. Often however, the reading is complicated because of the position of the body in relation to other rocks, its size and what happens to the body at depth. The corrected data are usually presented as field contour maps. The magnetic anomalies are usually numerous, erratic and less persistent and of large magnitude. From the field contoured maps, geophysicists can locate magnetic bodies interpret the nature of geological boundaries at depth, geologic structures like faults etc. An experienced interpreter in magnetics can usually see geological structure by merely looking at a magnetic map just as one can visualize surface features from the contours of a topographic map. When contour lines in a map are close together, they represent a sharp change in values or steep gradient, while widely space contour lines represent slow change in value or shallow gradient.

Generally, qualitative interpretation of a magnetic data is primarily a map or an image based recognition of patterns, trends, structural grains, discontinuity/offsetting faults and disrupting cross–cutting features (Dobrin and Savit, 1988). Qualitative interpretation is concerned essentially with the visual inspection of maps or profiles. Visual inspection involves identification of zones with different magnetic characteristics. Magnetically “quiet” and magnetically “perturbed” segments are qualitatively interpreted as caused by rocks with low and high magnetic susceptibilities respectively in the sub–surface (Dobrin and Savit, 1988). The quantitative interpretation on the other hand involves taking profiles on the residual anomaly map and plotting graphs in order to estimate the depth to the magnetic sources.

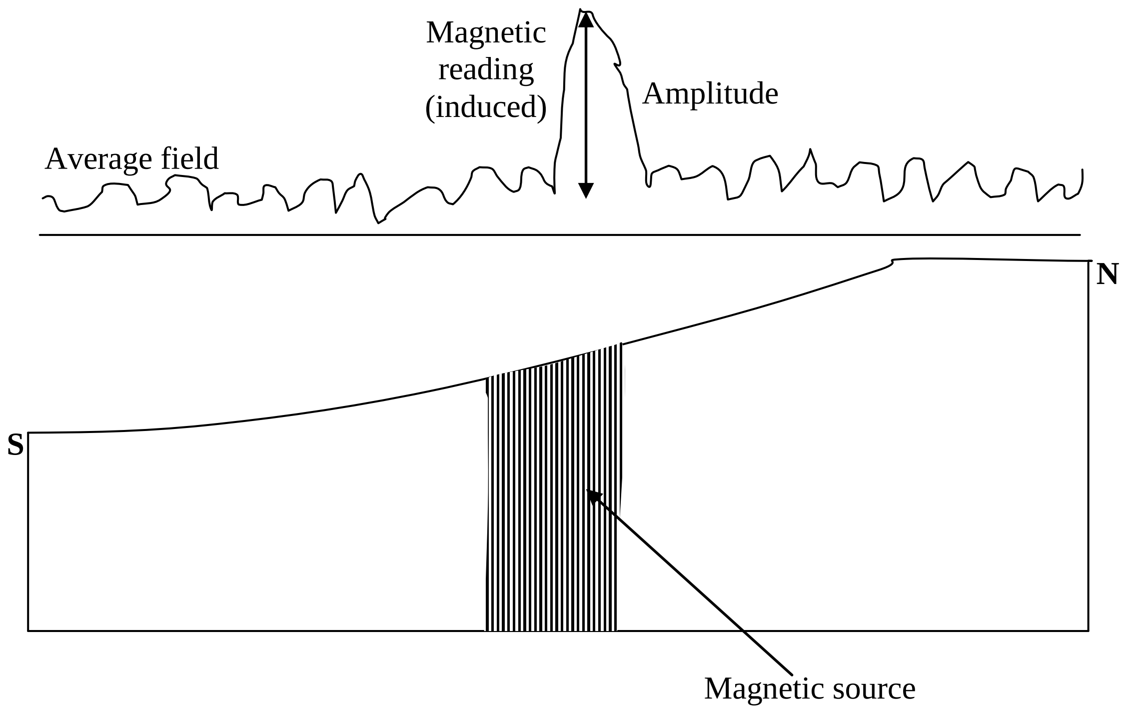

Fig 2.5: Description of rock's magnetism (After Lowrie, 1977)

2.6 Role of Faults and Fractures on Crustal Fluids

The roles of faults and fractures on crustal fluids have been of major interest in earth science including geology, seismology, hydrogeology and petroleum geology (Gudmundsson *et al.,* 2001). The static and dynamic effects of different stress on rock often produce change in rock mass such as fractures, faults and in general permeability which in turn control the flow of fluids in the earth crust. Fractures and faults are planes of tensile or shear failure at microscopic to regional scales in brittle rocks. These faults and fracture are developed mostly in competent rocks within the earth crust. In case of fractures, they are usually developed when the stress applied exceeds the elastic limit of the rocks. These two deformations are of great importance in crustal fluid distributions and control.

2.7 Geothermal System: Process and Model

Geothermal energy can be described as the heat generated within the earth which could be exploited for use. Geothermal resources, according to Mary and Mario (2004) are generally, associated with tectonically active region which are generated as a result of temperature differences between the different parts of the asthenosphere (below the lithosphere) where convective movement are formed. The slow convective movement is said to be maintained by the radioactive elements and heat from the deepest part of the earth. The less dense deep hotter rocks tend to rise with the movement towards the surface while the colder but heavier rocks close to the surface tend to sink, re- heat and rise again.

Generally, hydrothermal system is made up of the heat source, the reservoir, the recharge area and the connecting paths such as faults and fractures through which fluids percolate to the reservoir (the host rock) and in most cases are escaped to the surface as fumaroles and hot springs. The heat source is generally magmatic intrusion that has reached shallow depths of about 5-10km (Mary and Mario, 2004). The reservoir rocks are permeable rocks through which fluid circulate and extract heat from the heat source. This is often overlain by impermeable rocks and also connected through medium such as faults and fractures to a surfacial recharge area from which meteoric water replaces or partly replace the fluids which escape from the reservoir through springs or by drilling (Fig. 2.6). Large amounts of chemicals are carried along as the geothermal water percolates through the host rock; this dissolution of rock minerals mostly contributes to the salinity of most hot springs. The surface manifestations of geothermal energy are in form of hot springs.

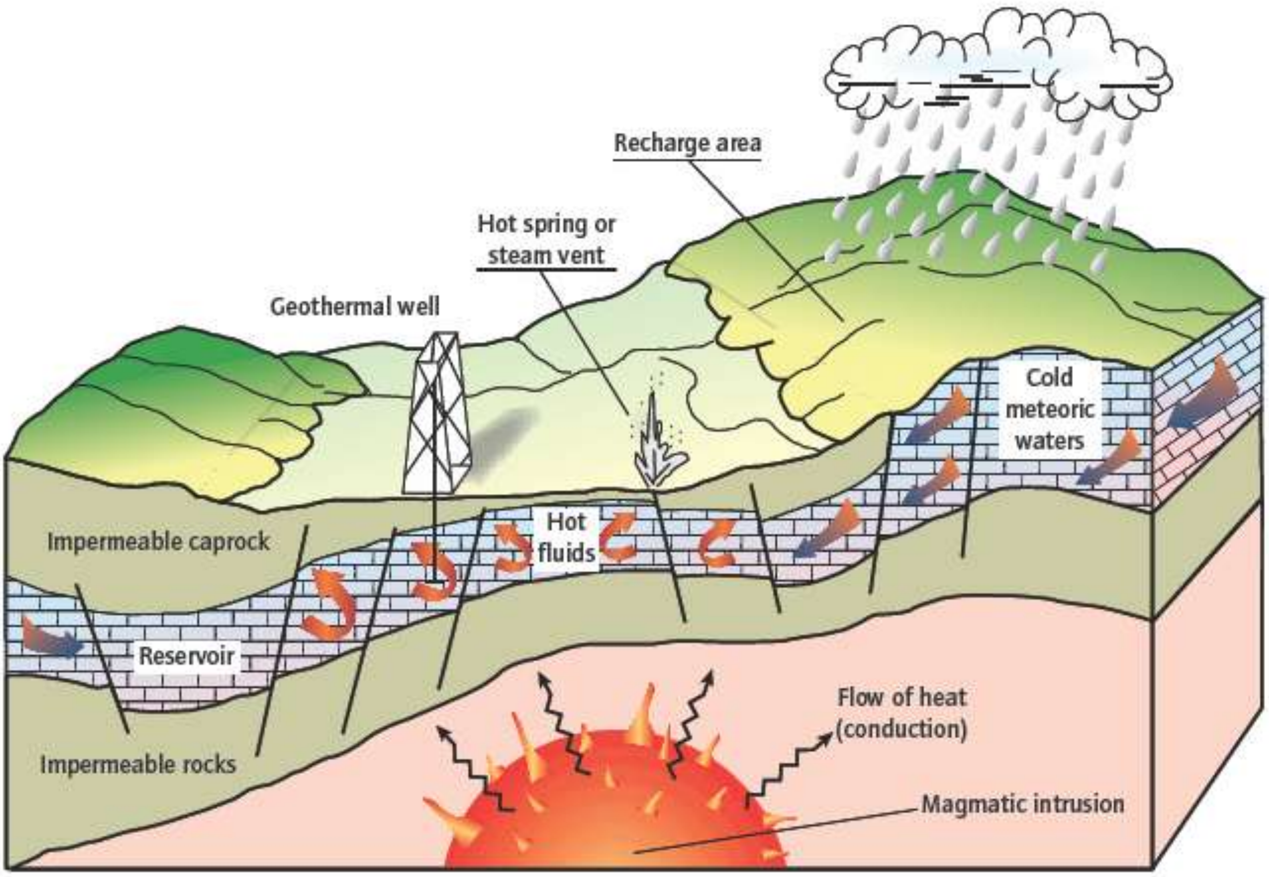

Fig. 2.6: Schematic representation of a typical geothermal system (After Mary and Mario, 2004)

CHAPTER THREE

MATERIALS AND METHODS

3.1 Data Availability and Description

The data for this study constitute the aeromagnetic sheets of Southwestern Nigeria. To achieve the objectives of the study earlier stated above, nine aeromagnetic sheets from the area: sheet 264 (Akure); sheet 265 (Owo); sheet 266 (Auchi); sheet 283 (Siluko); sheet 284 (Ifon); sheet 285 (Ubiaja); sheet 297 (Okomu); sheet 298 (Benin-city); sheet 299 (Agbor) were acquired through purchase, assembled and analyzed. The aeromagnetic data were obtained as part of nationwide aeromagnetic survey sponsored by the Geological Survey Agency of Nigeria (GSAN). The data were acquired along a series of Northwest-Southeast (NW-SE) flight line direction, flight lines spacing of 500 meters, tie line spacing of two kilometers (2km) tie lines direction of NE-SW and terrain clearance of 80meters. The geomagnetic gradient was removed from the data using the internationally geomagnetic reference field (IGFR). The data were made available in the form of contoured maps on a scale of 1:100, 000. The total area covered was about 27, 225 square kilometers.

The procedure involved in this study includes digitization of the aeromagnetic maps in order to extract the total field intensity values of the area. The regional anomaly was removed from the observed data by fitting a plane polynomial surface to the data. The residual data were subjected to computer processing techniques of filtering by spectral analysis in order to obtain quantitative parameter, which describe the depths to the magnetic sources (Curie point depth). Consequently, surface maps of depths to magnetic sources/layers were produced and analyzed. The Curie point depth information was then used to calculate the vertical geothermal gradient and heat flow of the study area respectively. Curie-isotherm map, geothermal gradient map and heat flow map were also produced. Finally, the Curie point depth information was used to estimate the depth to the cheat source (geothermal energy).

3.2 Methodology

3.2.1 Digitization of Aeromagnetic Maps

The nine aeromagnetic maps obtained were digitized and along flight lines at 2km intervals and the intersection points were picked and contoured using Surfer 32 contouring software. During the digitization of aeromagnetic maps, the following procedures were required:

1. Study of the aeromagnetic map itself to know the trend and the interval of the contours.
2. Measurements of the aeromagnetic map both in horizontal and vertical paths (usually each aeromagnetic map is 55km by 55km).
3. Drawing grids on the maps: the flight lines were used as grid lines of 2km interval.

4. Picking the intersection points: the intersections of the flight lines were picked with respect to their latitudes and longitudes
5. Contouring the digitized data: the data were plotted using Surfer 32 contouring software.

3.2.2 Separation of Digitized Aeromagnetic Data

The contoured digitized data which is referred to as total magnetic field intensity (TMI) map of the study area, contains both the regional and residual anomaly. To interpret the local field, the regional field was removed from the data. In this case, a linear trend surface was fitted on to the digitized aeromagnetic data by a multiple repression technique for the purpose of removing the regional magnetic gradient. The linear surface so fitted was removed from the digitized data to obtain the residual aeromagnetic map that would then be interpreted.

3.2.2.1 Vector plane for taking geophysical measurements

A vector plane is defined by two unit vectors i and j.

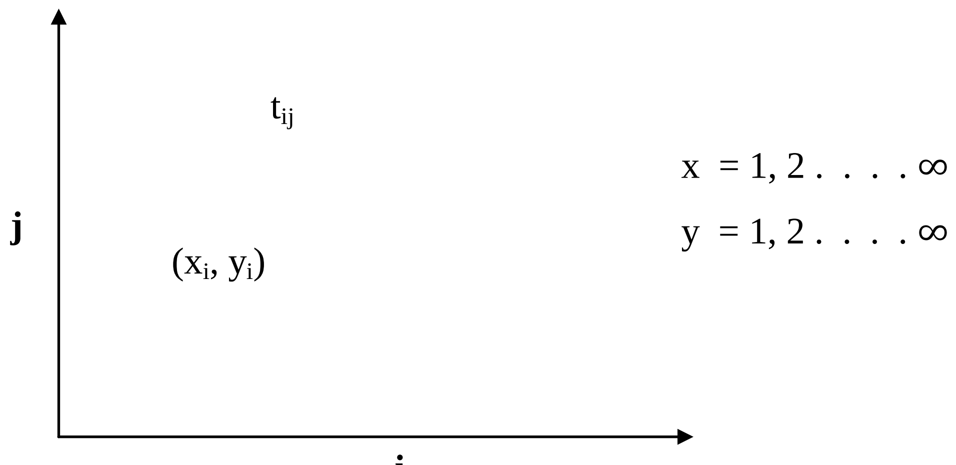

Fig. 3.1: Vector plane defining point measurement t_{ij} at coordinate $(x_i y_i)$

The coefficient of the unit vector along x – axis is i. Hence, we have x_i. Also, the coefficients of the unit vector along y – axis is j. Hence, we have y_i. Every point on ij vector will be defined by x_i and y_j.

3.2.2.2 Fitting of Empirical Data Onto a Linear Surface (Trend Surface)

A linear surface equation is given by $Ax_i + By_i + C$ 3.1

where, A, B and C are constant of the linear equations

i = 1, 2 . . . . .n and j = 1, 2 . . . . n

Where; n = maximum data point.

Let us assume that a certain geophysical reading t_{ij} is taken at co-ordinate (x_i, y_j), such that the data and the co-ordinate values range from:

$(x_i, y_{j,} t_i), (x_2, y_{2,} t_2)$ . . . . $(x_n, y_{n,} t_n)$ 3.2

where, n = maximum data point

Fitting the data t_{ij} onto a linear surface $(Ax_i + By_i + C)$ we have,

$t_{ij} = Ax_i + By_j + C$ 3.3

We need to maximize the error function of the variable A, B and C,

Thus,

$$g(A, B, C) = \sum_{i=1}^{n}\sum_{j=1}^{n}\left[\mathrm{t_{ij}} - (\mathrm{A_{xi}} + \mathrm{B_{yi}} + \mathrm{C}\right]^2 \qquad 3.4$$

Where,

g = error function of the variables A, B and C

The condition on which the error function g is maximum is that the partial derivative of g with respect to A, B and C is equal to zero.

Thus,

$$\left.\begin{aligned}\frac{\delta g}{\delta A} &= 0\\ \frac{\delta g}{\delta B} &= 0\\ \frac{\delta g}{\delta C} &= 0\end{aligned}\right\} \qquad 3.5$$

Solving equation (3.5) simultaneously,

Then,

$$\left.\begin{aligned}\frac{\delta g}{\delta A} &= -2\sum_{i=1}^{n}\sum_{j=1}^{n}\left(\mathrm{tij} - \mathrm{A_{xi}} - \mathrm{B_{yi}} - \mathrm{C}\right)\mathrm{x_i} = 0\\ \frac{\delta g}{\delta B} &= -2\sum_{i=1}^{n}\sum_{j=1}^{n}\left(\mathrm{tij} - \mathrm{A_{xi}} - \mathrm{B_{yi}} - \mathrm{C}\right)\mathrm{y_i} = 0\\ \frac{\delta g}{\delta C} &= -2\sum_{i=1}^{n}\sum_{j=1}^{n}\left(\mathrm{tij} - \mathrm{A_{xi}} - \mathrm{B_{yi}} - \mathrm{C}\right) = 0\end{aligned}\right\} \qquad 3.6$$

Dividing each of the equations (3.6) by – 2 we have;

$$\left.\begin{aligned}
&\sum_{i=1}^{n}\sum_{j=1}^{n}\left(\mathrm{t_{ij}} - \mathrm{A_{xi}} - \mathrm{B_{yi}} - \mathrm{C}\right)\mathrm{x_i} = 0\\
&\sum_{i=1}^{n}\sum_{j=1}^{n}\left(\mathrm{t_{ij}} - \mathrm{A_{xi}} - \mathrm{B_{yi}} - \mathrm{C}\right)\mathrm{y_i} = 0\\
&\sum_{i=1}^{n}\sum_{j=1}^{n}\left(\mathrm{t_{ij}} - \mathrm{A_{xi}} - \mathrm{B_{yi}} - \mathrm{C}\right) = 0
\end{aligned}\right\} \qquad 3.7$$

Opening the brackets in equation (3.7), we have;

$$\left.\begin{aligned}
&\sum_{i=1}^{n}\sum_{j=1}^{n}\mathrm{t_{ij}x_i} - \mathrm{A}\sum_{\mathrm{i-1}}^{\mathrm{n}}\mathrm{x_1^2} - \mathrm{B}\sum_{\mathrm{i=1}}^{\mathrm{n}}\sum_{\mathrm{j=1}}^{\mathrm{n}}\mathrm{y_jx_i} - \mathrm{C}\sum_{\mathrm{i-1}}^{\mathrm{n}}\mathrm{x_i} = 0\\
&\sum_{i=1}^{n}\sum_{j=1}^{n}\mathrm{t_{ij}y_i} - \mathrm{A}\sum_{\mathrm{i-1}}^{\mathrm{n}}\mathrm{x_iy_j} - \mathrm{B}\sum_{\mathrm{j=1}}^{\mathrm{n}}\mathrm{y_j^2} - \mathrm{C}\sum_{\mathrm{i-1}}^{\mathrm{n}}\mathrm{y_i} = 0\\
&\sum_{i=1}^{n}\sum_{j=1}^{n}\mathrm{t_{ij}} - \mathrm{A}\sum_{\mathrm{i-1}}^{\mathrm{n}}\mathrm{x_i} - \mathrm{B}\sum_{\mathrm{j=1}}^{\mathrm{n}}\mathrm{y_j} - \mathrm{nc} = 0
\end{aligned}\right\} \qquad 3.8$$

Re-writing equation (3.8) we have,

$$\left.\begin{aligned}
&\sum_{i=1}^{n}\sum_{j=1}^{n}\mathrm{t_{ij}x_i} = \mathrm{A}\sum_{\mathrm{i-1}}^{\mathrm{n}}\mathrm{x_i} + \mathrm{B}\sum_{\mathrm{i=1}}^{\mathrm{n}}\sum_{\mathrm{j=1}}^{\mathrm{n}}\mathrm{y_jx_i} - \mathrm{C}\sum_{\mathrm{i-1}}^{\mathrm{n}}\mathrm{x_i} = 0\\
&\sum_{i=1}^{n}\sum_{j=1}^{n}\mathrm{t_{ij}y_i} = \mathrm{A}\sum_{\mathrm{i-1}}^{\mathrm{n}}\sum_{\mathrm{j=1}}^{\mathrm{n}}\mathrm{x_iy_j} + \mathrm{B}\sum_{\mathrm{j=1}}^{\mathrm{n}}\mathrm{y_j^2} + \mathrm{C}\sum_{\mathrm{i-1}}^{\mathrm{n}}\mathrm{y_i} = 0\\
&\sum_{i=1}^{n}\sum_{j=1}^{n}\mathrm{t_{ij}} = \mathrm{A}\sum_{\mathrm{i-1}}^{\mathrm{n}}\mathrm{x_i} + \mathrm{B}\sum_{\mathrm{j=1}}^{\mathrm{n}}\mathrm{y_j} + \mathrm{nc} = 0
\end{aligned}\right\} \qquad 3.9$$

Putting equation (3.9) in matrix form, we have;

$$\begin{bmatrix} \sum_{i=1}^{n} x_i^2 & \sum_{i=1}^{n}\sum_{j=1}^{n} y_j x_i & \sum_{i=1}^{n} x_i \\ \sum_{i=1}^{n}\sum_{j=1}^{n} x_i y_j & \sum_{j=1}^{n} y_j^2 & \sum_{j=1}^{n} y_j \\ \sum_{i=1}^{n} x_i & \sum_{j=1}^{n} y_j & n \end{bmatrix} . \begin{bmatrix} A \\ B \\ C \end{bmatrix} = \begin{bmatrix} \sum_{i=1}^{n}\sum_{j=1}^{n} t_{ij} x_i \\ \sum_{i=1}^{n}\sum_{j=1}^{n} t_{ij} y_j \\ \sum_{i=1}^{n}\sum_{j=1}^{n} t_{ij} \end{bmatrix} \qquad 3.10$$

By matrix inversion the values of A, B and C will be obtained.

Note that, 100 data points were evenly selected as 10 by 10 grid data and by inserting values of the aeromagnetic data into equation (3.10) we obtain the matrix below;

$$\begin{bmatrix} 100 & 38.20 & 3070 \\ 3820 & 332140 & 166980 \\ 3070 & 166980 & 208750 \end{bmatrix} . \begin{bmatrix} A \\ B \\ C \end{bmatrix} = \begin{bmatrix} 752430 \\ 29782165 \\ 23632155 \end{bmatrix} \qquad 3.11$$

By matrix inversion, the values of A, B and C were obtained as:

A = 7371.4666

B = 6.3674

C = - 2.9446

The trend surface equation (regional gradient) becomes;

t_{ij} = 7371.4665x + 6.3674y -2.9446

Furthermore, the trends surface equation was then subtracted from the aeromagnetic (observed) data and the resultant residual anomaly obtained. Both the digitized data and the residual data were contoured using surfer 32 contouring software.

3.3 Delineation of Geothermal Energy/Heat Source Depth (Curie Point Depth)

Spectral analysis technique was adopted in this study to delineate the depth to the Curie temperature isotherm in the study area. An attempt to delineate the heat source depth will also delineate the geothermal energy of the area. Curie point depth in this study was used to infer transition depth of magnetite. Generally, rocks are usually non-magnetic at temperature greater than the Curie point of magnetite. The magma chamber acts as the hydrothermal source in most geothermal environment.

Delineation of heat source depth/geothermal energy (Curie point depth) was attempted based on spectral analysis method. The method relates depth to the top and bottom of the magnetic sources as stated in equation 2.8 in section 2.1.3. The spectral analysis was done using interactive filtering technique in Oasis Montaj software which is frequency domain processing of most potential field data. After preparing the magnetic grid (in space domain), it was then transformed to wave number (frequency) domain, using forward filtering transform (FFT) filters.

The transformation procedure involved application of different filtering functions such as upward and downward continuation. In this study, the upward continuation was applied to remove the effect of shallow sources since the analysis was aimed at estimating depth to deeper magnetic sources. After the filtering application, the inverse filter was applied to the space domain grid data which transformed it to wave number or frequency domain, from which power spectrum was generated. The power spectrum is a two dimensional (2D) function of energy and wave number. Radial Power Spectrum plot was generated from the transformed aeromagnetic data using Oasis Montaj software. The software automatically computes the depth corresponding to the power spectrum by plotting data from spectrum file. The result of the computed radial power spectral and depths to the top sources in the study area was obtained. So, estimating the heat source (Curie point depth) therefore was done by determining the depth to the bottom (Z_b) of the deepest anomaly using equation 2.8 in section 2.1.3.

3.4 Continuation

Magnetic data measured on a given plane can be transformed to data measured at a higher or lower elevation, thus either attenuating or accentuating shorter wavelength anomalies (Kellog, 1953). Continuation was employed on the magnetic data used for this study. Continuation is the mathematical projection of potential field data collected at one datum or level to another datum above or below the plane of observation. The basis of analytic continuation is the Laplace's equation which produces continuation equation. Continuation works well if there is no anomalous body between the datum and level of projection.

3.4.1 Upward Continuation

Upward continuation was employed in potential field interpretation in order to determine the form of regional variation over the study area. Upward continuation alternates the shallow feature anomalies and relatively enhances the anomalies of deeper seated sources. The frequency response of the upward continuation filter is given as:

$$F_u\,(u, v, h) = e^{-2\lambda(u^2+v^2)^{\frac{1}{2}}} \qquad 3.12$$

Where h is the height to which the field is continued. Thus, this form of continuation effectively smoothened the anomaly by suppressing the short wavelength components. Upward continuation is a straight forward operation because the projection is into a force free region. Upward continuation was applied to suppress the effects of small scale features near the surface and also to reduce topographic effects.

3.5 Estimation of Depth to Basement

In order to determine the number of magnetic horizons in the study area and their average depths, power spectrum of the magnetic data was computed and interpreted. The amplitude of the logarithm of radially average power spectrum was plotted against the radial frequency. Best fit least squares lines were then virtually fitted to the spectrum. The slopes of the linear segment of the spectrum correspond to separate depths.

Accurately, aeromagnetic data can be represented by an analytical function using Fourier series. In order to estimate depth to basement across the study area, the spectra analysis (Fourier transform) method was used in the interpretation of the aeromagnetic data. Six (6) profiles were taken on the residual anomaly map (Fig. 4.2) of the study area. These profiles were taken perpendicular to the direction of the magnetic anomalies. The profiles A-A^1, B-B^1, C-C^1, D-D^1, E-E^1 and F-F^1 were used for detailed interpretation. The method used in this study involves Fourier transformation of digitized aeromagnetic data to compute the amplitude spectrum. The respective spectrums of the profiles are shown in Fig. 4.6 (a - f). The gradients of the low frequency linear segment were evaluated and the depths to the magnetic sources were determined using equation 2.5. Depths to basement obtained from spectra analysis carried out in the study area are shown in Table 4.2.

3.6 Method of Interpretation

The interpretation of magnetic anomaly maps were both qualitatively and quantitatively interpreted.

3.6.1 Qualitative Interpretation

The qualitative interpretation of the aeromagnetic map was done by visual inspection of the total magnetic intensity map (TMI) and the residual anomaly map. The qualitative interpretation was done by visual inspection of the total magnetic field intensity map, noting the following;

i. The trend of contours

ii. The positive and the negative values of the contours

iii. The minimum and maximum values of the contours and their aerial extent.

Thus there are three features that are important in qualitative interpretation namely;

a. Sharp changes in contours gradients defines structural trends
b. The alignment of lateral shift (which offset the main anomaly) suggests faulting
c. The alignment of closed anomalies suggest presence of magnetic bodies

3.6.2 Quantitative Interpretation

A complete quantitative interpretation of potential field data estimates was carried out in the study area. The purpose of quantitative interpretation is to obtain information about the depth to magnetic sources, its shape and size and probably about its susceptibility, with the aim of estimating the sedimentary thickness variations, map the configuration of the Curie temperature isotherm and the associated geothermal gradient, reveal the origin of hot spring close to the study area and to reveal the petroleum potential of the study area. So in order to achieve the above stated objectives across the study area using the Fourier transform method, several profiles were taken on the residual aeromagnetic map of the study area. The method was chosen because of its advantage of filtering all the noise away from the data. Moreover, during the application of this method, information is not lost in the process unlike other methods. In this study, six selected magnetic profiles namely A-A^1, B-B^1, C-C^1, D-D^1, E-E^1, F-F^1, were used for detailed interpretation and these served as representative of others since they behave almost the same way.

Consequently, graphs of the natural logarithms of the amplitude against frequencies obtained for the various profiles were plotted. Linear segment from the low frequency portion of the spectral, representing contributions from the deep-seated causative bodies were drawn from each graph. The gradients of the linear segment were evaluated and the depths to magnetic sources were determined along the selected profiles.

A plot of the logarithm of the amplitude versus frequency usually shows straight line segments which decrease in slope with increasing frequency and the slopes of the segment give estimates of the depth to the magnetic sources (Spector and Grant, 1970).

The magnetic field observation made at or above the surface of the earth and the magnetization at the top of the magnetic parts of the crust are characterized by relatively short spatial wavelengths, while magnetic field from the magnetization at the Curie-point depth are characterized by longer wavelengths and lower amplitude magnetic anomalies. This difference in frequency characteristics between the magnetic effects from the top and bottom of the magnetized layer in the crust was used to separate magnetic effects at the two depths to determine the Curie depth. To estimate the centroid depth, Z_0, the slope of the longest wavelength part of the spectrum, gives the value of Z_0. In the second step, the spectrum was drawn against the wave number in order to estimate the top depth, Z_t from the second longest wavelength part of the spectrum.

In summary, two satisfactory algorithms were developed to invert the gridded data based upon a distribution of point dipoles. The first algorithm estimates x_o,y_o and z_o, the co-ordinates of the centroid of the distribution, by computing a least-squares fit to the radical frequency of the Fourier transform, the second algorithm estimates centroid depth only by computing a least-squares fit to the square of the frequency estimates. The average depth to the top, z_t of the collection of point dipoles was estimated by a variation of the second algorithm. The depth of the bottom of the dipoles inferred as the Curie point depth of the study area was then obtained using the formula:

$$Z_b = 2Z_0 - Z_t \quad \text{(from equation 2.8)}$$

The depth estimates was contoured to produce the Curie isotherm map of the study area. For the purpose of computing the geothermal gradients, it was assumed that the temperature changes within the earth and are linear and of the form.

$$T_h = mh + T_0 \qquad \text{(from Onwuemesi, 1997)}$$

Where:

T_h = temperature in ^0C at depth h

m = geothermal gradients

h = depth of interest

To = surface temperature

It was assumed that the surface temperature was 27^0C while Curie temperature was 580^0C (Onwuemesi, 1997). Subsequently, geologic models for the magnetic anomalies, depth to basement map, 3D surface plot for the basement topography, Curie- isotherm map, 3D surface plot for the Curie isotherm configurations, geothermal gradient map, 3D surface plots for the geothermal gradient configuration, heat flow map and its associated 3D surface plot for the heat flow configuration of the study area were constructed.

3.7 Precautions

It was ensured that the effect of aliasing was avoided or reduced. The effect of aliasing arises from the ambiguity in the frequency represented by the sampled data. Frequencies greater than the Nyguist frequency, tend to impersonate the lower frequencies and this is known as aliasing effects. So in order to avoid or reduce the effect of aliasing, frequencies greater than the Nyguist frequency must be removed through the use of an alias filter, which provides high attenuation above the Nyguist frequency.

More so, effect of aliasing can be reduced through the use of small sampling intervals such that the Nyguist frequency is equal to or greater than the highest frequency component present in the function being analyzed.

Again, when a limited portion of an aeromagnetic map or short profile is subjected to Fourier analysis, it is difficult to reconstruct the sharp edges of the anomaly with a limited number of frequencies and this produces what is known as the Gibb's phenomenon. The truncation effect can therefore be reduced by selecting a large centered on the anomaly or a long profile centered on the feature of interest. According to Ofoegbu and Onuoha (1991), an alternative and more effective approach to reducing the truncation effects is by the application of cosine taper to the observed data.

CHAPTER FOUR

RESULTS AND DISCUSSION

4.1 Result Presentation

The maps of the total field intensity and residual magnetic anomalies of the study area are shown in Figs. 4.1a, 4.1b and 4.2. The figures show that the total magnetic field and residual anomalies range from 7650 to 8340nT and – 60 to 100nT respectively. The maps show areas with both widely-spaced and closely–spaced contour lines indicating area with low and high intensity of magnetization respectively. Total magnetic field intensity map shows that the contour lines of the southeastern parts are widely spaced indicating that the depth to magnetic basement in this area is relatively high. But at Akure (northwestern part) area, the contour lines are closely spaced indicating that the depth to basement is shallow in this area.

Examination of the map reveals that the magnetic highs and lows are bounded by high gradient zones (Fig. 4.1b) trending in the Northeast-Southwest (NE–SW) and Northwest-Southeast (NW-SE) directions. Several sections of broad magnetic anomalies in the northwestern and northeastern part of the area are bounded by relatively steep magnetic gradients. The high gradient zones are indicative of fracture/shear zones (Bain, 2000). Moreover, closely spaced linear sub parallel orientation of contours between the north-eastern and north-western and the southern parts of the study area suggest the presence of faults or local fractured zones that may have possibly passed through these areas (Fig. 4.1b).

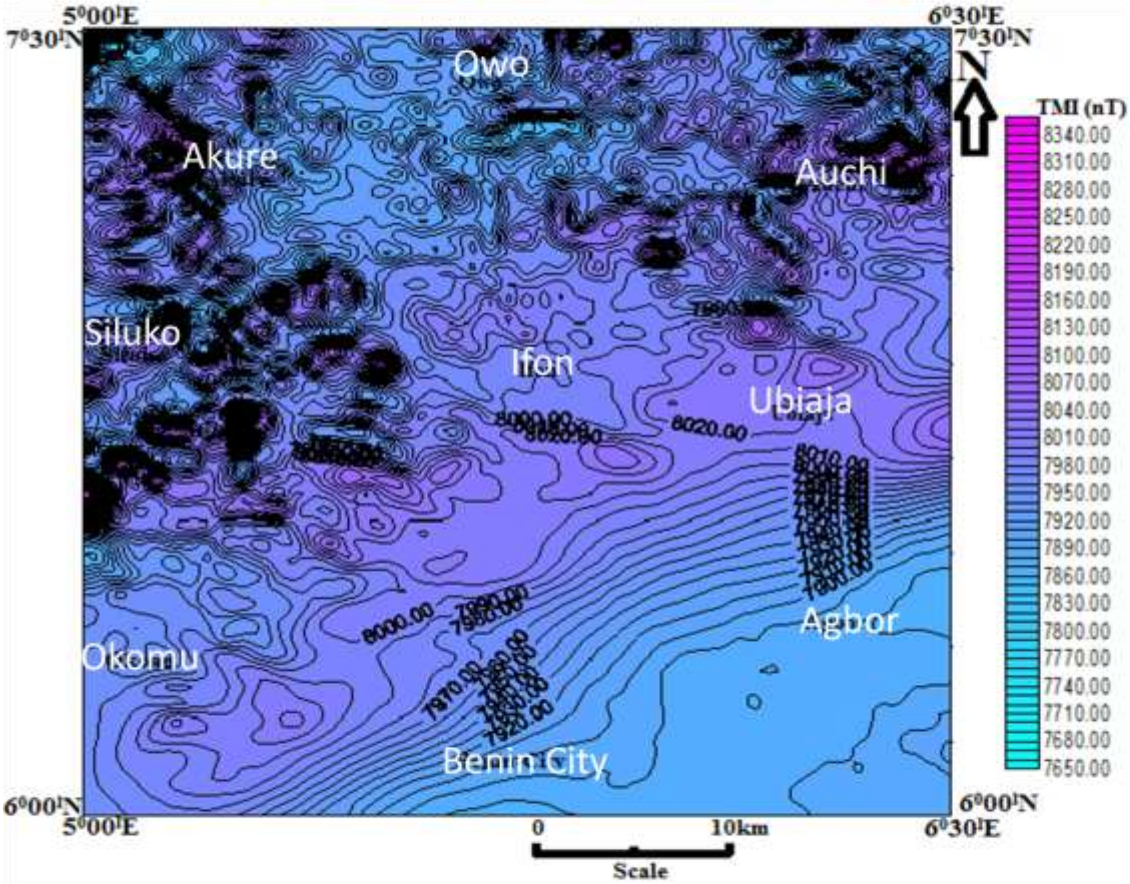

Fig. 4.1a: Total Magnetic Intensity Map of the study area (Contour Interval-10nT)

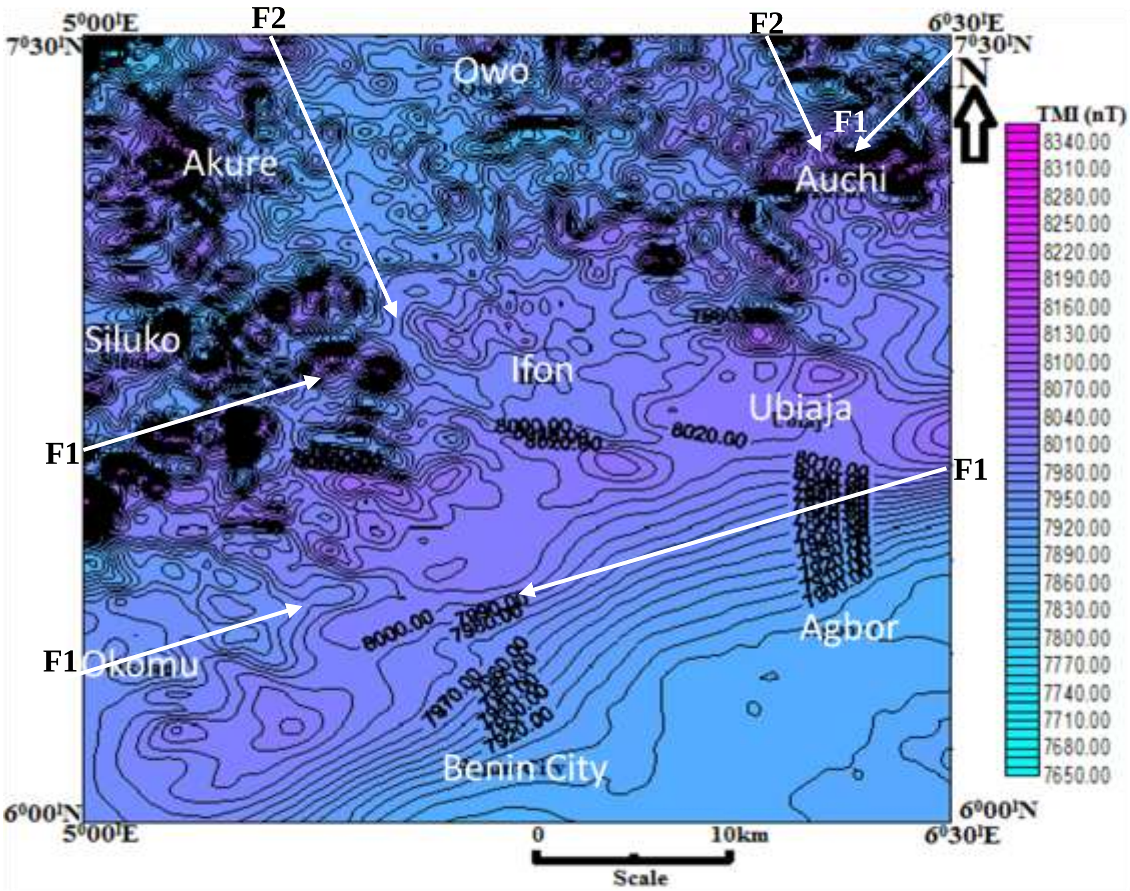

Fig. 4.1b: Total magnetic intensity map showing the high gradient zones (fault/fracture zones F_1 and F_2)

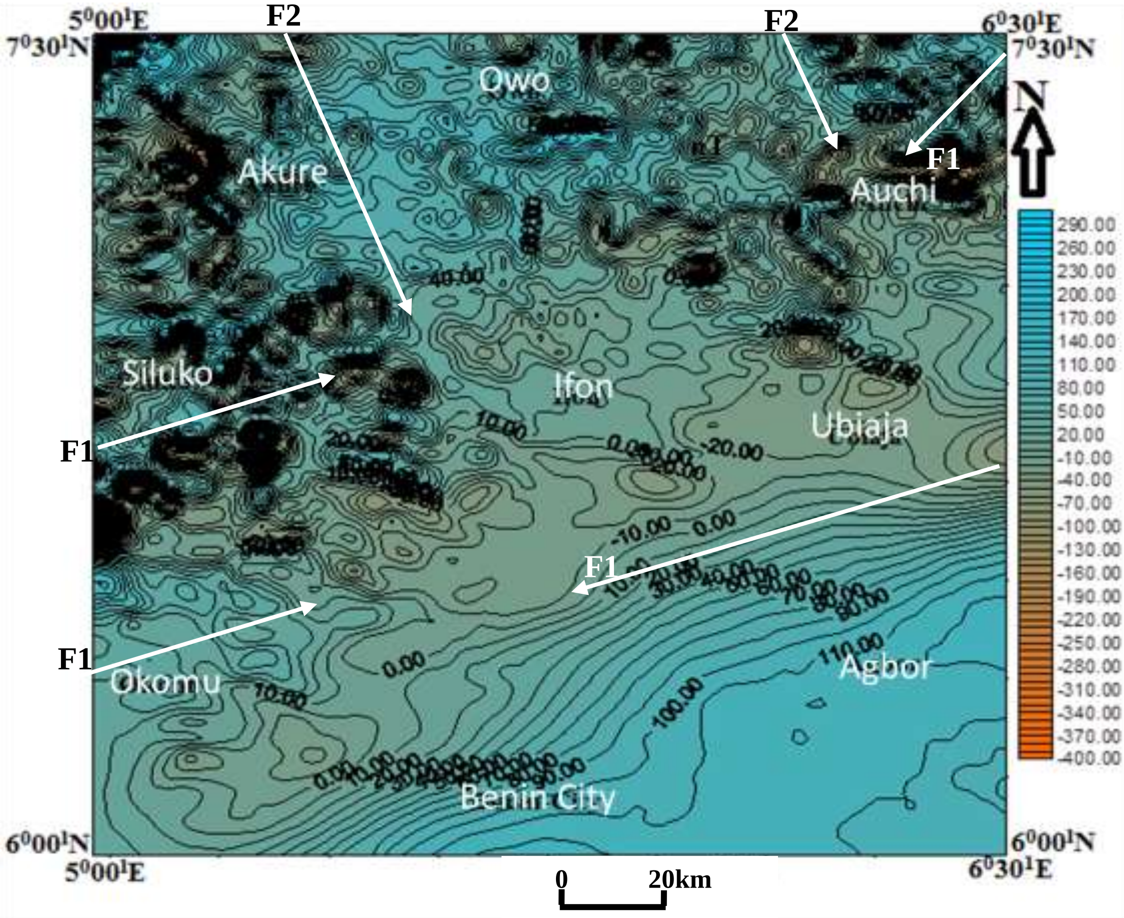

Fig. 4.2: Residual map of the study area (contour interval of 10nT) showing fault/fracture zones F_1 and F_2

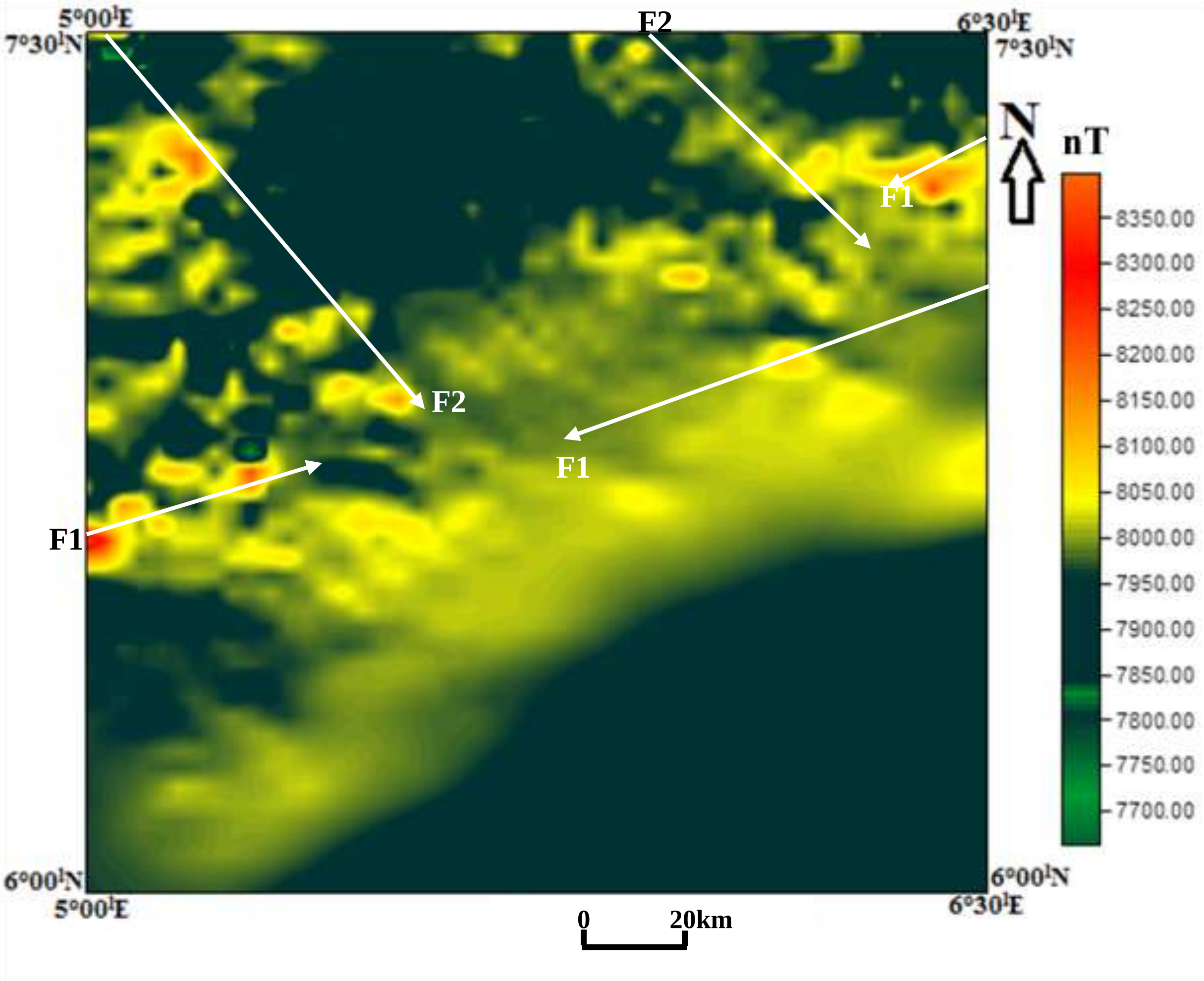

Fig. 4.3: Upward continuation of residual anomaly showing the northern boundary of the Niger Delta Basin and scattered intrusives within the Basement Complex

According to Chinwuko *et al.*, (2012), there would always be a magnetic susceptibility contrast across a fracture zone due to oxidation of magnetite to hematite and or infilling of fracture planes by dyke-like bodies whose magnetic susceptibilities are different from those of their host rocks. Such geologic features may appear as thin elliptical closures or nosing on an aeromagnetic map. The elliptical contour closures seen in the study area suggest the presence of magnetic bodies.

Again, visual inspection of the aeromagnetic map over the study area indicates that the contour lines are widely spaced in the southern and southeastern part which shows thicker sediments. This shows that the depth to the basement is higher in the southern and southeastern parts compared to closely spaced contours in the north eastern and north western parts which suggest shallow sedimentary thickness. In addition, the residual anomaly map shows positive magnetic anomaly and larger sedimentary thickness indicating deeper depths at the southern parts of the study area, while the northern and central portions of the study area show negative magnetic anomaly with smaller sediment thickness which indicates shallow depths.

In the northwestern part of the study area, (Akure-Siluko), there is a dome shaped linear feature. This linear feature is of intermediate depth and seems to be hosted in the basement structure. This feature is thought to be a major divide (fault or fracture) which is making a boundary. In general, there is an indication of a ridge around Akure-Siluko region with a depression/graben around Owo-Ifon region separating the north western flank from the northeastern flank (Auchi-Ubiaja). The fact that this structure is close to the major River, River Osse makes it desirable for further study. The depression/graben conforms to the river Owena, Ofosu, Osse etc. there is a strong influence of lateral variations and contrast in magnetic properties of the shallow sedimentary covers, which are as a result of some combination of faulting, deposition and possibly mineralization associated with structural displacements.

In a nutshell, the aeromagnetic map shows two major areas of differing magnetic pattern. The first is the area of magnetic high extending northwest of Akure and down towards Siluko. Another area of high magnetism is the Owo and northern flank of Auchi. These areas are associated with the intrusive masses or volcanic domes and the geothermal area. The second area is an area of relatively smooth magnetic pattern associated with the Niger Delta Basin. The magnetic anomalies represent variations in the amount and susceptibility of magnetic minerals (mainly magnetite) and the intensity of their remnant magnetization (Griscom and Muffler, 1971).

4.1.1 Area of Magnetic High

The area of magnetic high consists of magnetic anomalies that differ in order of magnitude ridge extending northwest ward and southwest ward from Akure area. This area consists of elliptical anomalies associated with volcanic domes. These anomalies are presumably caused by concealed volcanic dunes or intrusive masses that are close to the surface. These volcanic dunes area shows that the intensity of the earth's magnetic field is at ground level and this indicates that many masses of igneous rocks may be concealed at shallow depths beneath the surface.

4.1.2 Area of Smooth Magnetic Field

On the southwestern and southeastern border of the study area, the depth to the basement increases greatly and the magnetic field becomes smooth. In the area of relatively smooth magnetic pattern, the magnetic rocks are so far below the surface and the local magnetic anomalies are greatly attenuated and smoothened out. It should be noted that the magnetic low on the Southern part of the study area is caused by the same magnetic body that causes the high, only that the magnetic rocks are far below the surface.

It is noteworthy to state that there is a major fault in the southwestern border of the study area (Fig. 4.1a, 4.1b, 4.2 and 4.3). The boundary here is of much structural and geothermal interest in that it is a fault that extends from the northwestern flank of the study area towards the

Niger Delta region and may provide channels for recharge of meteoric water to the geothermal system. Much of Earth's geologic activity such as earthquakes, volcanism, moving plates and the origin of mountains, is caused by internal heat. In fact the slow release of heat from Earth's interior is one major factor that makes it such a dynamic earth. So, the aeromagnetic map shows that this boundary is a major fault and indicates that it was due to downwarping along the northwestern boundary, caused as a result of geothermal energy originating from the northwestern flank of the study area.

Generally, the elliptical anomalies are probably due to clusters of small igneous intrusions associated with dike that extends into the overlying sedimentary rocks. The elliptical anomaly to the northwest indicates a possible source of geothermal energy. Based on the six selected profiles (Fig. 4.4 and 4.5a – f) which were used for detailed interpretation, depth of the shallowest and deepest magnetic sources were obtained based on spectral analysis and presented in Tables 4.1 and 4.2. The depth to the centroid obtained ranges from 3.99 to 14.09km while the depth to the top of the magnetic bodies ranges from 0.79 to 4.81km. According to Offor and Udensi (2014), the centroid depth is the depth that relates to the point where magnetism is lost in the crust. The regional distribution of the thickness of the magnetized crust is illustrated in Figs. 4.8 and 4.10. The result shows that the area is underlain by Curie depth as shallow as 7.19km around Akure area (northwestern part) while a Curie depth of about 21.31km can be found in the southeastern part of the study area.

Also, using Curie-point temperature of 580^0C and calculated Curie-point depths, the geothermal gradient variations of the study area were obtained using equation 2.11 (Table 4.2 and Fig. 4.13). The values of geothermal gradients and thermal conductivity of 2.5 W/m^0C (Nwankwo *et al.*, 2009) were subsequently used to estimate the corresponding heat flow anomalies in the study area (Table 4.2 and Fig. 4.15).

From the results obtained the geothermal gradient and the associated mantle heat flow range from 22.53 to 76.91^0C/km and from 56.33 to 192.28mW/m^2 respectively. There is a general increase in the geothermal gradient of about 76.91^0C/km towards Akure (northwestern) part of the study area and this provides a source of geothermal energy. The result of the analysis on the six selected profiles (Fig. 4.4) are presented for discussion.

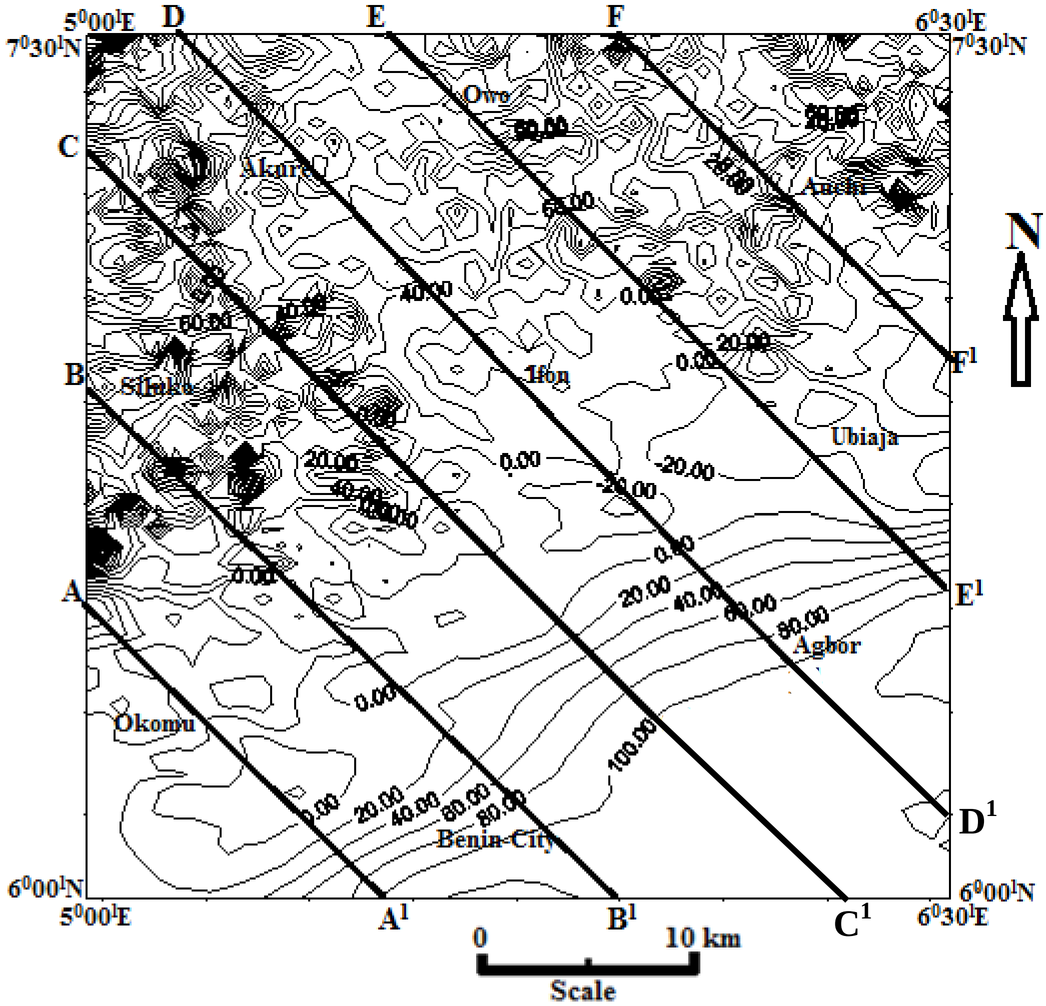

Fig. 4.4: Profiles along various anomalies within the residual map (contour interval of 20nT)

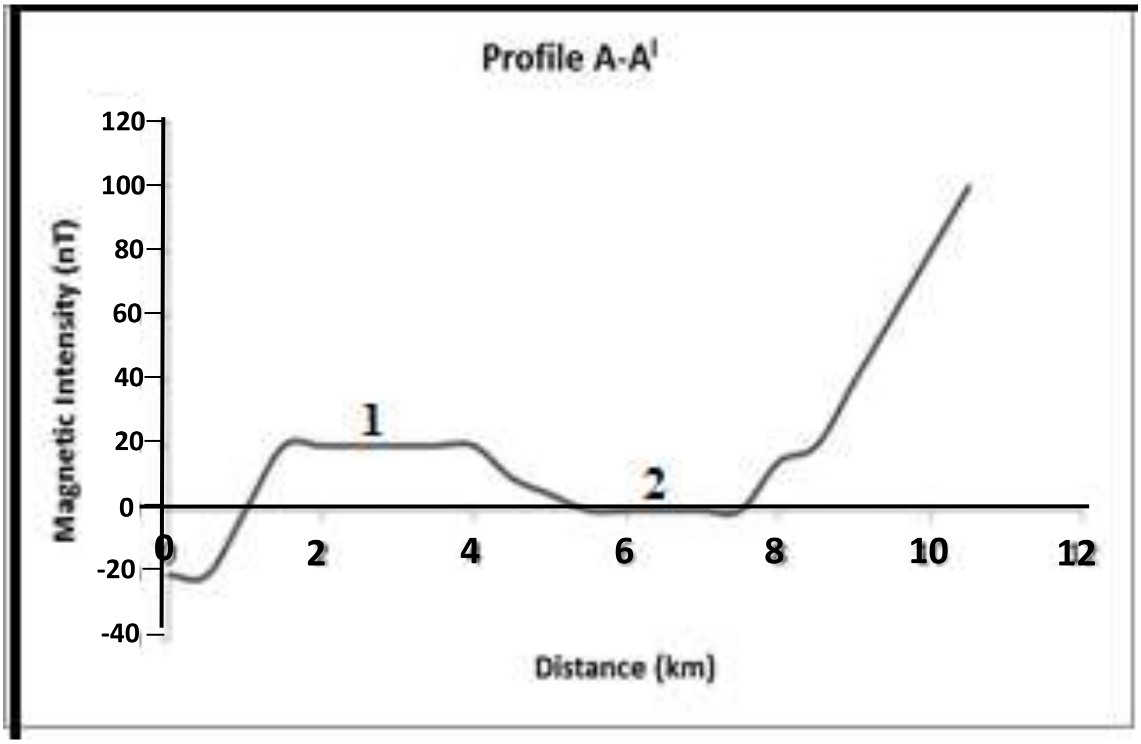

(a)

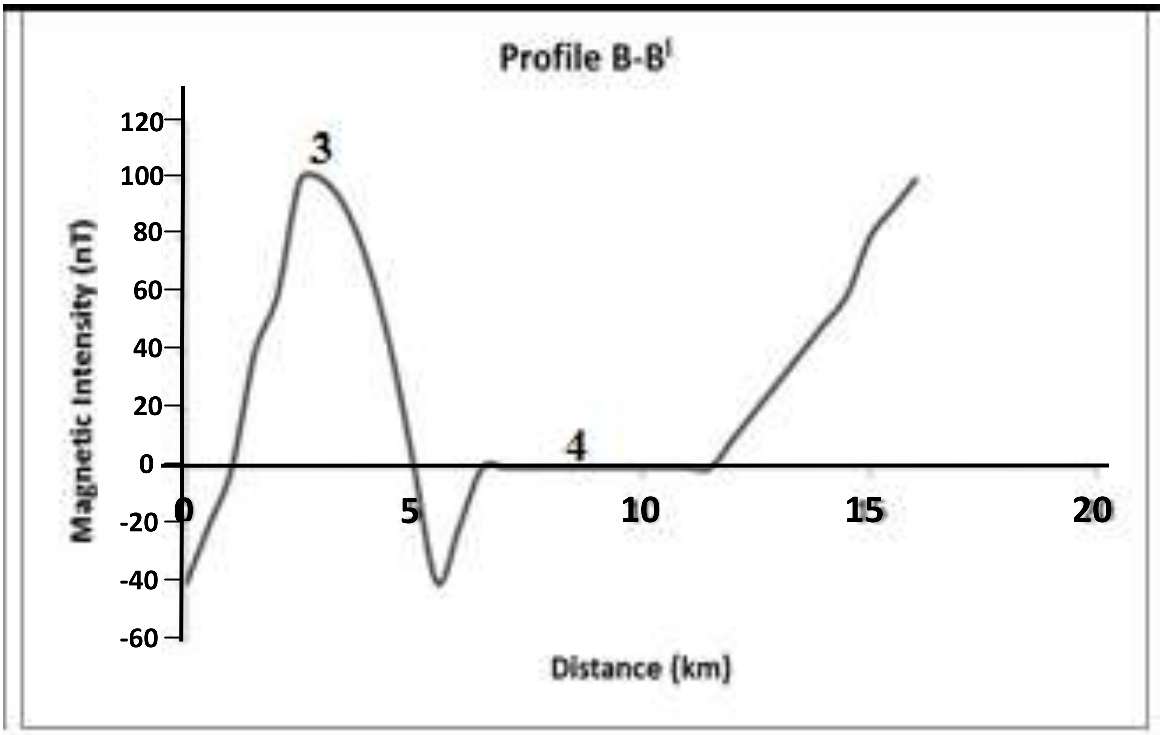

(b)

Fig. 4.5 (a) and (b): Profiles of sections A – A^1 and B – B^1

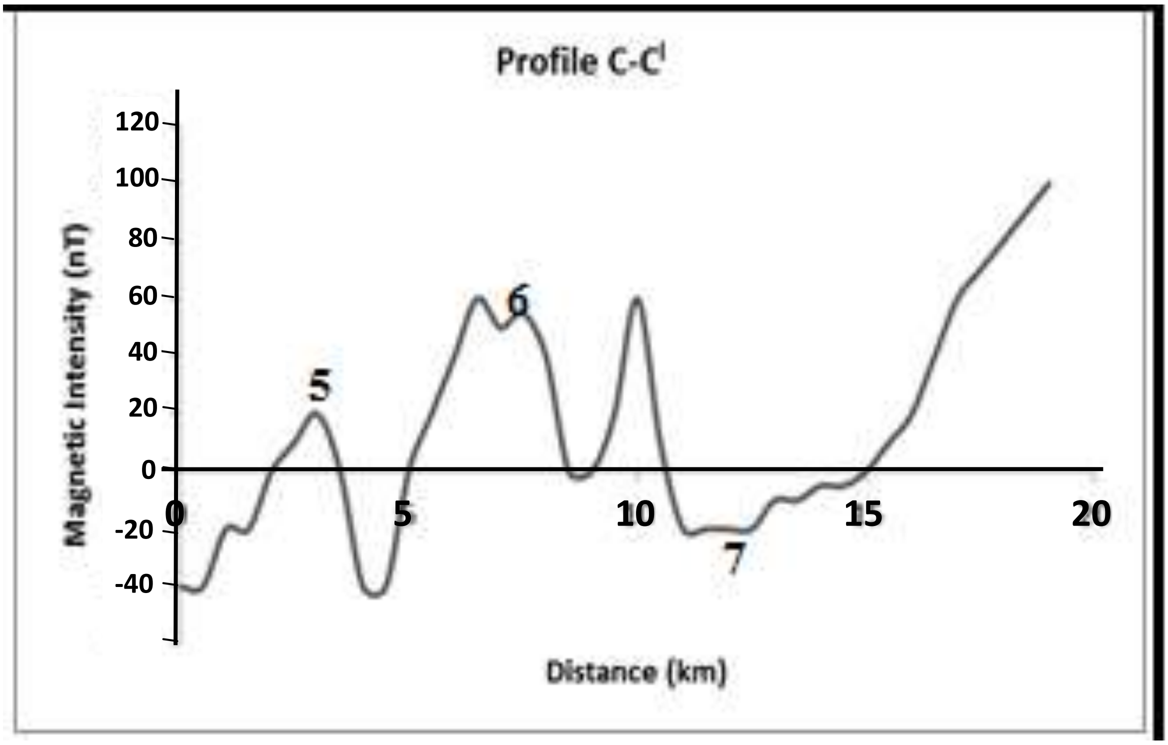

(c)

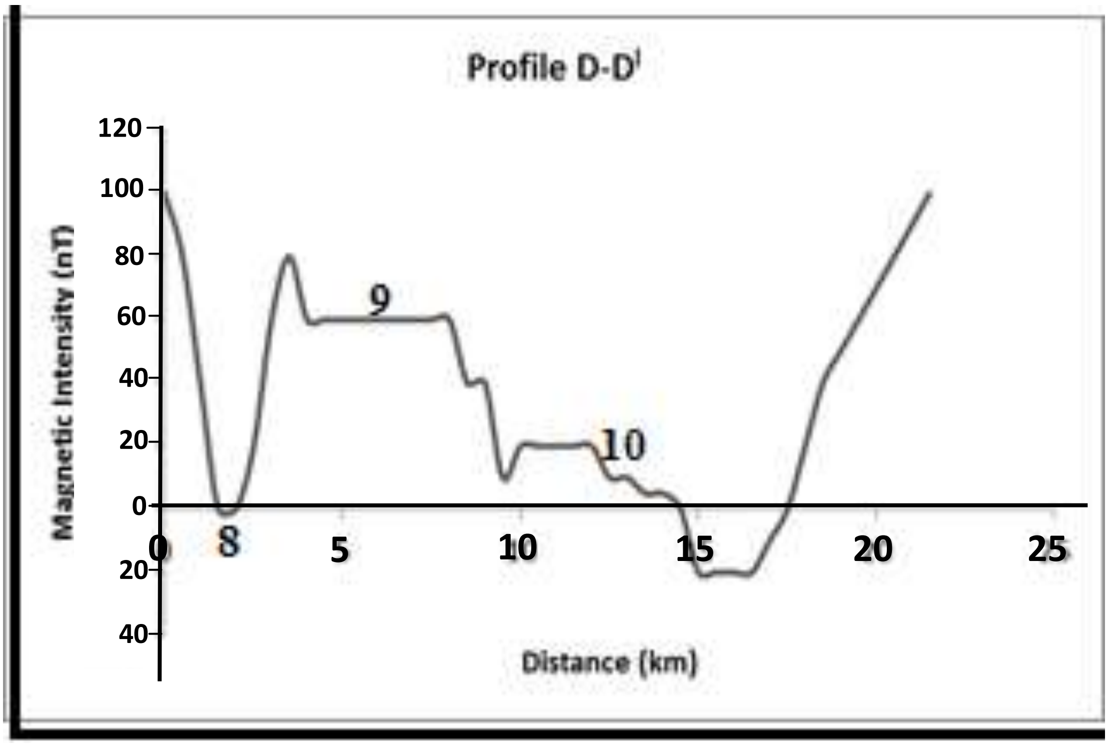

(d)

Fig. 4.5 (c) and (d): Profiles of sections C – C[1] and D – D[1]

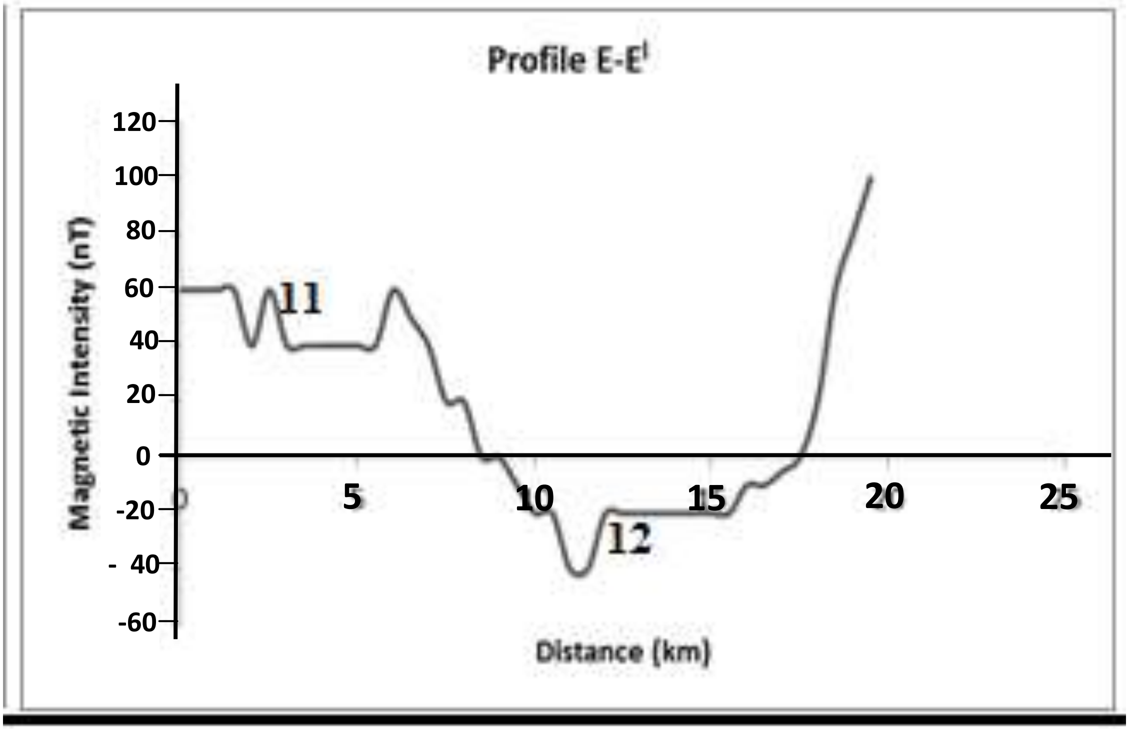

(e)

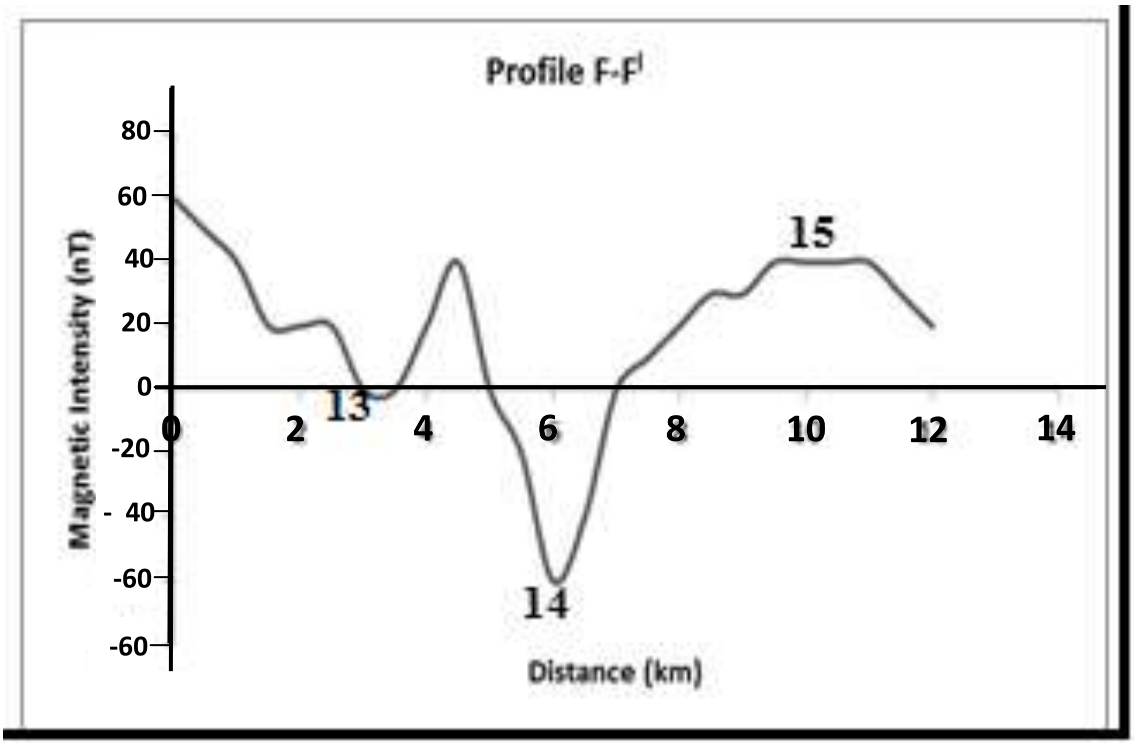

(f)

Fig. 4.5 (e) and (f): Profiles of sections E – E^{1} and F – F^{1}

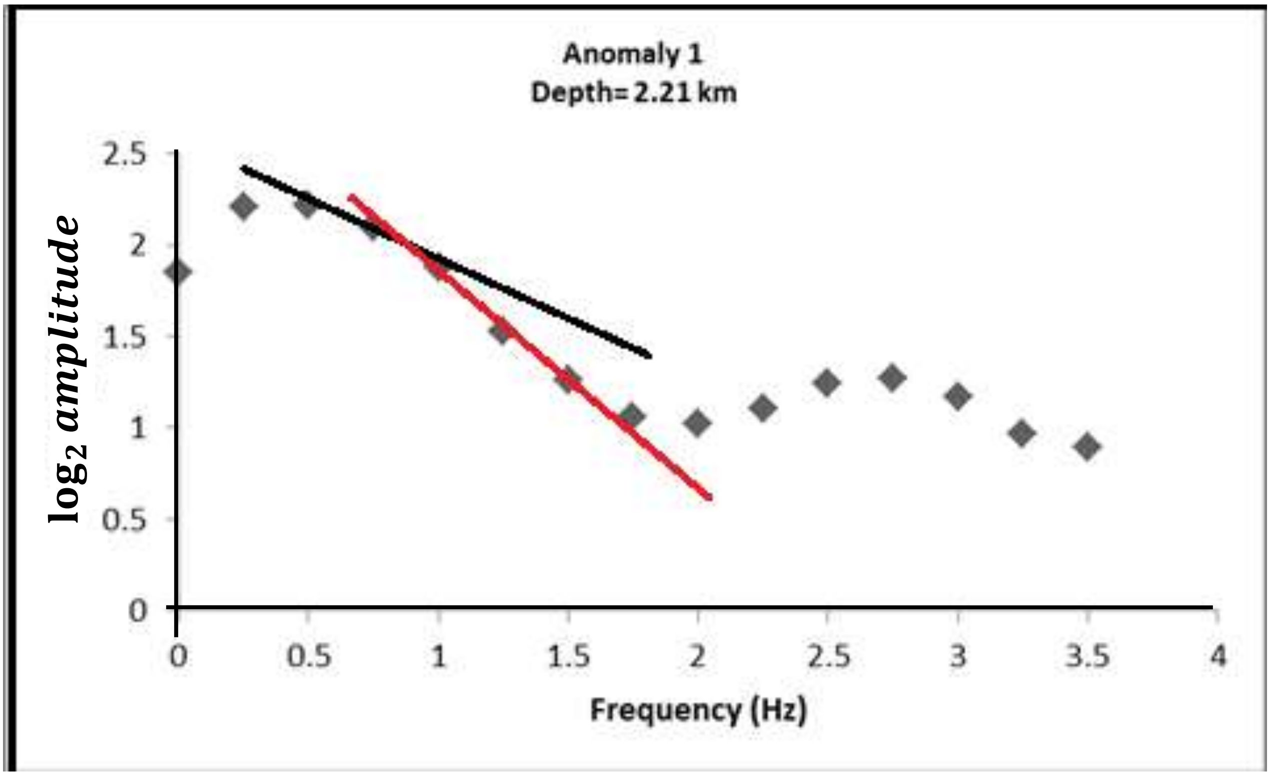

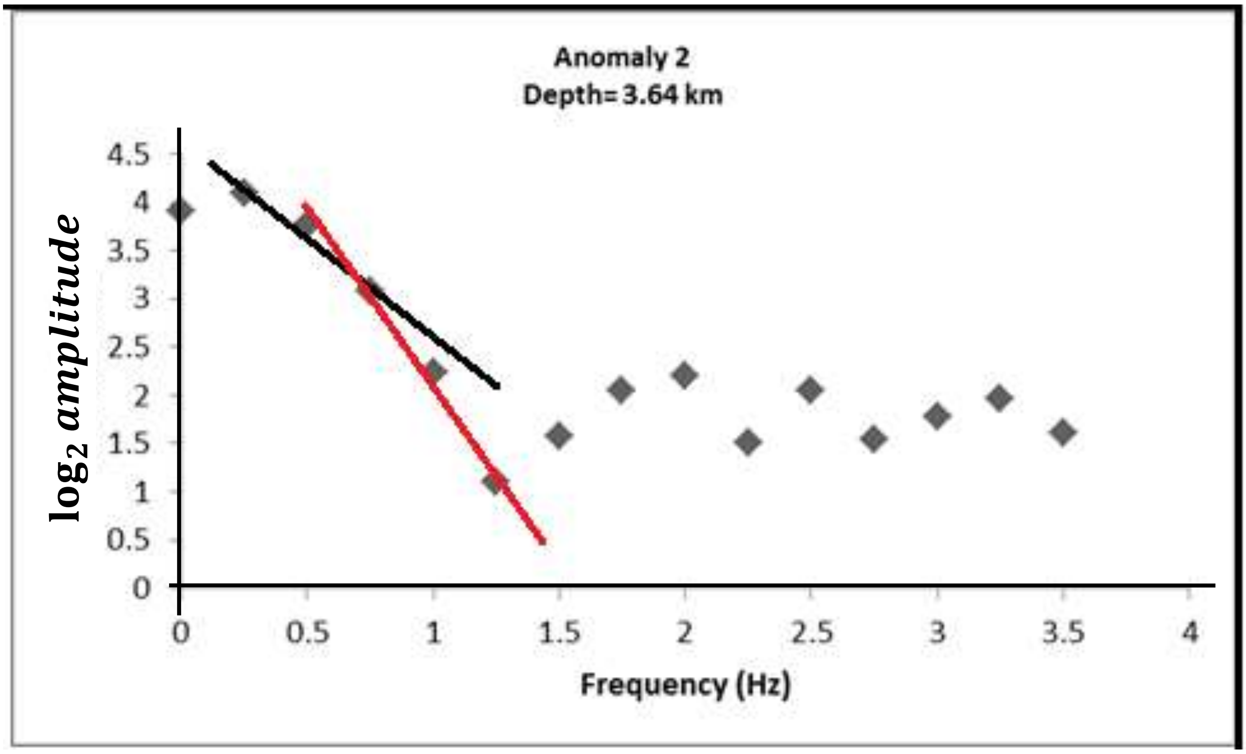

Fig. 4.6a: Amplitude spectra for profile A – A[1]

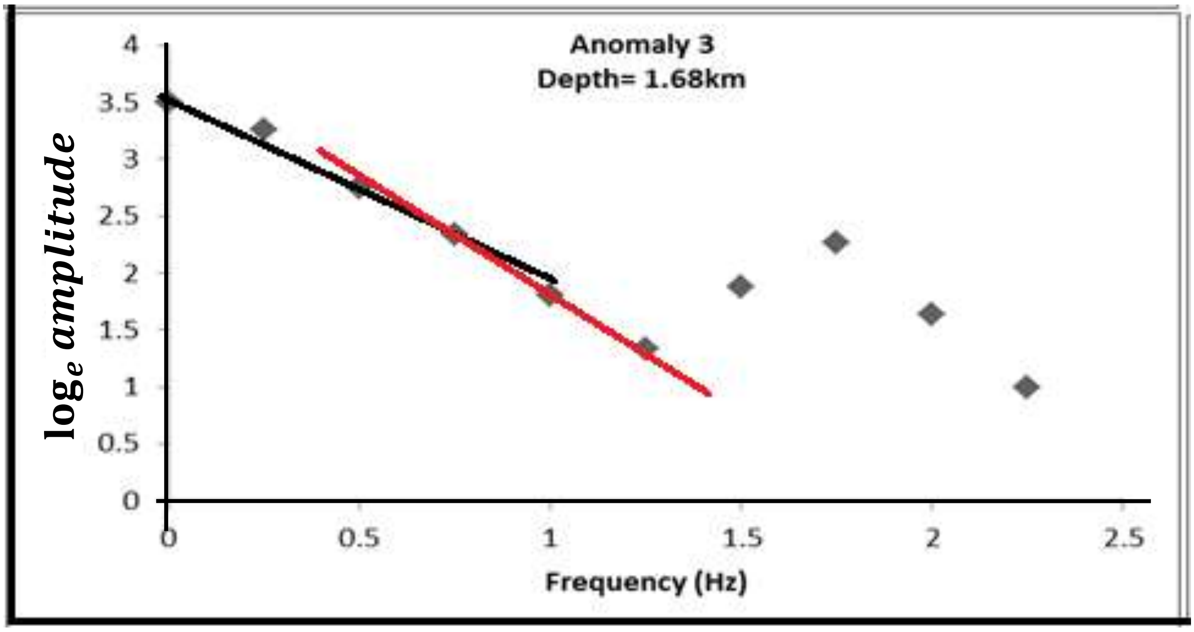

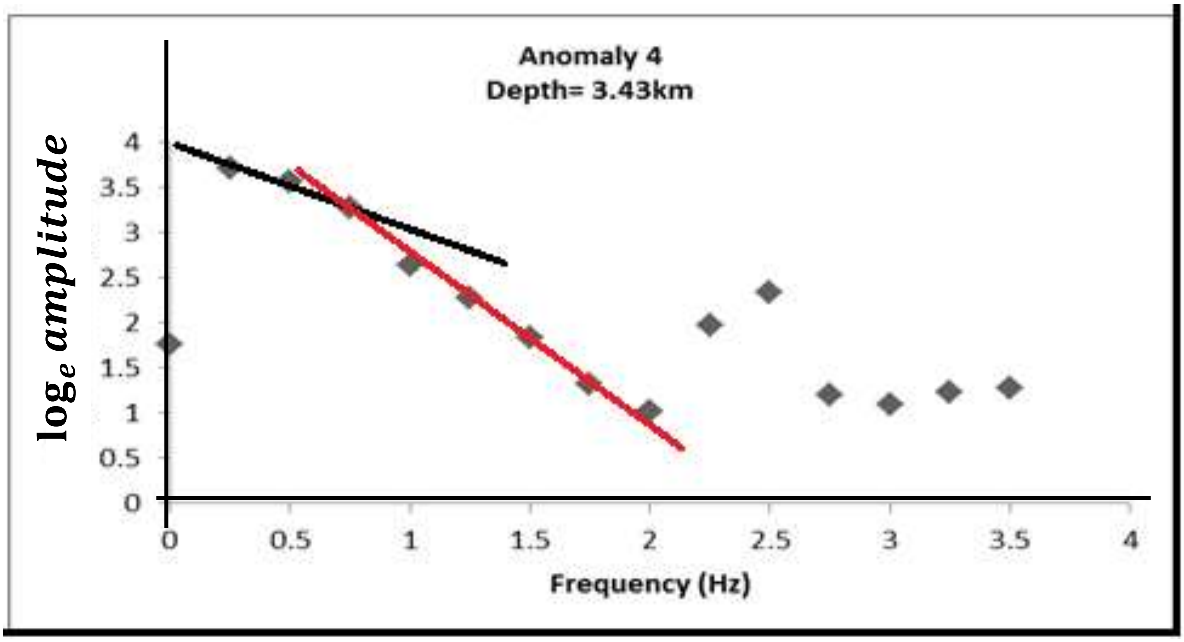

Fig. 4.6b: Amplitude spectra for profile B – B^1

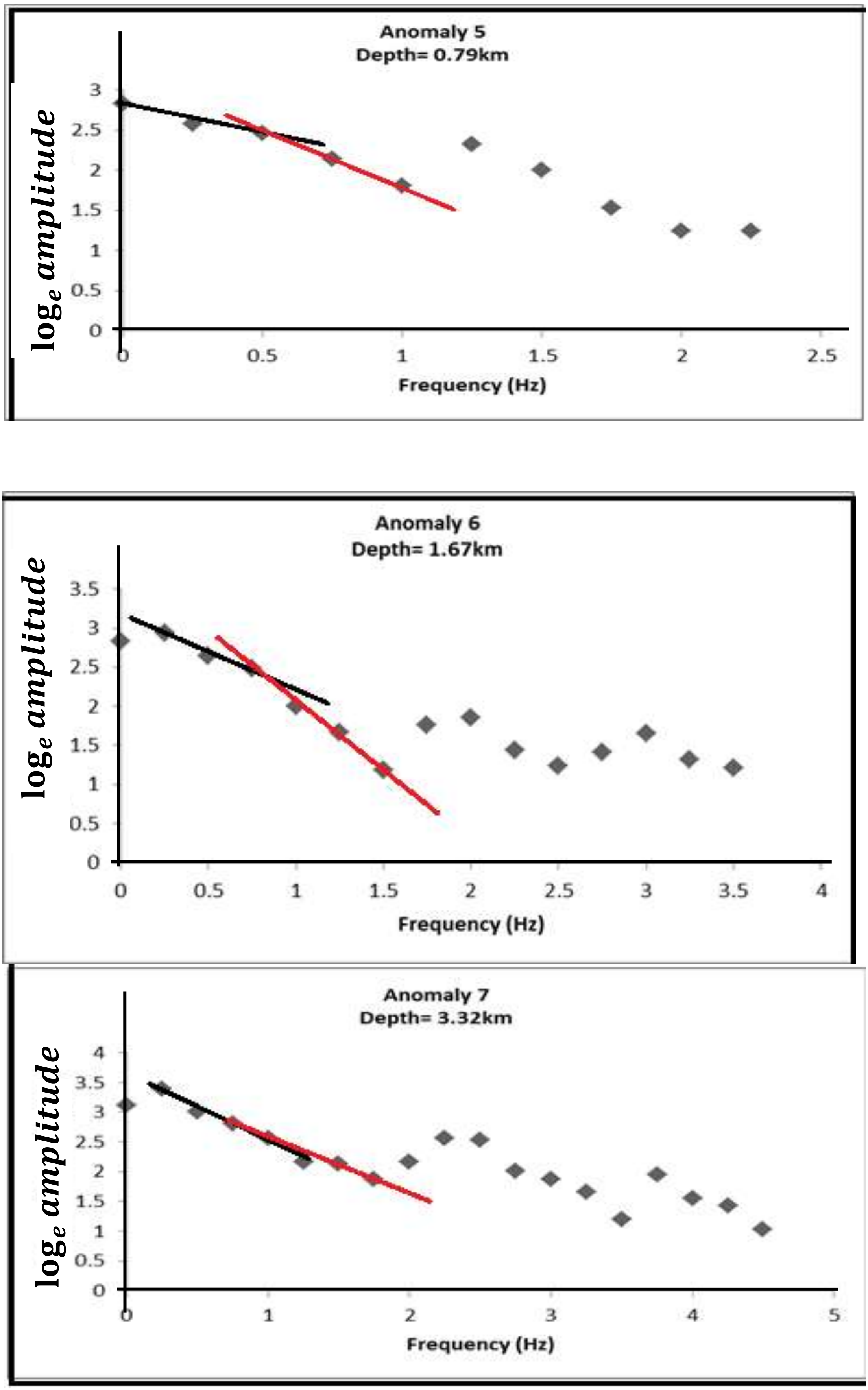

Fig. 4.6c: Amplitude Spectra for profile C – C[1]

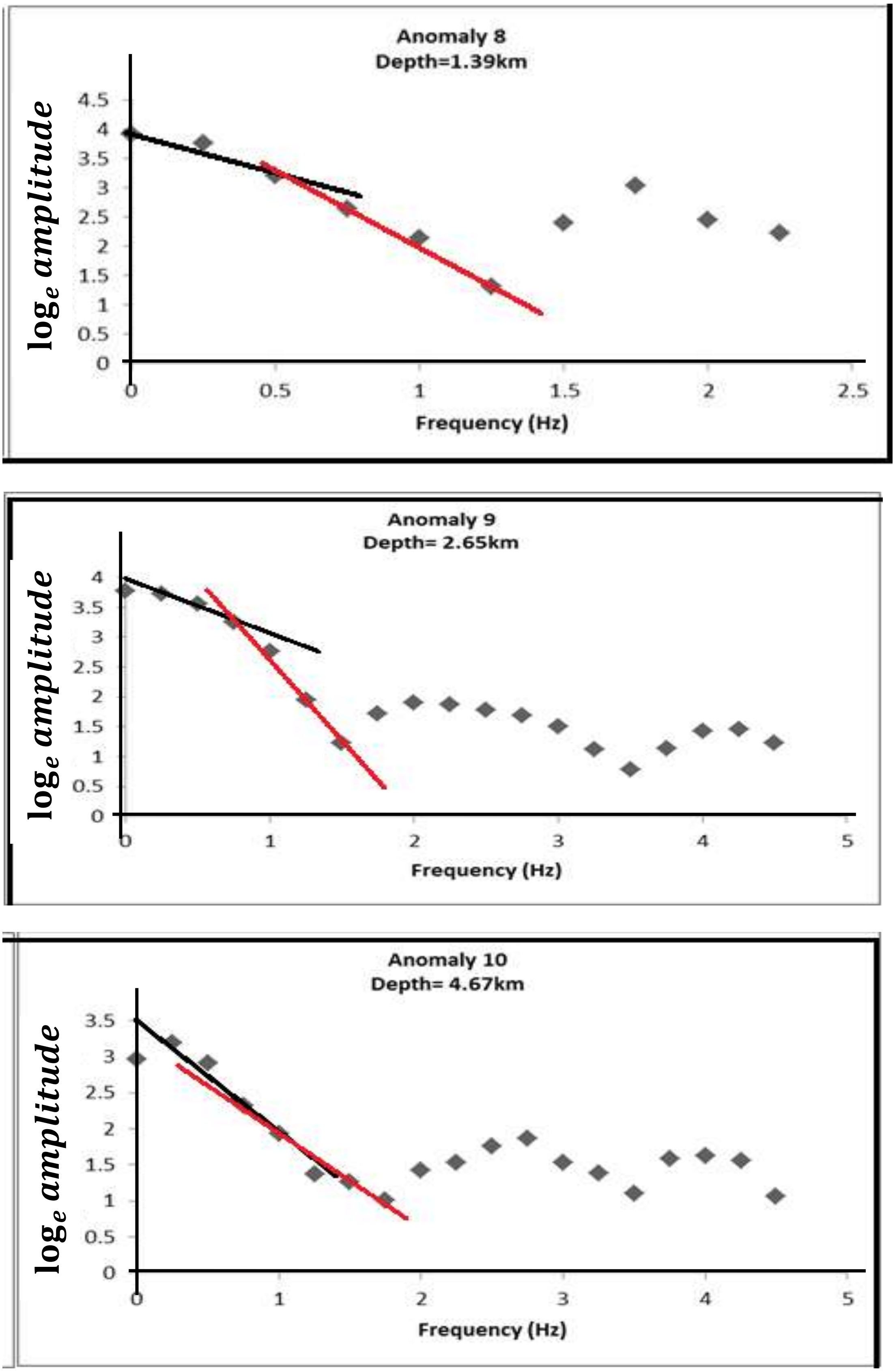

Fig.4.6d: Amplitude spectra for profile D – D[1]

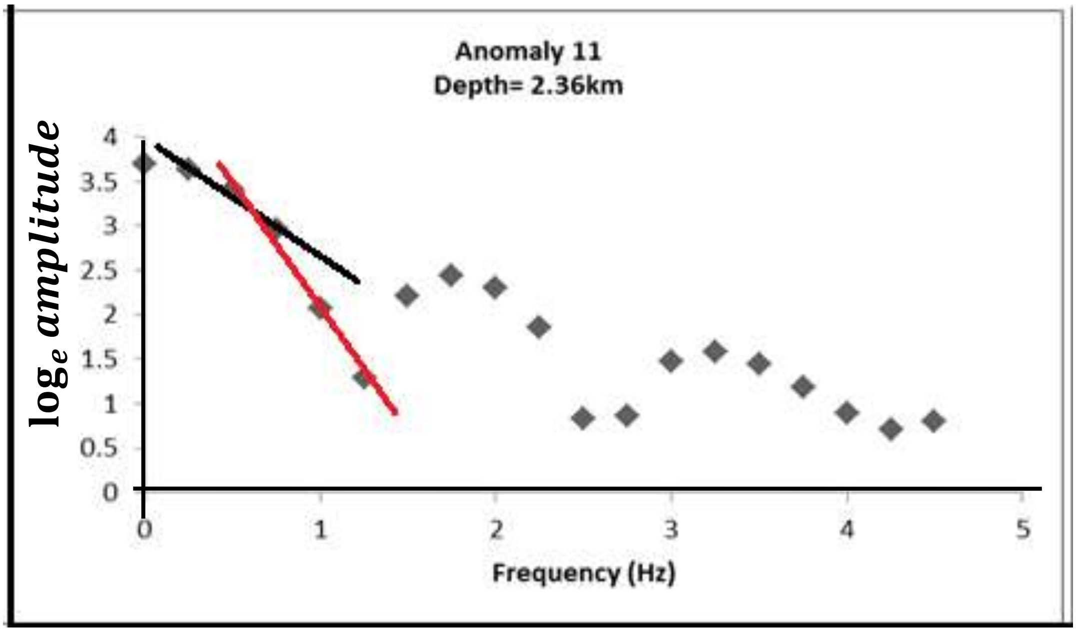

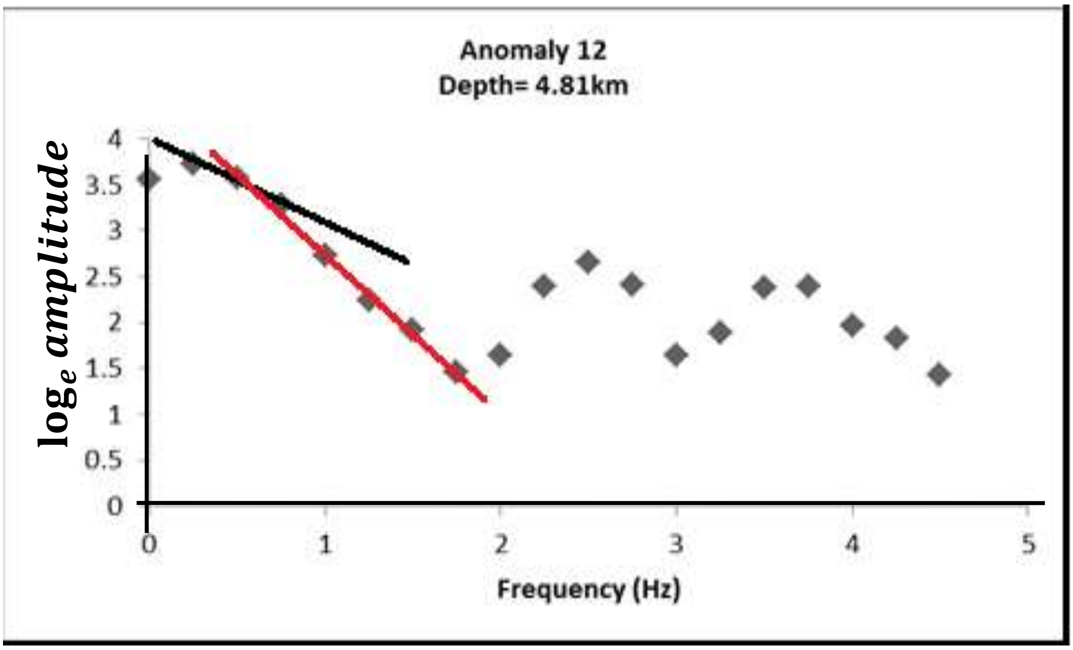

Fig. 4.6e: Amplitude spectra for profile E – E^1

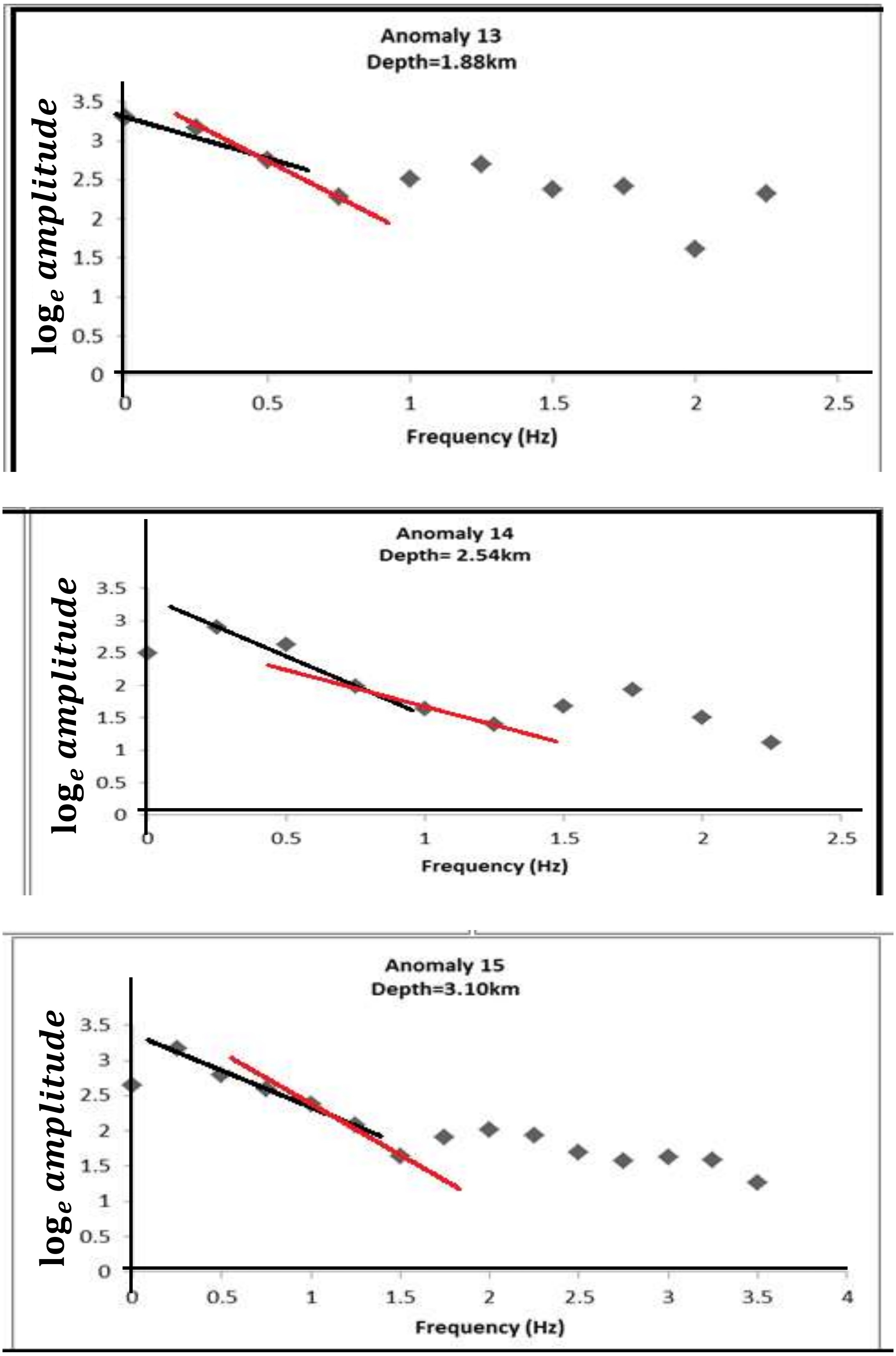

Fig.4.6f: Amplitude spectra for profile F – F[1]

Table 4.1: Basement depths obtained from spectral analysis of the study area

Profile name	Profile direction	Anomaly	Depth (km)
A-A^1	NW-SE	1	2.21
(Along Okomu)	NW-SE	2	3.64
B-B^1	NW-SE	3	1.64
(Along Siluko and Benin-City)	NW-SE	4	3.43
C-C^1	NW-SE	5	0.79
(Along Akure and Benin-City)	NW-SE	6	1.67
	NW-SE	7	3.32
D-D^1	NW-SE	8	1.39
(Along Akure and Agbor)	NW-SE	9	2.65
	NW-SE	10	4.67
E-E^1	NW-SE	11	2.36
(Along Owo and Ubiaja)	NW-SW	12	4.81
F-F^1	NW-SE	13	1.88
(Along Auchi)	NW-SE	14	2.54
	NW-SE	15	3.1

Table 4.2: Depths to the Curie isotherm and corresponding geothermal gradient with surface heat flow, based on spectral analysis of aeromagnetic data

Anomaly No.	**Depth to the Top (km)**	**Depth to the Centroid (km)**	**Curie Point Depth (km)**	**Geothermal gradient (^{o}C/km**	**Heat Flow (mW/m^2)**
1	2.21	10.14	18.07	30.60	76.50
2	3.64	14.09	24.55	22.53	56.33
3	1.64	6.38	11.12	49.73	124.33
4	3.43	12.11	20.79	26.60	66.50
5	0.79	3.99	7.19	76.91	192.28
6	1.67	5.20	8.73	63.34	158.36
7	3.32	5.90	8.48	65.21	163.02
8	1.39	5.70	10.01	55.24	138.11
9	2.65	9.64	16.63	33.25	83.13
10	4.67	13.47	22.27	24.83	62.07
11	2.36	7.97	13.58	40.72	101.80
12	4.81	13.06	21.31	25.95	64.88
13	1.88	8.47	15.06	36.72	91.80
14	2.54	9.61	16.68	33.15	82.88
15	3.10	11.11	19.12	28.92	72.30
Average	2.67	9.13	15.57	40.91	102.29

4.2 Profiles

4.2.1 Profile A-A^1

This profile runs in the direction of NW-SE in the south-western part of the study area. It cuts parts of sheet 297 (Okomu). The maximum magnetic intensity value along their profile is 100nT and the minimum is -20nT. The broad parts of the curve which is anomaly 1 and 2 indicate deep magnetic sources: the estimated depth to the top and the depth to centroid along this profile range from 2.21 km to 3.64 km and 10.14 km to 14.09 km respectively. The estimated Curie point depth and the associated geothermal gradients and heat flow values along this profile range from 18.07 km to 24.55 km, 30.60 ^{0}C/km to 22.53 ^{0}C/km and 76.50 mW/m^2 to 56.33mW/m^2 respectively.

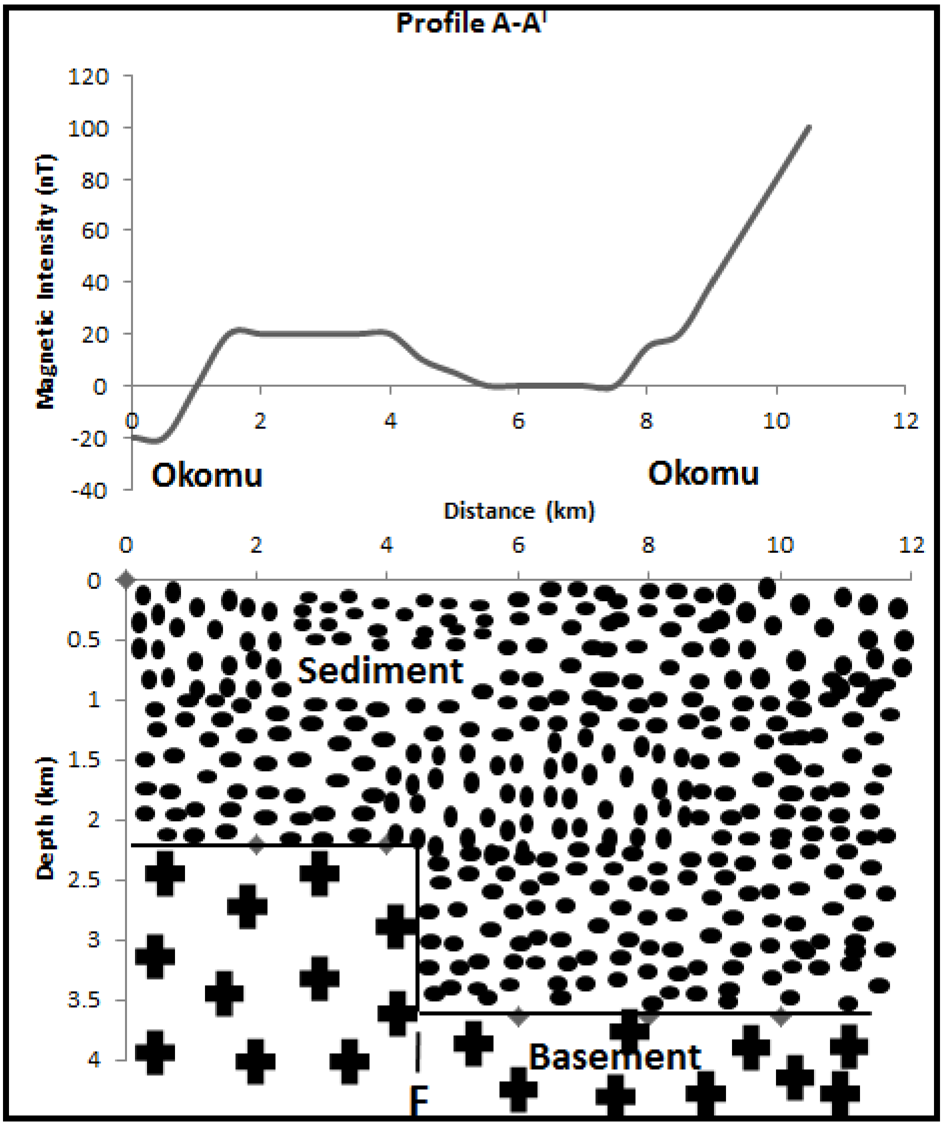

Fig. 4.7a. Geologic modeling of anomalies along profile A-A[1]

4.2.2 Profile B-B^1

This profile passes through the southern part in the direction of NW-SE direction of the study area. The maximum magnetic intensity value along this profile is 100nT and the minimum is -40nT. It cuts parts of Siluko (sheet 283) and Benin-city (sheet 298). The depth estimated to top and depth to the centroid on observed anomalies 3 and 4 ranges from 1.64 km to 3.43km and 6.38km to 12.11km respectively. The estimated Curie point depth and associated geothermal gradients and heat flow values along this profile ranges from 11.12km to 20.79km, 49.73^{0}C/km to 26.60^{0}C/km and 124.33^{0}C/km to 66.50^{0}C/km respectively.

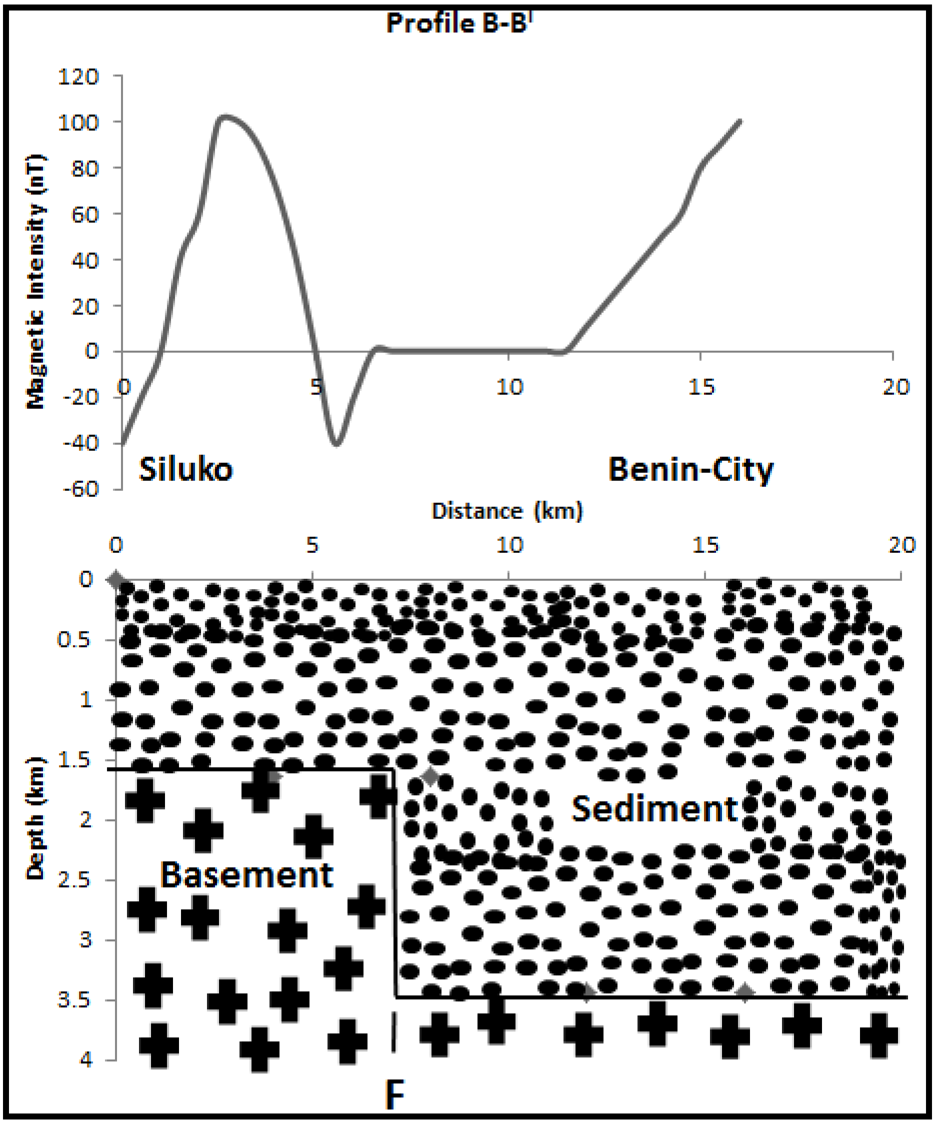

Fig 4.7b: Geologic modeling of anomalies along profile B-B[1]

4.2.3 Profile C-C^1

This profile runs in the direction of NW-SW and cuts across Akure (sheet 264) and western, central and south eastern part of the study area. The maximum magnetic intensity value is 60nT and the minimum is -40nT. The estimated depth to the top and depth to the centroid for anomalies 5, 6 and 7 are 0.79 km. 1.67 km, 3.32 km and 3.99 km, 5.20 and 5.90km respectively. The estimated Curie depths of anomalies along this profile are 7.19 km, 8.73km and 8.48 km; the associated geothermal gradients are 76.91^0C/km, 63.34^0C/km and 65.21^0C/km while the heat flow values are 192.28 mW/m^2, 158.36 mW/m^2 and 163.02 mW/m^2.

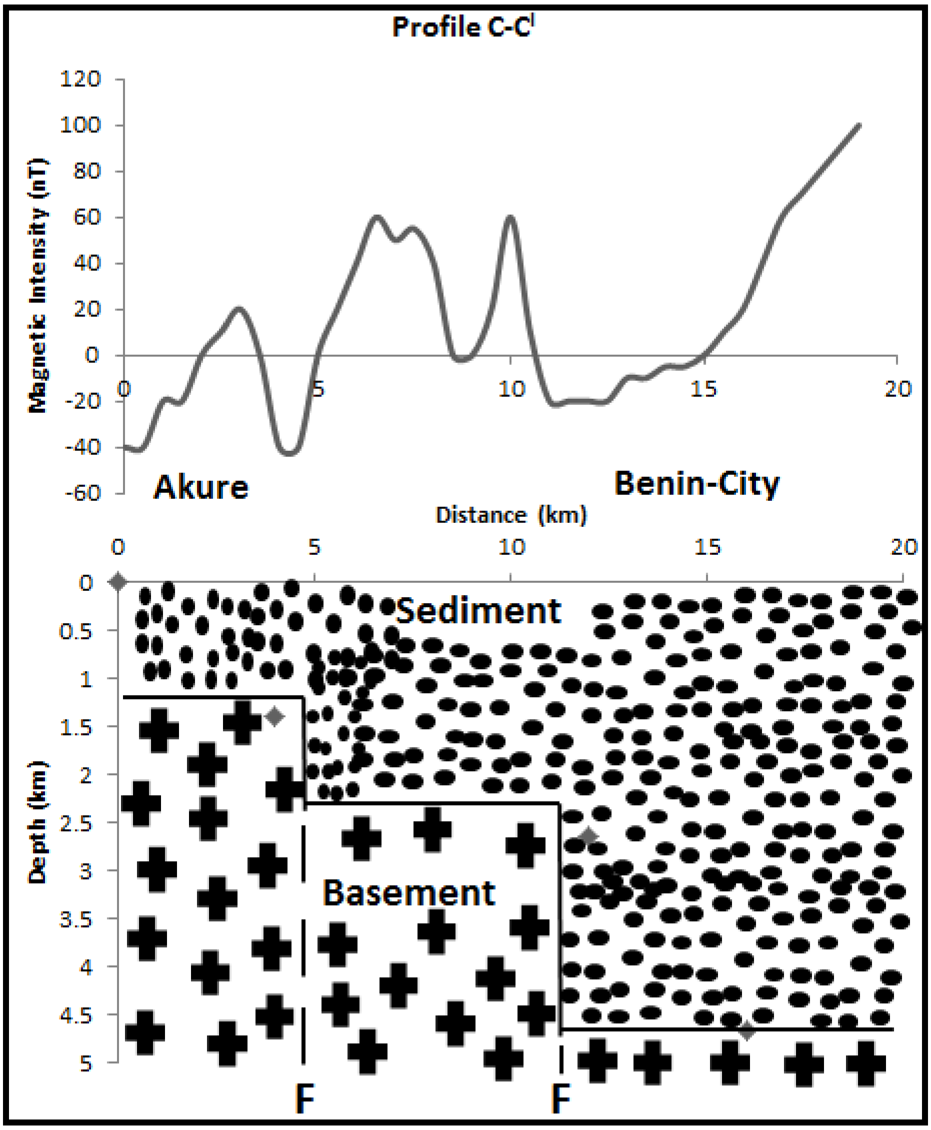

Fig. 14.7c: Geologic modeling of anomalies along profile C-C[1]

4.2.4 Profile D-D^1

This profile passes through Akure and Agbor (sheet 264 and sheet 299 respectively). The maximum magnetic intensity value along this profile is 100nT while the minimum is -20nT. The estimated depth to the top and depth to the centroid for anomalies 8, 9 and 10 are 1.39 km, 2.65, 4.67km and 5.70km, 9.64km and 13.4km respectively. The estimated Curie point depths of anomalies along this profile are 10.01 km, 16.63 km and 22.27 km, the associated geothermal gradients are 55.24^{0}C/km, 33.25^{0}C/km and 24.83^{0}C/km while the heat flow values are 138.11 mW/m^2, 83.13 mW/m^2 and 62.07 mW/m^2.

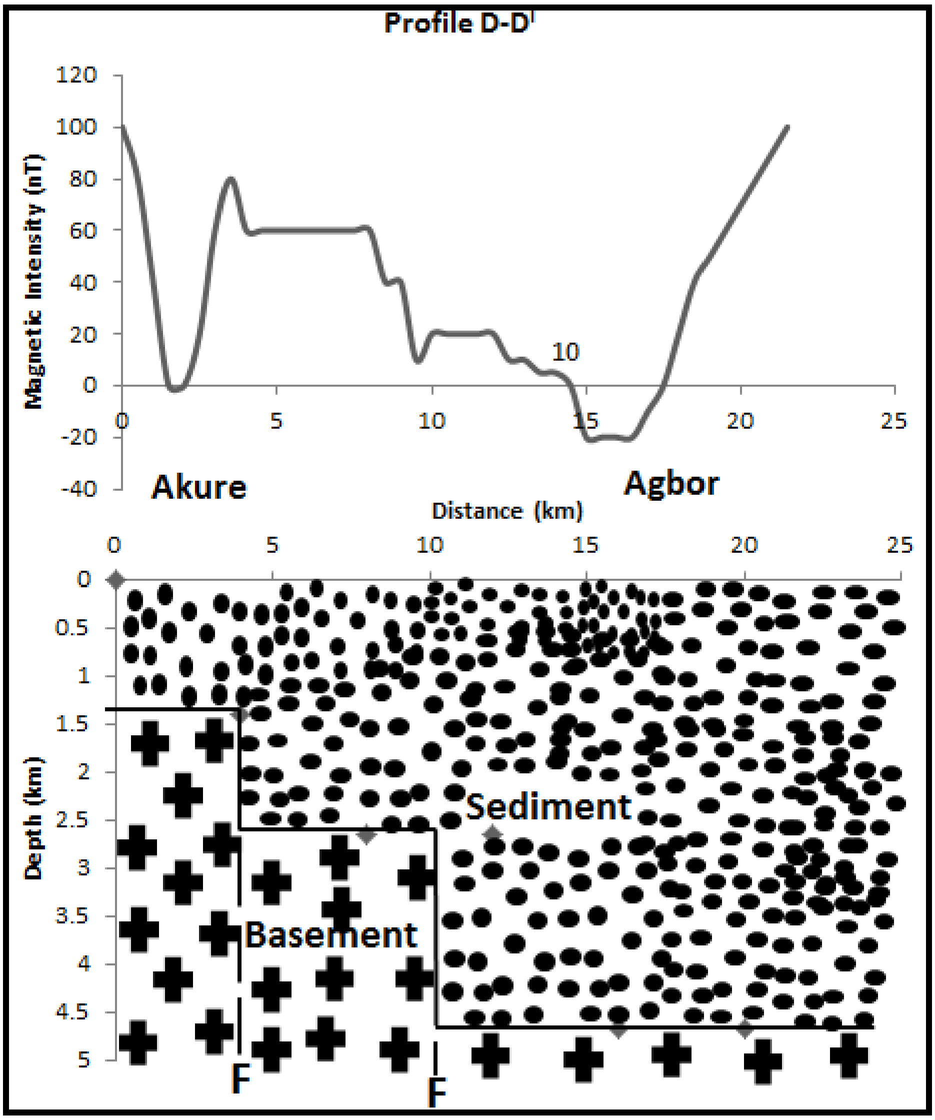

Fig. 4.7d: Geologic modeling of anomalies along profile D-D[1]

4.2.5 Profile E-E^1

This profile runs in the direction of NW-SE in the north-eastern part of the study area. It cuts through Owo and Ubiaja (sheets 265 and 285 respectively). The maximum magnetic intensity value along this profile is 100nT and the minimum is -40nT. The depth estimated to the top and the depth to the centroid along this profile range from 2.36 km to 4.81 km and 7.97 km to 13.06 km respectively. The estimated Curie point depths and the associated geothermal gradients and heat flow values along this profile range from 13.58 km to 21.31 km, 40.72 ^{0}C/km to 25.95 ^{0}C/km and 101.80 mW/m^2 to 64.88 mW/m^2 respectively.

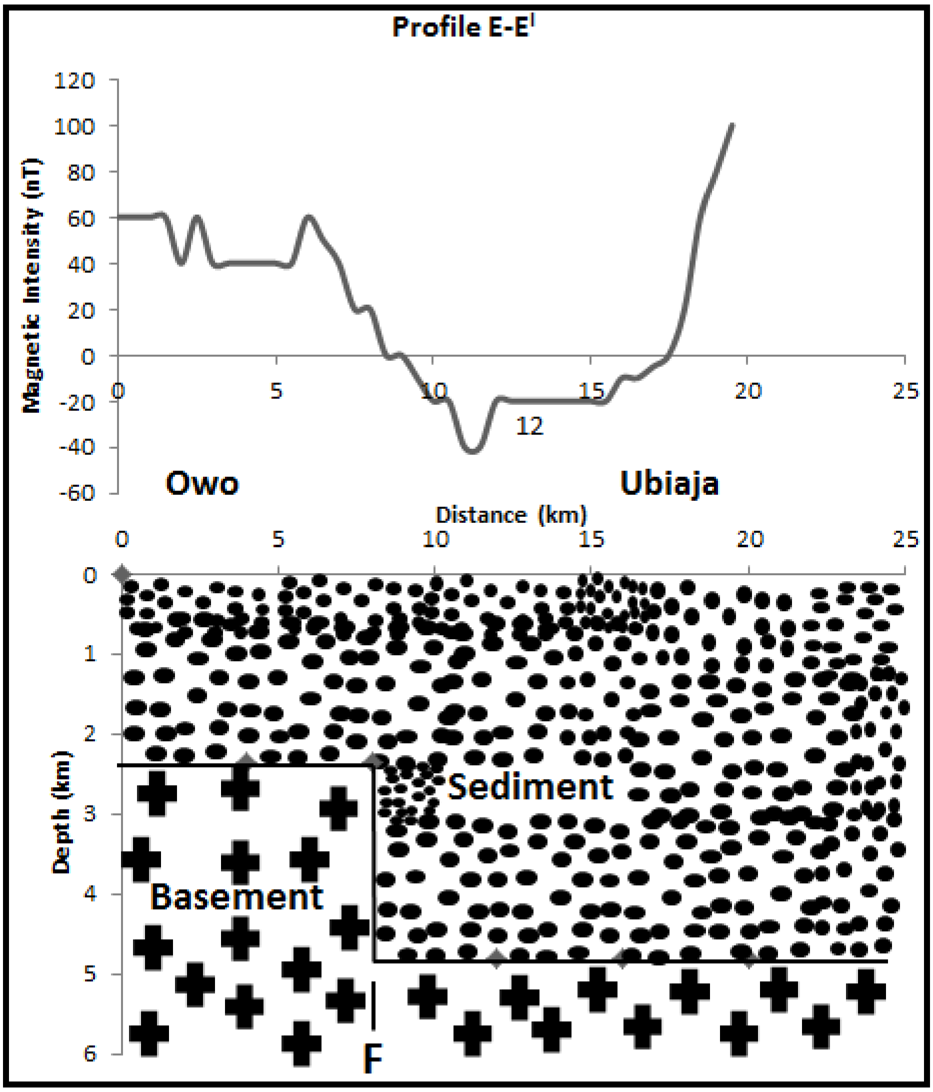

Fig. 4.7e: Geologic modeling of anomalies along profile E-E[1]

4.2.6 Profile F-F^1

This profile runs in the direction of NW-SE and cuts through Auchi (sheet 266) in the north-eastern part of the study area. The maximum magnetic intensity value along this profile is 45nT and the minimum is -60nT. The estimated depth to the top and the depth to the centroid for anomalies 13, 14 and 15 are 1.88 km, 2.54 km, 3.10 km and 8.47 km, 9.61 km and 11.11 km respectively. Also the estimated Curie point depth of anomalies along this profile are 15.06 km, 16.68 km and 19.12 km, the associated geothermal gradients are 36.72^{0}C/km, 33.15 ^{0}C/km and 28.92 ^{0}C/km, while the heat flow values are 91.80 mW/m^2, 82.88 mW/m^2 and 72.30 mW/m^2.

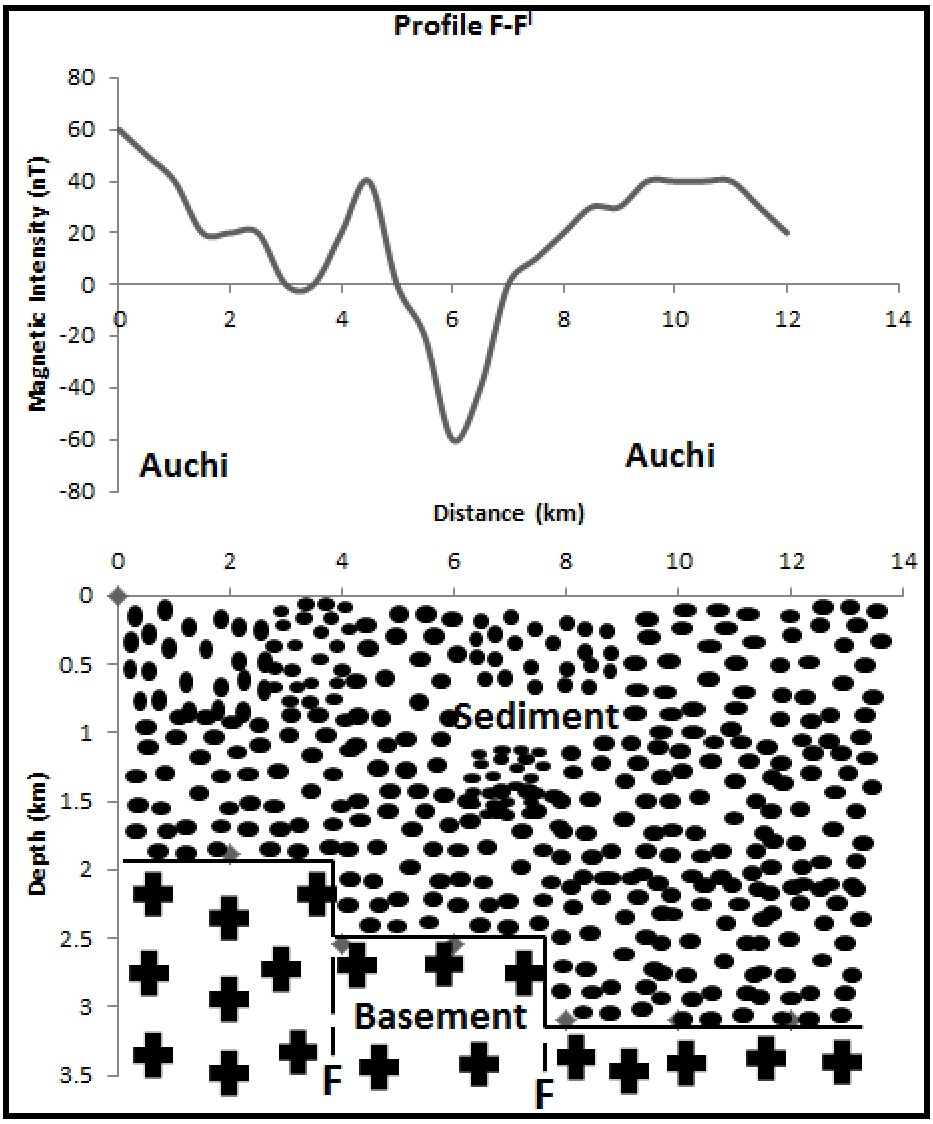

Fig. 4.7f: Geologic modeling of anomalies along profile F-F[1]

4.3 Discussion

4.3.1 Basement Topography

As a matter of quality assurance, investigation of the depth estimate in this study was carried out. From the depth values determined from the spectral analysis, two depths to magnetic sources were revealed; the deeper magnetic sources and the shallow magnetic sources. The shallow magnetic sources range from 0.79 km to 1.88 km, while the deeper magnetic sources range from 2.21 km to 4.81 km (Fig. 4.8 and 4.9).

The deeper magnetic sources may probably represent depths to Precambrian basement, while the shallower magnetic sources represent depths to basic intrusions and/or magnetized bodies within the sedimentary cover. The depth to basement is deeper in the southern and southeastern part of the study area and shallower in the northwestern and northeastern parts.

Consequently, the depth to basement map (Fig. 4.8) and 3D–surface map (Fig. 4.9) representing the topography of the study area were produced, based on the depth values obtained from spectral analysis. These give the basement configuration as well as the sedimentary thickness within the study area. The 3D – surface plot shows a linear depression/graben at the northwestern part of the study area, indicating thick sediments which trend northwest - southeast direction while the northwestern and northeastern parts have thin sedimentary thicknesses

(Fig. 4.9). This depression separates the two ridges in the northwestern and the northeastern part of the study area. This depression is in good agreement with the linear feature of intermediate to deeper depths caused by rifting that gave rise to the formation of River Osse, River Ofosu and River Ogbese.

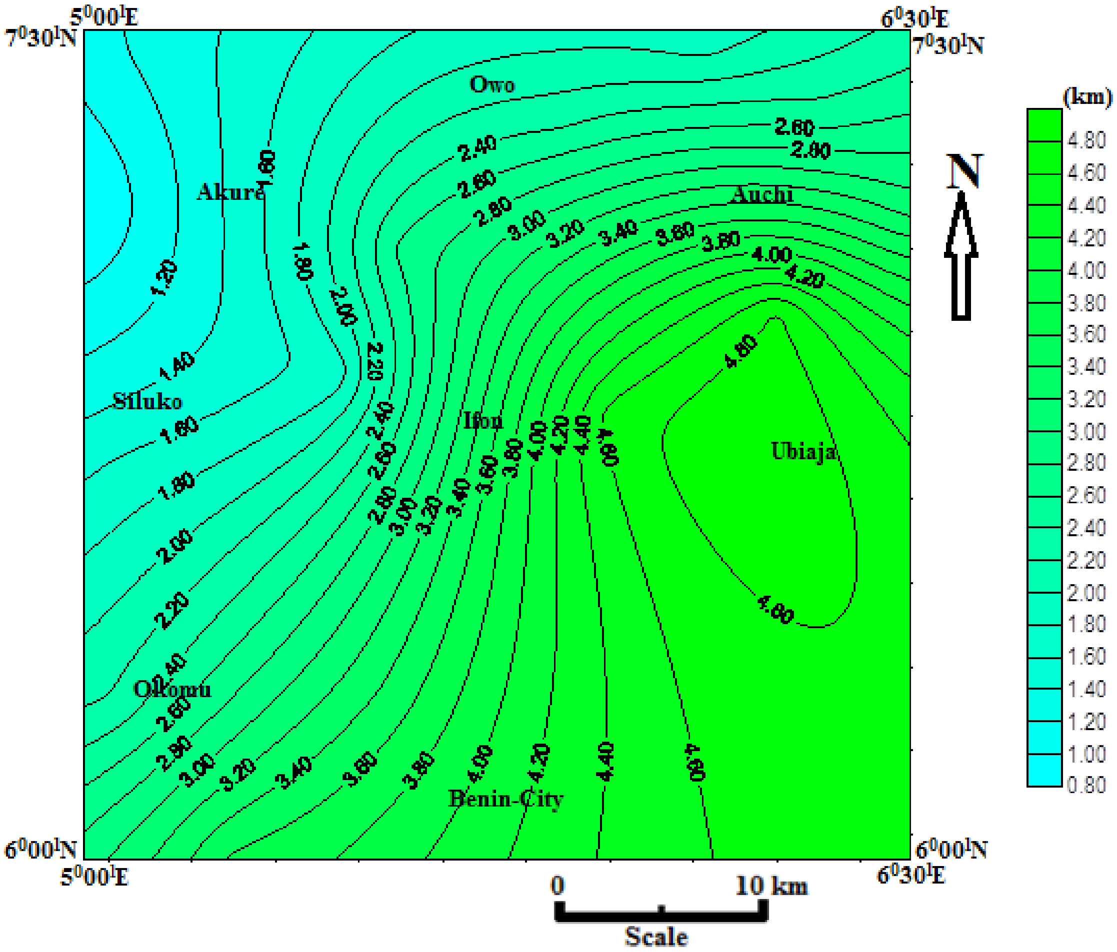

Fig. 4.8: Depth to basement within the study area (contour interval ≈ 0.2 km)

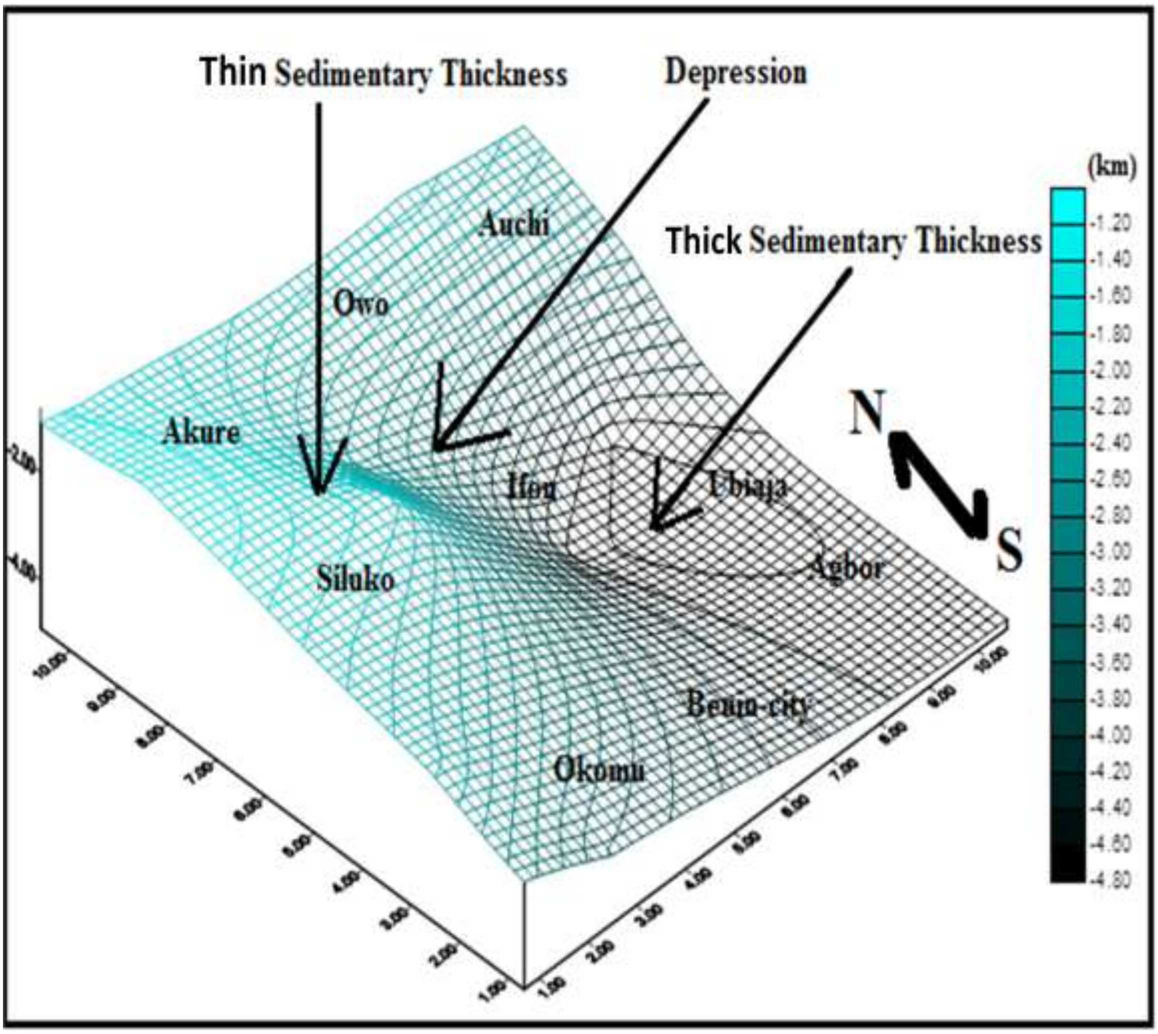

Fig. 4.9: 3D Surface plot for the basement topography of the study area

4.3.2 Curie-Point Depth Isotherm and their Associated Geothermal Gradient and Heat Flow

Figure 4.10 shows two Curie point depth regimes; shallow and deep Curie point depths. The shallow Curie point depths are located in the northwestern and northern parts of the study area. The deep Curie point depths are located in the southern and southeastern part of the study area. These two inferred thermally (shallow and deep Curie point depths) anomaly regions are separated by an intermediate anomaly region of NNE – SSW trending belt located at the central northeastern and southwestern region.

The results of the spectra analysis of aeromagnetic anomalies in the study area show Curie point depth minimum estimates range between 7.19km and maximum estimates of 24.55km (Table 4.2) with an average value of 15.57km. The observed/estimated results thus agree fairly well with Abraham *et al.*,(2014) where an average Curie point depth estimate of 15.1±0.6km was obtained over parts of Ikogosi warm spring (which is about 10km away from the northern part of my study area).

It should be noted that the earth acts as a heat engine and at the surface there is a continuous heat flux comprising the heat flow from the mantle and the lower crust supplemented by heat production from the radioactive isotopes which are largely concentrated in the upper crust.

A local thermal dome is believed to be present in the northern and northwestern part of the study area. While the southern part of the study area, is characterized by a cooler crust (Fig. 4.10 and 4.11). The study area also shows that the Curie temperature isotherm for the study area is undulating with an axial ridge configuration. The morphology shows a linear relationship with the topography of the basement floor and the thickness of the sediments. In areas where the basement floor is elevated and the sedimentary thickness is thin, the Curie isotherm is also found to be elevated and vice versa (Onwuemesi, 1997). This is due to the differential subsidence of the faulted basement as a result of the overlying basement load. Where there are thick sedimentary deposits, the Curie isotherm (base of the magnetized crust) lies at a deeper level than in areas where there are thin sediments (Fig. 20). The implication of the undulating nature of the Curie isotherm is the variation in the geothermal gradients within the basin, the values of which are found to be comparatively higher where the Curie isotherm is elevated than in areas where it is deeper. In this section, I hereby discuss the Curie point variations across the study area and relate/compare them with the regional geology of the area and their associated geothermal gradients and heat flows.

4.3.2.1 Profile A – A^1

This profile cuts across the Southern area in the NW – SE direction of the study area. It passes through parts of Okomu (sheet 297). The intermediate to deep Curie Point Depth (CPD) region of Okomu trends in NE - SW direction. The estimated depths to the Curie point isotherm ranges from 18.07 km to 24.55 km (Table 3). The estimated geothermal gradients and heat flow vary between 22.53 and 30.60 ^{0}C/km and between 56.33 and 76.50 mW/m^2 respectively.

Geologically, this area is dominated by Quaternary activity with coastal plain sands in the upper part of this profile and alluvium and mangrove swamps in the Southern part, which are of Quaternary age. This area is drained by River Okomu, River Osse and River Siluko. This area has been tectonically less active and in general had little or no intrusive or extrusive activity at the surface (shallow depth) but rather buried at a deeper depth.

A crustal zone of weakness is believed to be present in this area, beneath the large Quaternary sedimentary basin fill of between 2.21 – 3.64km. Crustal thickening and/or rapid subsidence is thought to be responsible for thermal cooling in this zone. Low to average heat flow anomaly contours of 56.32 – 76.51 mW/m^2 is present in this area.

4.3.2.2 Profile B – B^1

This profile passes through parts of Siluko (sheet 283) and Benin City (sheet 298) in the NW – SE direction of the study area. This region is characterized by shallow to deep (CPD) that range from 11.12 km to 20.79 km and a sedimentary thickness of between 1.64 to 3.43 km.

The estimated geothermal gradients and heat flow varies between 26.60 – 49.73 ^{0}C/km and 66.50 to 124.33 mW/m^2 respectively (table 3). The ages of the rocks gets younger as one transverses southwards. The upper part of this profile, around Siluko is characterized by undifferentiated basement complex of Precambrian to Upper Cambrian age. This is overlain by sediments of Cretaceous to Tertiary age, consisting basically of shale and mudstone, coal, sandstone, clays, coal and limestone. The lower part of the profile, around Benin is made up of sedimentary fill of Tertiary to Quaternary age, consisting of lignite, shale and clay. The shallow CPD estimates of 11.12 km (and the corresponding high heat flow anomalies of 124.33 mW/m^2) in the northwestern part of the study area (profile B – B^1) show some relationship or closeness to intrusive or extrusive activity. This area is drained by Rivers Owena, Ofosu and Ogbesse respectively. The southern part of the profile around Benin- City is characterized by deep CPD estimates of 20.79 km and a corresponding geothermal gradient of 26.60 ^{0}C/km and associated low heat, low to average heat flow of 66.50 mW/m^2. This region is dominated by a thick sedimentary fill of Tertiary to Quaternary age, consisting basically of sand, clay and lignite. The southern part of this profile is drained by River Ikpoba, River Osiomo and River Ogba.

4.3.2.3 Profile C – C^1

This profile cuts across the north-western, central and south-eastern parts of the study area (Akure, Ifon and Benin – City). This area is characterized by shallow CPD that ranges from 7.19 to 8.48 km. The shallow CPD estimates (and the corresponding geothermal gradient of 63.34 and 76.91^{0}C/km and the associated heat flow of between 158.36 and 192.28 mW/m^2) coincide with the site of intrusive activity around Idanre Hill when correlated with the high heat flow values. Idanre Hill found in southwestern part of Akure is characterized by Older Granite and undifferentiated basement complex of Precambrian to Upper Cambrian age has a height of about 300 ft above sea level.

Moreover, the region in the southwestern part of the study area (eastern part of Idanre Hill) is also characterized by shallow CPD and corresponding heat flow. The central part of this profile around the northwestern part of Ifon region is also characterized by shallow CPD and high heat flow. This area is an intrusive province of Quaternary age that erupted on a Cretaceous metamorphic basement. Southern part of this profile (northern part of Benin) is also characterized by a shallow CPD (and a corresponding high heat flow anomalies of 163.02 mW/m^2) (Fig. 23 and Table 4.2).

Depths to the bottom of the magnetic sources indicate a general increase in the geothermal gradient of 63.34 ^{0}C/km to 76.91 ^{0}C/km towards the Idanre Hill, located southwest of Akure.

The magnetic map, Curie point depth map, geothermal gradient map, the heat flow map show a good correlation between exposed geologic units and magnetic signatures. This tends to correspond with the exposed undifferentiated basement complex rocks found around northern and southern part of Akure. These observations were traced to the Older Granites emplaced in this region. These findings are consistent results from the spectral analysis of aeromagnetic data for geothermal investigation of Ikogosi warm spring, Ekiti State, southwestern Nigeria by Abraham *et al.*, (2014) who, from their investigation show that the low CPD at the spring source location could be due to magnetic intrusion at depth in the highly fractured quartzite unit. They equally observed that the shallow Curie depth observed could be as a result of the intruded Older Granite unit spotted in that region.

4.3.2.4 Profile D – D^1

This profile cuts across the northern part of Akure (sheet 264) through Ifon (sheet 284) to Agbor (sheet 299). The shallow CPD region of northern part of Akure is characterized by a geothermal gradient and associated heat flow of 55.24 ^{0}C/km and 138.11 mW/m^2 respectively. The central portion of the profile around Ifon is marked by shallow to intermediate CPD and towards the southern part around Agbor region is characterized by a deep CPD of 22.27km, corresponding geothermal gradient of 24.83 ^{0}C/km and associated low heat flow contours of 62.07 mW/m^2.

Geologically, the area is dominated in the northern part by Older Granite and undifferentiated basement complex of Precambrian to Upper Cambrian age. The central part of the profile, around Ifon is characterized by the Cretaceous to Quaternary activity and the southern part, around Agbor is dominated by sedimentary fill of Quaternary age. The deep CPD region located in the southeastern part of this profile and the shallow CPD region located in the north- western part of this profile is separated by a shallow to intermediate CPD at the Central part of the profile. A crustal zone of weakness may be present around the central region, separating the large Quaternary Sedimentary fill and the shallow CPD rocks of the Precambrian to Upper Cambrian age in the Northern sector of the profile.

Crustal thickening and/or rapid subsidence is thought to be responsible for thermal cooling along this zone.

Commonly, these anomalies are caused by the intrusion of granitic magmas into the upper crust at depths of several kilometers. These heat the meteoric water circulating in the fractures and faults through the overlying rocks. The geothermal significance of this event is that regions north and south of suture may lie in different heat – flow provinces. Another geothermal significance of the event that took place around this region is the initiation of the graben that now forms the valley that run from Akure, through Ifon down to Agbor Area.

4.3.2.5 Profile E – E^1

This profile cuts through the northeastern part of the study area across Owo and Ubiaja. The Owo region is marked by shallow CPD of 13.58 km, corresponding geothermal gradient of 40.72 ^{0}C/km and associated heat flow of 101.80 mW/m^2. This area of shallow CPD is characterized by high heat flow and is dominated by rock of undifferentiated basement complex rocks and undifferentiated metasediments of Precambrian to Upper Cambrian age.

The southeastern portion of the profile is characterized by deep CPD of 21.31 km, corresponding geothermal gradient of 25.95^{0}C/km and associated heat flow of 64.88 mW/m^2. There is a thick Cretaceous to Tertiary sedimentary basin consisting basically of false bedded sandstone, Coal, shale with limestone. This area in the southern part of the profile has been tectonically less active and in general had little or no intrusive or extrusive activity at the surface or shallow depth. A zone of weakness may be present in the central portion of the profile. This suture zone is now mainly buried with deposits in the Southern part of the profile. Thermal cooling of this zone can be attributed either to crustal thickening, inherited from the Tertiary times or to rapid subsidence related to deposition of the sediments.Deposition of thick sediments in the subsidizing portion in the central portion further contributed to the depression and deposition of more sediment. The present deeper CPD may only reflect a stage in which the crust is trying to reach a thermal re-equilibrium.

4.3.2.6 Profile $F – F^1$

This profile passes through parts of Auchi (sheet 266) in the NW – SE direction of the study area. The profile cuts across the northeastern part of the study area. The shallow to intermediate CPD of Auchi trends in the E – W direction. The estimated Curie point isotherm along this profile ranges from 15.06 to 19.12 km with a geothermal gradient that ranges from 28.92 to 36.72 $^0C/km$. Heat flow anomaly values of 72.30 to 91.80 mW/m^2 are present in this area.

Geologically, this area is characterized by Precambrian to Upper Cambrian Undifferentiated complex and Undifferentiated metasediments in the Upper region of the profile. The central region of the profile is marked by Cretaceous rocks consisting of shale, mudstone, coal, limestone, shale and false bedded sandstones, while at the southern part of the profile is dominated by Tertiary sediments consisting of clay, shale with limestone. This area is a vast area of undifferentiated basement complex and metasediemnts, and an average topography of about 2200 ft around Semolika (NW of Auchi), 1500 ft around Ososo (northern part of Auchi) and 1500 ft around Ojeaga and Ido (northeastern part of Auchi). The shallow to intermediate CPD coincide with the intrusive activity around this region. The shallow to intermediate CPD are well correlated with the heat flow values around this area.

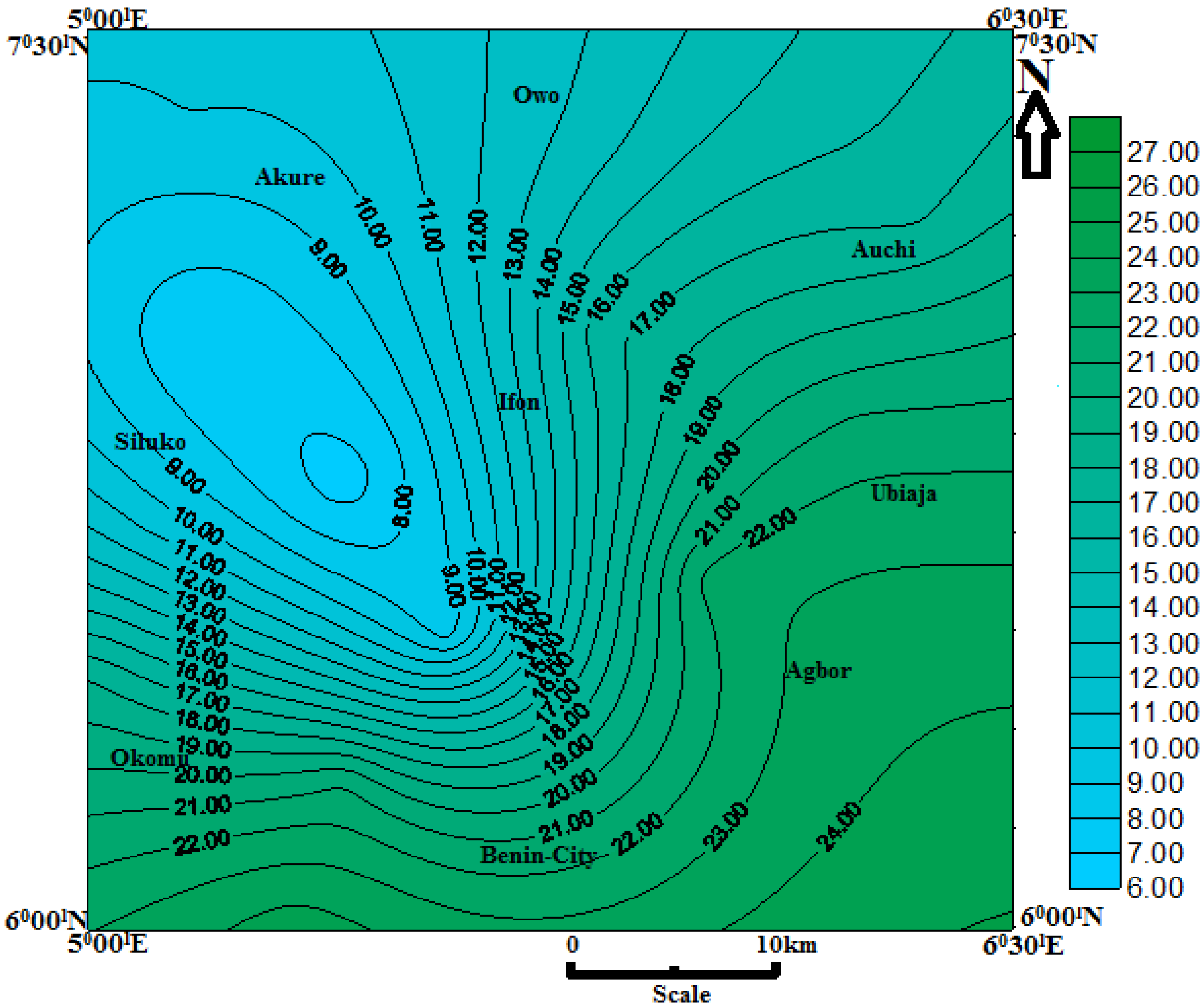

Fig. 4.10: Curie isotherm map of the study area (contour interval ≈ 1.0km)

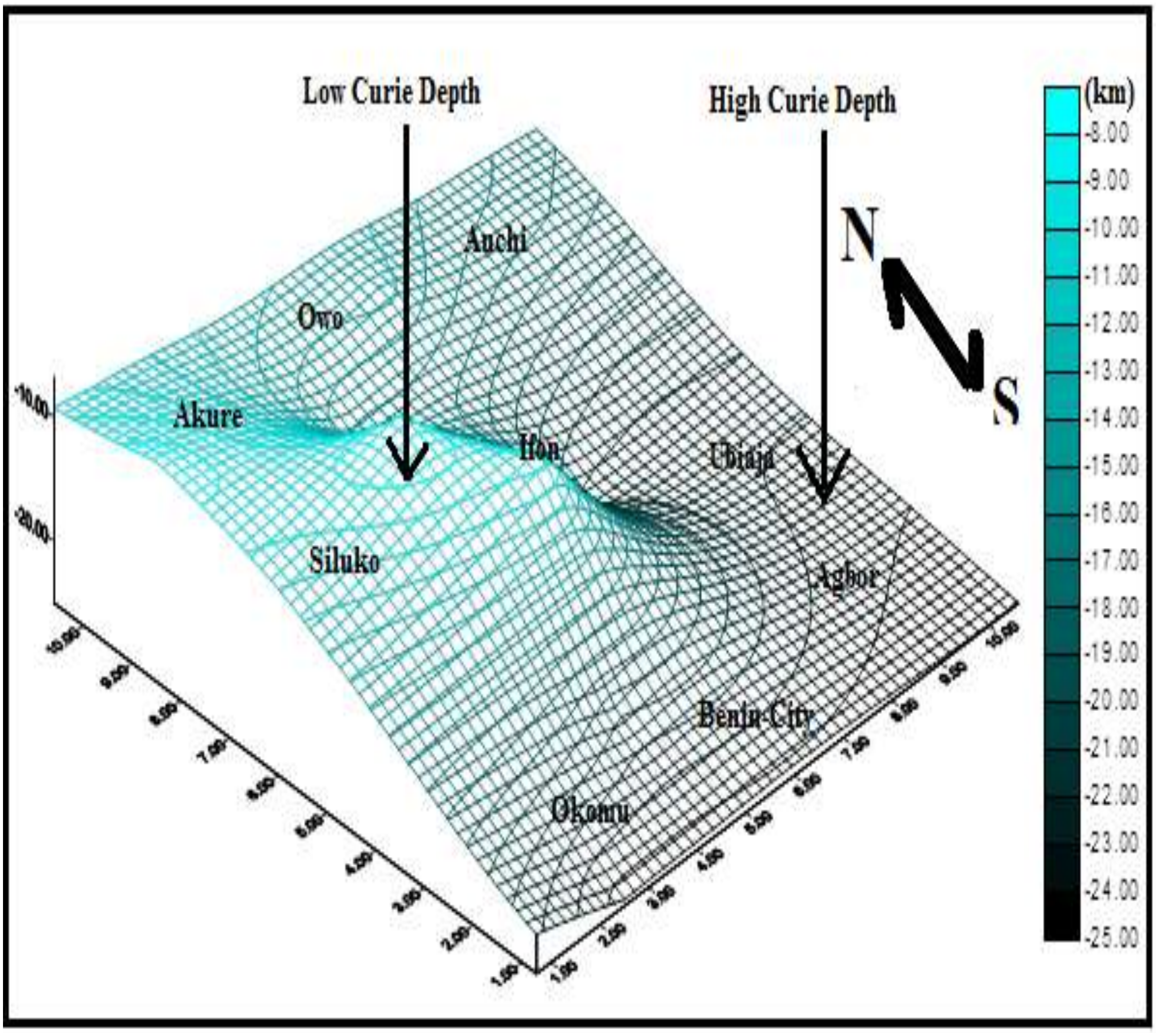

Fig. 4.11: 3D Surface plot for the Curie isotherm configuration of the study area

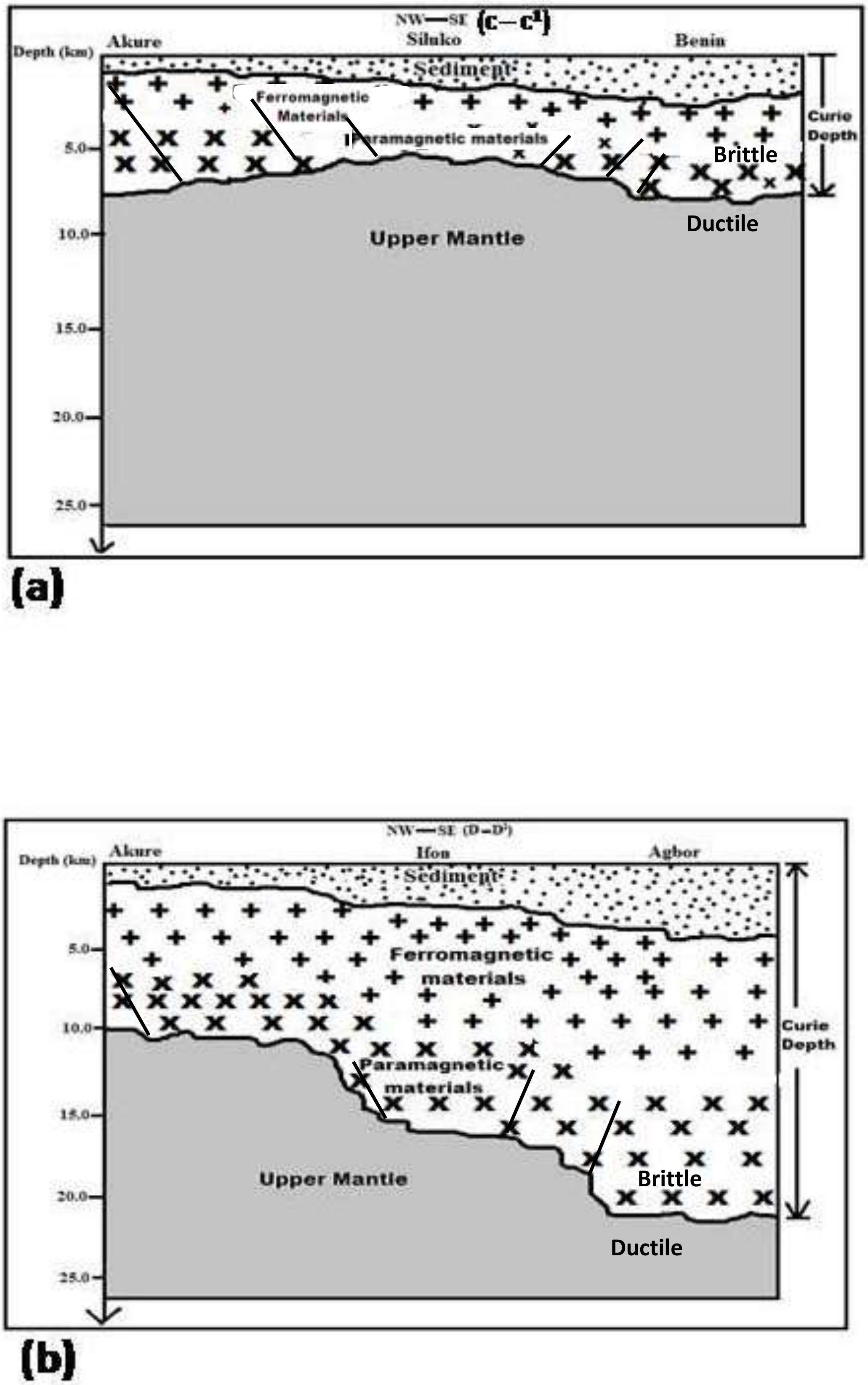

Fig. 4.12: Curie Isotherm model of the study area (a) Akure – Benin (b) from Akure – Agbor. The dashed lines are projections of the faults and fractures

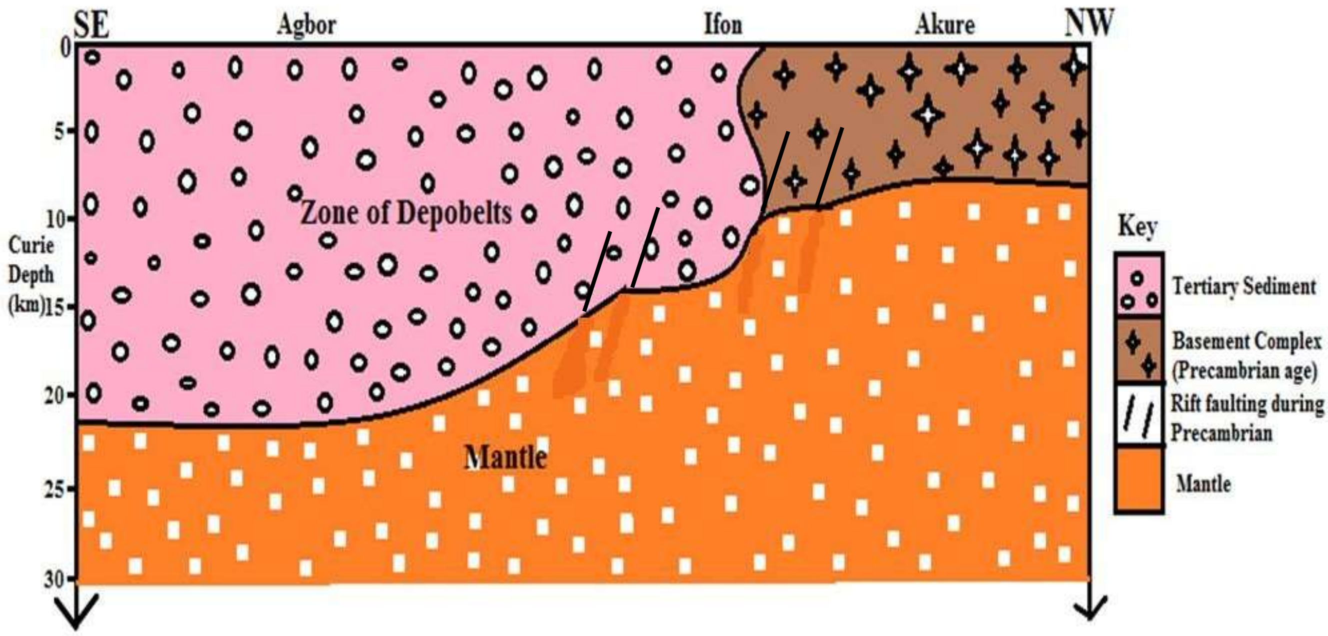

(C)

Fig. 4.12: Curie Isotherm model of the study area (c) From Akure to Agbor Showing zones of depobelt. The dashed lines are projections of the faults and fractures

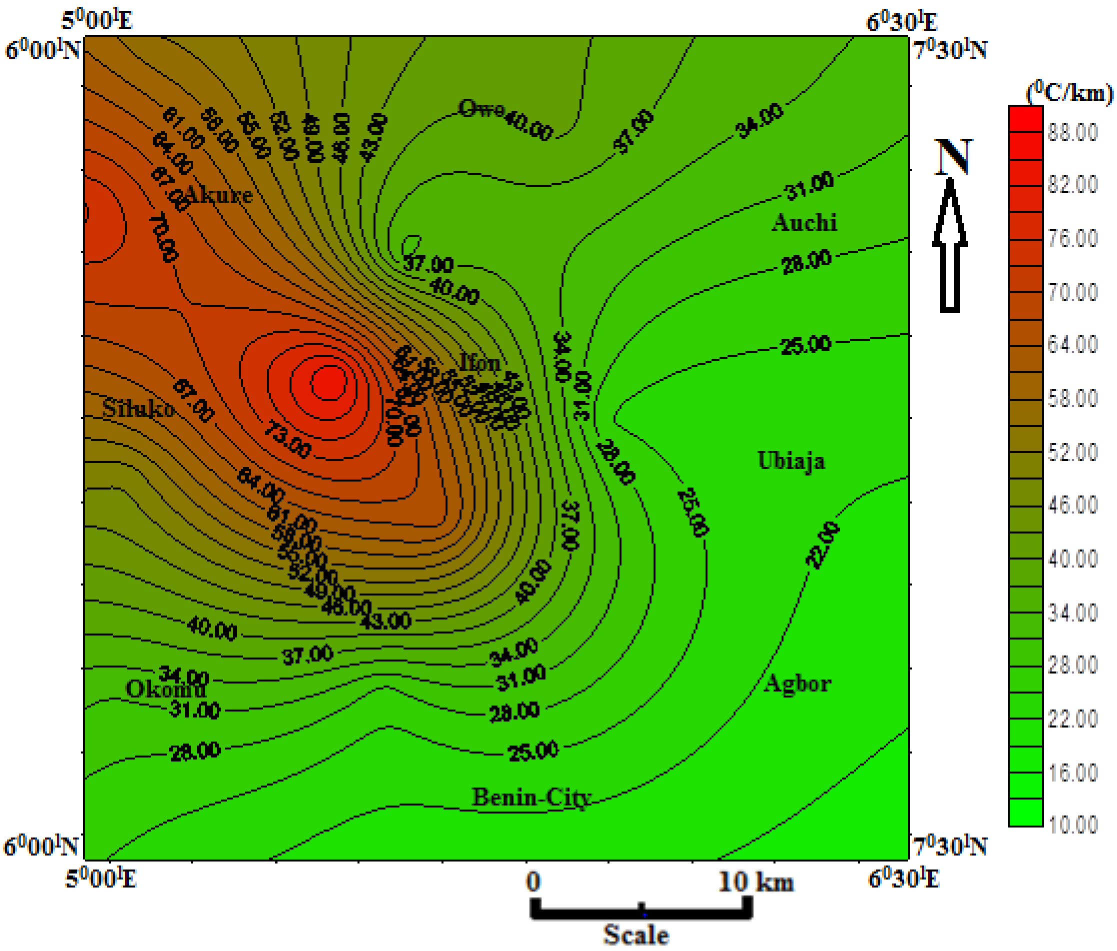

Fig. 4.13: Geothermal gradient map of the study area (contour interval ≈ 3.0 ^{0}C/km)

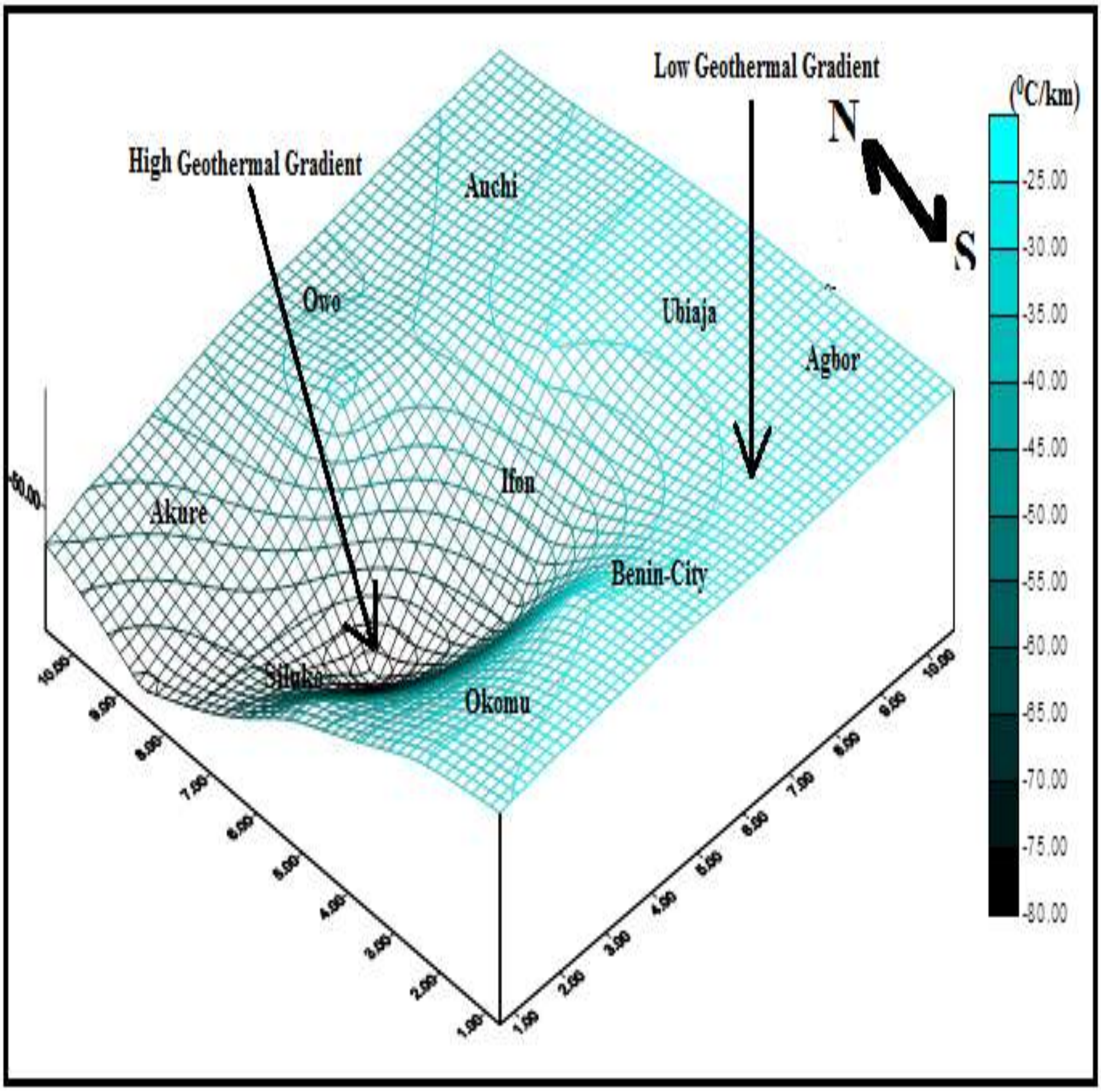

Fig. 4.14: 3D Surface plot for the geothermal gradient configuration of the study area

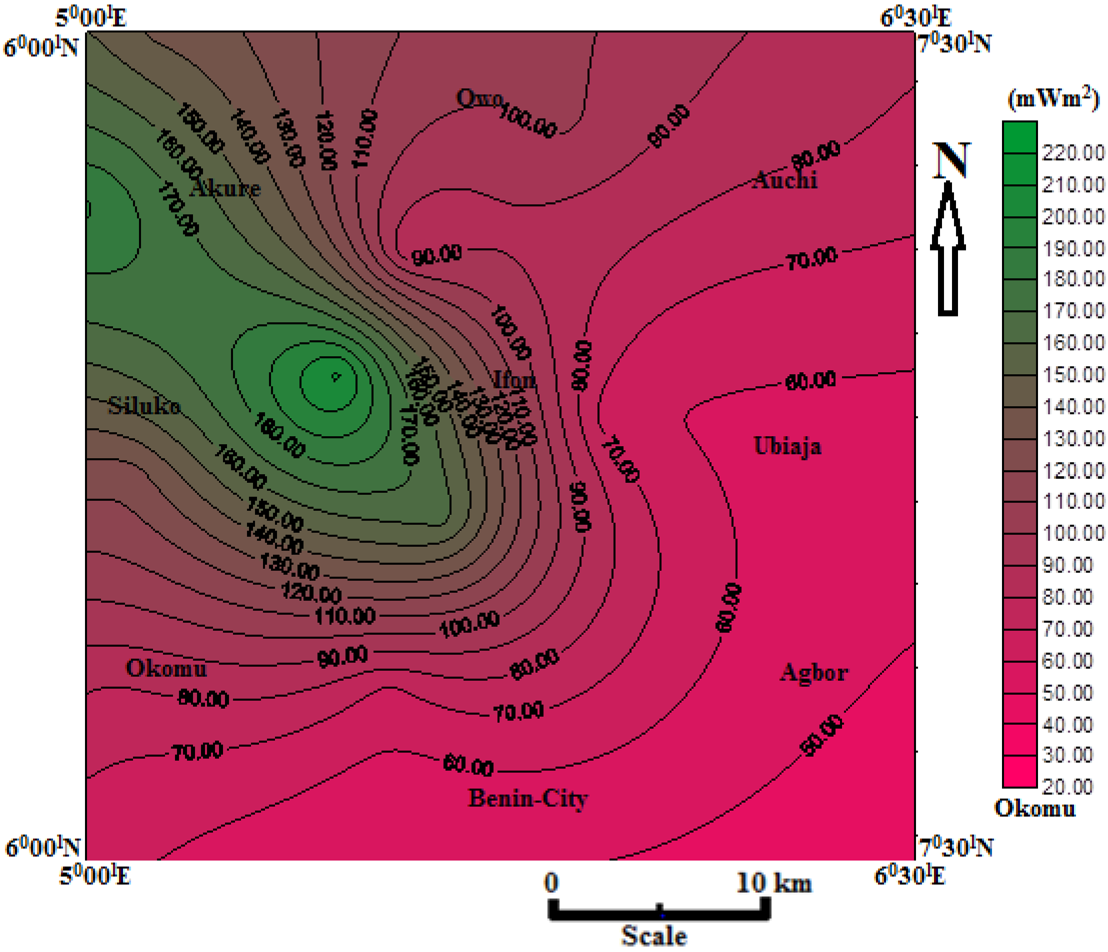

Fig. 4.15: Heat flow map of study area (contour interval ≈ 10.0 mWm^2)

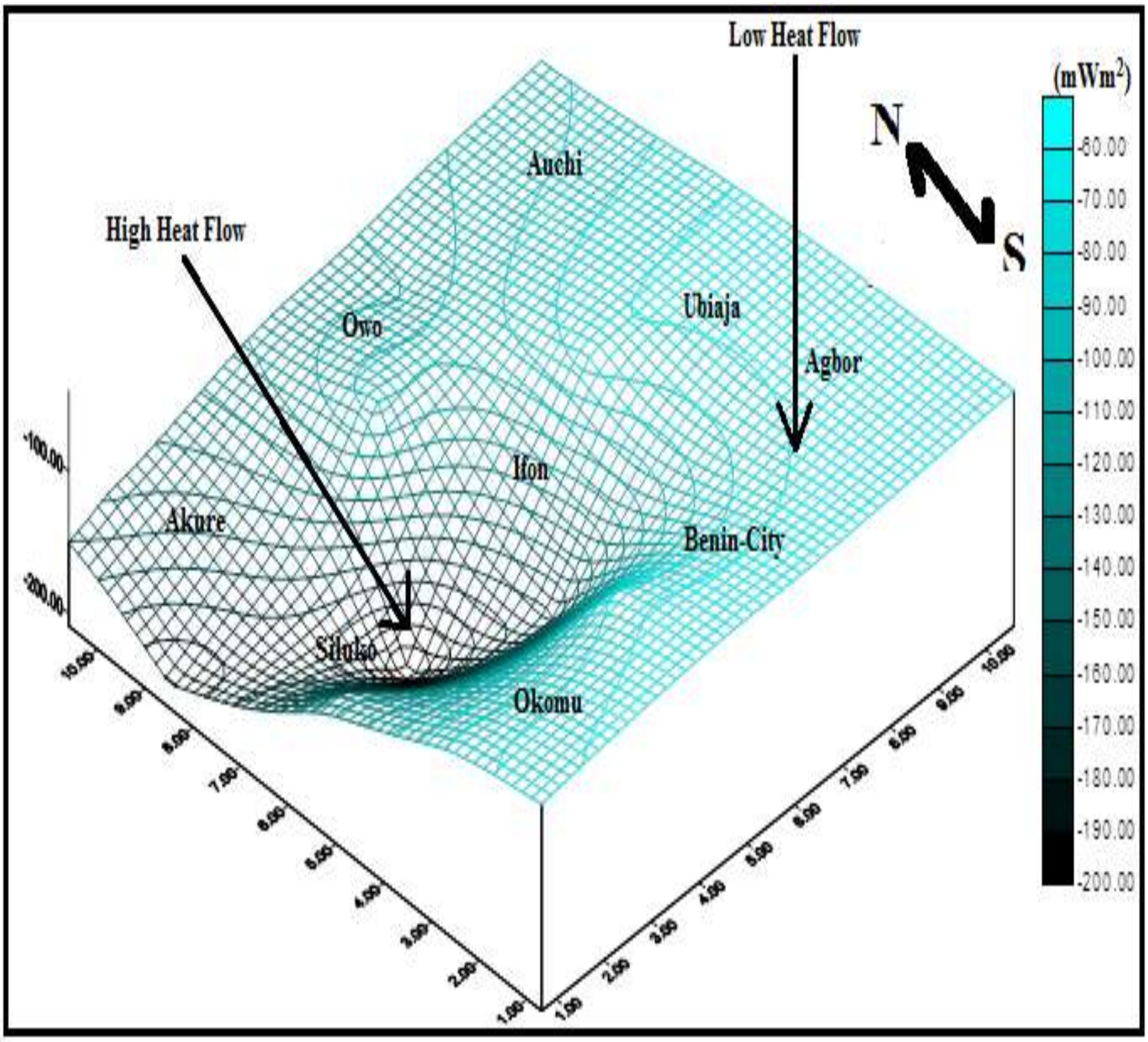

Fig. 4.16: 3D Surface plot for the heat flow configuration of the study area

4.4 Curie-Point Depth: Implication on the Geothermal Energy/Resources of the Study Area

The implication of the results are best illustrated by considering the graphs of the logarithms of the spectra energies (Fig. 4.6 a-f) from which the Curie isotherm depth was computed. According to Mishina (2009), the penetration of the magma to the crust produces different geophysical phenomena such as crustal deformation, volcanic activity and seismicity. In the northwestern part of the study area, geologic activity has been attributed to the geothermal processes as a result of the magma intrusion to the crust.

Comparing the estimated top and bottom of the deepest magnetic source (from spectral analysis) with the crustal model/structure (Fig. 4.12a and 4.12b), it is clear that the top and bottom depths coincide with the top of the crystalline upper crust (the Precambrian basement), which is of high magnetic property while the bottom falls within the middle crust, at the bottom of the basement near heat source. The heat source/geothermal energy source in the study area is inferred to be the magnetic body which is emplaced at approximately depth of 7.19km. The brittle-ductile transition is related to the movement of magma to the mid crust (Fig. 4.12a and 4.12b). The model is consistent with Curie point depth estimated in this study. The Curie depth that defines elevated temperature corresponds to magmatic intrusion which drives other processes such as stress accumulation, earthquake generation and emplacement of hydrothermal solutions. The shallowness of the northwestern zone of the study area must have resulted in the pronounced deformations and surface manifestation of hydrothermal fluids some distance away from the northwestern flank of the study area.

Moreover, the shallowness of the estimated Curie point depth of 7.19km implies that the heat flow around the northwestern part of the study area should be above the average value (Stampolidis and Tsokas, 2002). The cause of a high heat flow in most geothermal regions is the tectonically induced magmatism (Espinosa-Cardena and Campos-Enriquez, 2008).

On the whole, at a certain threshold of increased temperature, rocks response to stress results in brittle to ductile deformation. This ductile condition reduces the open passages (pore fluid connection) through which fluids can be transported or connected to the convecting fluid at shallower depths and as such, heat is predominantly by conduction through a conductive medium to the fluid reservoir. Within the reservoir therefore, the heat is transported through a convection of geothermal fluid via connected pores (Bibby *et al.*, 2009). This and the presence of active faults and fractures are responsible for the surface manifestations of the warm spring, some kilometers away from the northwestern part of the study area. Apart from using the knowledge of Curie-depth isotherm to delineate heat source/geothermal energy, some attributes such as fault trends, uplifted crust/mantle boundary and high geothermal energy can be delineated. A NE-SW and a NW-SE fault trends were delineated from the study. The manifestations of hot spring close to the area are largely supported by these faults (Fig. 4.17). The study has equally shown that the high heat flow around the area is enough to cause the surface geothermal manifestations. The study has equally revealed an uplifted crust/mantle boundary towards the northwestern part of the study area.

The results from this work also show that the Akure area (northwestern part) provides a great source of geothermal energy as temperatures greater than 100^0C can be reached at depths less than 2km. According to Jessop *et al.*,(1976), the average heat flow in thermally "normal" continental regions is around 60mW/m^2 and values in excess of about 80–100mW/m^2 indicate anomalous geothermal conditions have been assigned to all heat flow values which are all well above 100mW/m^2.

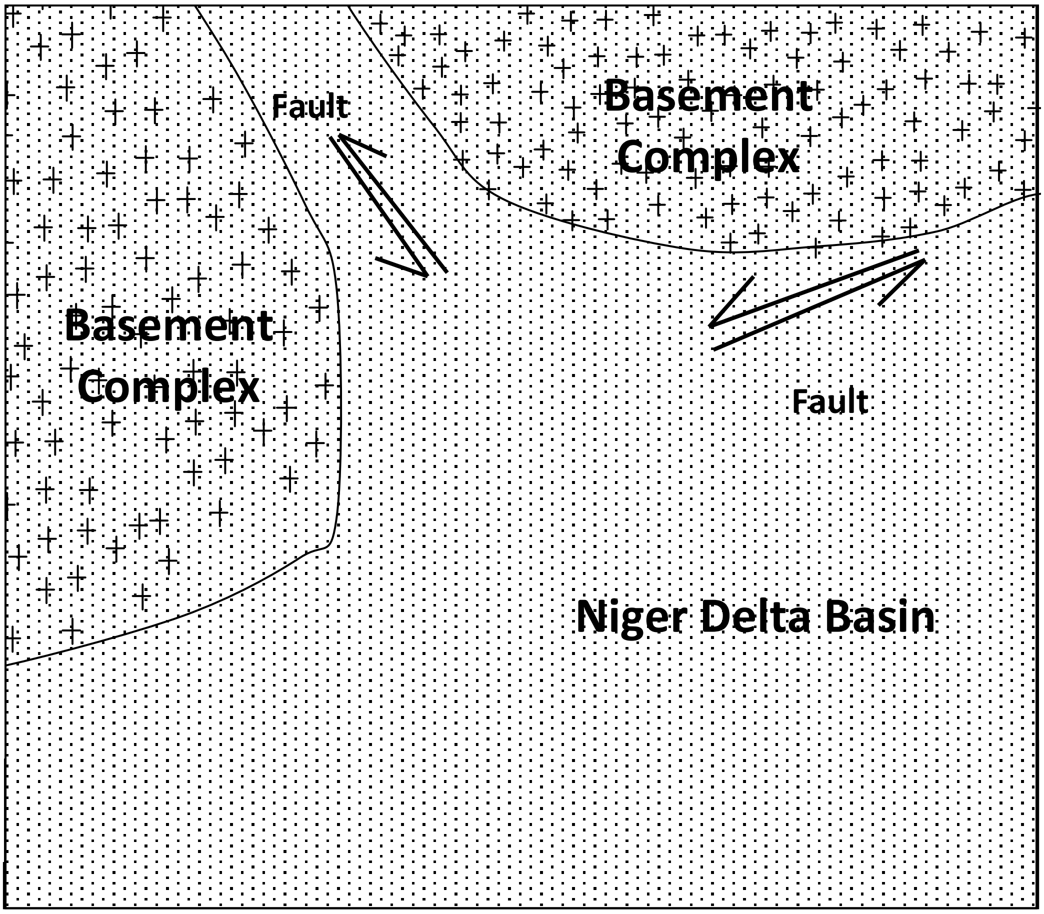

Fig. 4.17: Model of the northern boundary of the Niger Delta Basin and major faults running in NW – SE and NE – SW directions.

4.5 Structural Features Within the Study Area

The structural pattern of the study area was delineated using the aeromagnetic data obtained as shown in (Fig. 4.1a and 4.2). The area is intensely faulted with faults trending in NE -SW and NW- SE directions.

Fig. 4.17 shows map of the study area indicating the northern boundary of the Niger Delta Basin and a major fault running in the northwestern direction. Several contour closures are found in the northwestern and northeastern part of this lineament, which indicate shallow basement. The northeast – southwest (NE - SW) anomaly trend of the regional field may be attributed to the southwest – northeast strike of the Benue Trough which is part of a down -faulted “failed arm” of a triple junction that formed when Africa and South America separated during the Cretaceous (Cratchley *et al.,* 1984).

4.6 Petroleum Potential

The knowledge of the depth to the basement provides the thickness of the sedimentary fill which in turn is a key indicator in determining whether the deeper parts of the basin have been buried to sufficient depth to reach maturation window. So, for any area to be viable for hydrocarbon formation, the thickness of sediment must be up to 2.30 km as well as other conditions necessary for hydrocarbon formation (Wright *et al.,* 1985). Based on the sedimentary thickness of 0.70 - 4.81km, the possibility of hydrocarbon generation is feasible. It is hereby noted that one of the economic significance of this study is the consideration of hydrocarbon potential and it can be seen from the result that sedimentary thickness obtained in this analysis is sufficient to allow for accumulation of hydrocarbon. Gracefully, some oil companies such as the Platform Petroleum Company and the Pan Ocean Petroleum Company have their wells and gas flow stations located in the Southern part of the study area, located in the Niger Delta. Figures 4.18 and 4.19, shows the potential areas of hydrocarbon generation and warm spring in relation to the geothermal gradient and associated heat flow in the study area.

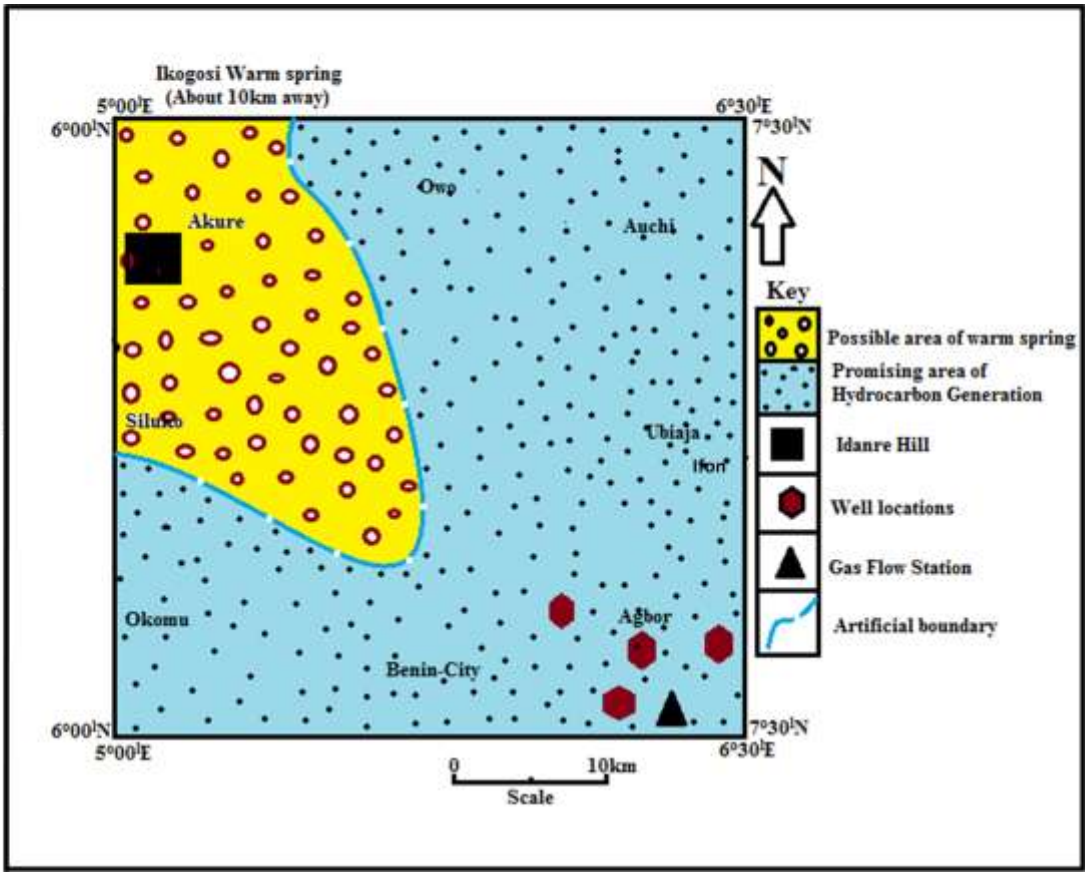

Fig. 4.18: Potential areas of hydrocarbon generation and warm spring (geothermal energy)

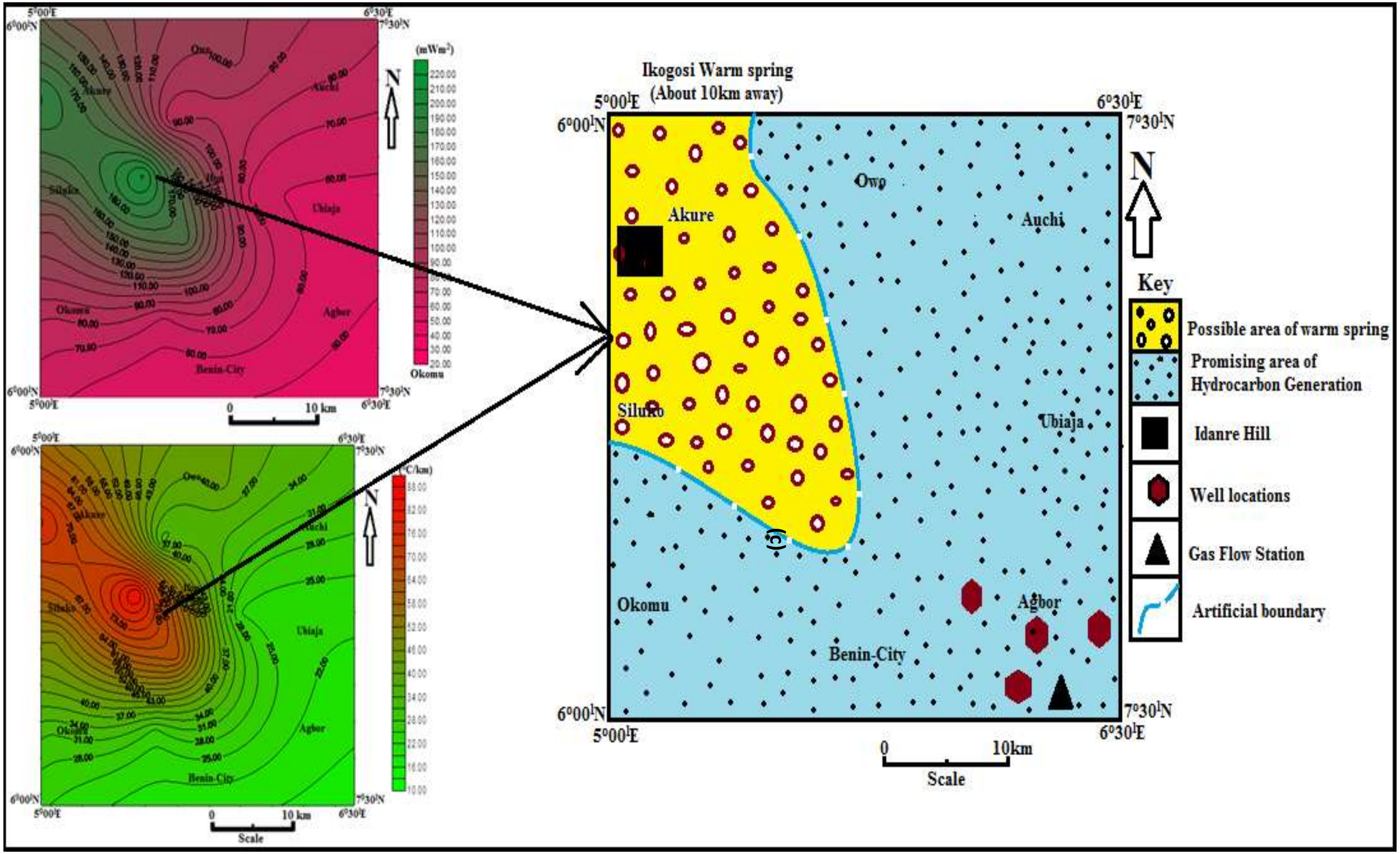

Fig. 4.19: Correlation of the (a) geothermal gradient (b) the heat flow in relation to the (c) model of the potential areas of hydrocarbon generation and warm spring

CHAPTER FIVE

SUMMARY, CONCLUSIONS AND RECOMMENDATIONS

5.1 Summary

There had been a rapid increase in the quest all over the world for the development of renewable energy resources, of which geothermal resources is one of them (Hildernbrand *et al.*, 1996). The present study provides thermal information that will guide regional geothermal energy exploration in the study area and Nigeria as a whole. The source of geothermal energy used by mankind is the earth's natural heat which is derived primary from the decay of the long -lived radioactive isotopes of Uranium, Thorium and Potassium but probably with a contribution from a slight cooling of the earth (Downing and Gray, 1986).

The earth acts as a heat engine and at its surface there is a continuous heat flux comprising the heat flow from the radioactive isotopes which are largely concentrated in the upper crust. As a consequence, a study of heat flow is a principal exploratory technique for the identification and location of geothermal resources as it permits the prediction of temperatures to depths below those reached by shallow drilling.

Spectral analysis of aeromagnetic anomalies from the South western Nigeria has been applied with the aim of delineating the geothermal energy and its attributes in parts of southwestern Nigeria. Discrete Fourier transform method was applied to a set of aeromagnetic data over part of the southwestern Nigeria comprising of the Niger Delta Basin. From the depth values determined from the spectral analysis, two depth models were established: The deeper magnetic sources and the shallow magnetic sources range from 2.21 km to 4.81 km while the shallow magnetic sources range from 0.79 km to 1.88 km .The thickness of the sediments ranges between 0.79 and 4.81 km, and the floor of the basin is characterized by block faults, whose widths vary from the other. It is these multiple and intermittent block faults that gave rise to the elongated lobes of magnetic anomalies for the basin. The block faults are vertical and their downward movements along the fault planes, due to the load of the overlying sediments, have contributed significantly in the subsidence of the basin. The depths to the basement are deeper in the southern, southeastern and central part and shallower in the north eastern and northern parts of the study area.

The structural pattern of the study area was mapped using the aeromagnetic data. The area is intensely faulted with faults trending in NE -SW and NW- SE directions. According to Jiakang and Igor (2005), these trends often coincide with litho-tectonic domains and depend on the scale of investigation. The result also shows a linear structure that is found in the north western part of the study area, of intermediate depth and seems to be hosted in the basement structure and is thought to be a major (divide) marking the boundary. Several contour enclosures are found in both the northwestern and the northeastern part of the study area, which indicate shallow basement. The sources of seismicity in Nigeria include inhomogeneities and zones of weakness in the crust created by the various episodes of magnetic intrusion and other tectonic activities. The possible mechanism for Nigeria's seismicity have been attributed to the locations of earth movements associated with NE- SW trending fracture and zones of weakness extending from the Atlantic ocean into the country (Ajakaiye *et al.,* 1987).

The result of investigation of the Curie point isotherm of the study area reveals the Curie isotherm depth varies between 7.19 and 24.55 km. The study also reveals that the geothermal gradient and associated heat flow values vary between 22.53 -76.91 ^{0}C/km and 56.33 -192.28 mW/m^{2} respectively. The investigation also revealed that the regions with the shallowest CPD lie, at the north-western and northern part of the study area. Therefore, the Curie point depths are shallower than 15 km and this, according to Tanaka *et al.,* (1999), reveals that the northwestern region is volcanic and geothermal fields since Curie point depth is greatly dependent on geologic conditions. Therefore these areas with variations less than 15 km may be recommended for further investigations for geothermal reconnaissance studies. The southern and south eastern portion of the study area show respectively high values of CPD representing areas with cooler crust. Interestingly, the Curie isotherm for the basin is undulating with an axial ridge configuration. The morphology depicts a linear relationship with the topography of the basement floor, and the thickness of the sediments. In areas where the basement floor is elevated and the sedimentary thickness is thin, the Curie temperature isotherm is also found to be elevated and vice versa. This is due to the differential subsidence of the faulted basement as a result of the overlying sediment load. Where there are thick sedimentary deposits, the Curie isotherm (base of the magnetized crust) lies at a deeper level than in areas where there are thin sediments. The implication of the undulatory nature of the Curie isotherm is the variation of the geothermal gradients (and the associated heat flow) within the basin, the values of which are found to be comparatively higher where the Curie isotherm is elevated than in area where it is deeper.

So, application of spectral analysis to aeromagnetic anomalies in order to delineate geothermal energy and its attributes in parts of southwestern Nigeria was carried out. The result shows a general inverse correlation between the calculated Curie depths and the heat flow in the southwestern Nigeria, with high heat flow regions (around Idanre Hills, South western part of Akure and northwestern part of Akure area) characterized by shallow Curie depth and low-heat-flow regions (around Agbor, Benin-City and Ubiaja) corresponding to deeper Curie depths.

In addition, the estimated Curie depths agree generally with locations of intrusive or extrusive activity across the study area, providing confidence that is sampling the Curie-temperature isotherm and assessing reasonable average thermal conditions for the crust of the study area.

This study has shown that both tectonics and magnetism play an important role in generating the thermal structure of the crust. The smallest values of CPD (shallow CPD) were obtained in the southern part of the study area where some areas with significantly high heat flow are presented. The sources' nature of these anomalies should be classified as zones of late magmatism, sharply expressed neotectonic or recent movements or increased seismic activity.

5.2 Conclusions

A study of interpretation of aeromagnetic data over parts of southwestern Nigeria in order to delineate geothermal energy and its attributes has been carried out using spectral analysis. It has been discovered that the depth to the top of magnetic sources varies from 0.9 to 4.81km for the region. The study revealed that the region is characterized by shallow Curie depths and high heat flow. The Curie point depth estimated the average depth of magnetic sources and is concluded to reflect thermal structures. The study area is underlain by a Curie point isotherm as shallow as 7.19km (extending northwest from Akure to southern part of Akure) and a deep Curie point isotherm as 24.55km towards the southern part of the study area. The result was also subjected to geothermal gradient computation and heat flow, where an estimated values range from 22.53 to 76.91^{0}C/km and 56.33 to 192.28mW/m^2 respectively.

The results from this work show that the northwestern and southern part of Akure provides a great source of geothermal energy as temperatures greater than 100^{0}C can be reached at depths less than 2km. The average heat flow in thermally “normal” continental regions is around 60mW/m^2. Values in excess of about 80 – 100mW/m^2 indicate anomalous geothermal conditions (Jessop *et al.*, 1976). For this study anomalous geothermal condition have been assigned to all determined heat flow values which are all well above 100mW/m^2.

It is hereby noted that the shallow CPD observed in the northwestern part of the area is due to magnetic intrusion at depth. The magnetic high extending northwest from Akure into the southern part of Akure is caused by magnetic mass, consisting of intrusive rocks. The elliptical anomalies are due to clusters of small igneous intrusions associated with dykes that extend into the overlying sedimentary rocks.

Large volume of metamorphosed sedimentary rock associated with the magnetic anomalies and with the geothermal area shows that large amounts of heat have been generated in this area, doubtless by cooling igneous rocks far below the surface. The presence of the magnetic anomaly indicates that the temperature of the large volumes of igneous rocks above the basement in the study area probably do not exceed 580^{0}C, the Curie temperature of magnetite, so that the igneous rocks must for the most part have cooled to a temperature well below their liquidus.

In summary, the study has revealed the capability of aeromagnetic data in analyzing thermal structures of the area using spectral method. Significantly, it has been able to define subsurface constituents of the faults and their impacts on the subsurface manifestations of the geothermal resources of the study area. The result shows two depth sources: the deeper sources ranges from 2.21 – 4.81 km, while the shallow magnetic sources ranges from 0.79 – 1.88 km. The structural pattern reveals that the most dominant trend in the study area is NE – SW and NW – SE directions. The area is underlain by a Curie- point depth isotherm as shallow as 7.19km Depths to magnetic sources vary from 0.79 to 4.81km. The geothermal gradient and associated heat flow range from 22.53 to 76.91^{0}C/km and from 56.33 to 192.28mW/m^2 respectively. Possibility of hydrocarbon generation in some part of the study area is feasible based on the sedimentary thickness range of 0.79 – 4.81km. There is a general increase in the geothermal gradient of about 76.91^{0}C/km towards the northwestern part of study area. This provides a source of geothermal energy. Consequently, the northwestern part of the study area is an area with great geothermal energy potential for geothermal exploitation.

5.3 Contributions to Knowledge

The study has brought to the fore several capabilities of magnetic method that have not been adequately utilized.

i. **Origin of warm spring:** The study has identified that the Ikogosi warm spring (which is about 10km from the study area and associated with a faulted and fractured quartzite band sandwiched between schists) is associated with intrusive masses/volcanic domes of granites/rhyolite that cut across the northwestern part of the study area. These intrusive masses and volcanic domes cause elliptical anomalies to the northwestern part of the study area and this indicate a possible source of geothermal energy. The Ikogosi warm spring area is associated with these volcanic domes and intrusive masses.

ii. **Sedimentary thickness:** The knowledge of the depth to the basement provides the thickness of the sedimentary fill which in turn is a key indicator in determining whether the deeper parts of the basin have been buried to sufficient depth to reach maturation window. Based on the sedimentary thickness of 0.79-4.81km, obtained from our study, the possibility of hydrocarbon generation is feasible.

iii. **Fault trends:** A major northeast – southwest (NW – SW) anomaly trend of the regional field was delineated. This trend may be attributed to the southwest – northeast strike of the Benue Trough which is part of a down faulted "failed arm" of a triple junction that formed when Africa and South America separated in the Cretaceous (Cratchley *et al.*, 1984). The structural pattern reveals that the most dominant trend is NE – SW which is related to the Pan – African trend. Another trend observed is the NW–SE in the northwestern part of the study area.

iv. **Uplifted crust/mantle boundary:** The study has revealed an uplifted crust/mantle boundary towards the northwestern part of the study area. In areas where the basement floor is elevated and the sedimentary thickness is thin, the Curie temperature isotherm is also found to be elevated and vice versa.

v. **High geothermal energy:** The study has revealed variations of the geothermal gradients and associated heat flow within the study area, with high anomalous geothermal energy in northwestern area where the Curie isotherm is elevated than in the southern and southeastern part where the Curie isotherm is deeper.

Generally, the knowledge of the Curie point depth has offered a window for a better view of the thermal structure of the crust via aeromagnetic data. Moreover, the variations in the bottom of the magnetically active layer of the lithosphere, has offered an essential tool for the structural interpretation of the area. In addition, the geological framework of the study area has a significant bearing on heat flow through the upper crust and because of variations in thermal conductivities of different rock types on the geothermal gradient and hence the occurrence and recognition of regions favourable for exploitation of geothermal energy.Lastly, the information derived from this study has been used as a basis for making a first assessment of the geothermal energy resources of the area.

5.4 Recommendations

The results obtained in this work have provided important geophysical/geological inputs which are very useful to further geothermal energy exploitation in the area. Based on the results the following recommendations are proposed:

i. This method has been successfully used to delineate areas of geothermal energy potential in the study area and should be used in other suspected areas of geothermal energy potential across Nigeria and other parts of the world. This will serve as a contribution to filling the gap in the crustal temperature information in those areas.

ii. A detailed temperature measurement at various depths through a series of boreholes to be located at adequate intervals within the crystalline Basement Complex should be carried out in the area. This would provide the much needed data for further studies of the origin, emplacement, geophysical and geological characteristics of the Basement Complex of South Western Nigeria.

iii. An in – depth assessment of the geothermal potential in selected areas where heat load exists should be made. This involves more detailed geological studies and possibly seismic surveys leading to the identification of potential development site which may then be invested by drilling a preliminary exploratory well in the area.

REFERENCES

Abraham, E. M., Lawal, K. M., Ekwe, A. C., Alile, O., Murana, K. . and Lawal, A. A. (2014). Spectral analysis of aeromagnetic data for geothermal energy investigation of Ikogosi warm spring – Ekiti State, southwestern Nigeria. *Geothermal energy*, 2(6): 1 – 21.

Adegbuyi, O. and Abimbola, A. F. (1997). Energy resource potential of Ikogosi warm spring area, Ekiti State, southwestern Nigeria. *African Journal of Science,* 1(2): 111 – 117

Adepelumi, A. A., Ako, O. B. D., Ajayi, T. R., Olorunfemi, A. O. and Felebita, D. E. (2008). Integrated geophysical mapping of the Ifewara transcurrent fault system, Nigeria. *Journal of African Earth Science.* 52: 161 – 166.

Adetona, A. A., Udensi, E. E. and Agelaga, A. G. (2007). Determination of depth to buried magnetic rocks under the lower Sokoto Basin, Nigeria, using aeromagnetic data. *Nigeria Journal of Physics* 19(2): 21 – 32

Ajakaiye, D. E., Daniyan, M. A., Ojo, S. B. and Onuoha, K. M. (1987). Southwestern Nigeria earthquake and its implications for tectonics and evolution of Nigeria. *J. Geodynamics*, 7: 205 – 214

Akujeze, C. N. and Oteze, G. E. (2007), Deteriorating quality of groundwater in Benin – City, Edo State, Nigeria, *Water Resources*, 17: 17 – 23

Allen; J.R.L. (1965). Late Quaternary Niger Delta and adjacent areas, *AAPG Bull* 49(5), 547 – 600.

Anakwuba, E.K., Onwuemesi, A.G., Chinwuko, A.I. and Onuba, L.N. (2011). The Interpretation of aeromagnetic anomalies over Maiduguri Dikwa depression, Chad Basin, Nigeria: A structural view. Scholars Research Library. *Archives of Applied Science Research*, 3(4), 499 – 508.

Anakwuba, E. K. and Chinwuko, A. I. (2015). One dimensional spectral analysis and Curie depth isotherm of eastern Chard Basin, Nigeria. *Journal of Natural Sciences Research.* 5: 14 – 22

Bain, J. E. (2000). Eastern Gulf data reveal play concepts, *The American oil and Gas Reporter*, 38 – 41

Balogun, O.Y. (2003). Senior secondary atlas. (2nd Ed.) Longman, Nigeria.

Baranov, W. (1975). Potential fields and their transformations in applied geophysics. Gebruder publishing company, Bornteager, Berlin, 1 – 35.

Bhattacharyya, B.K. and Morley, L.W. (1965). The declination of deep crustal bodies from total field aeromagnetic anomalies. *J. Geomag. and Geoelec*. 17, 237 – 253.

Bhattacharyya, B.K. (1966). Continuous spectrum of the total-magnetic-field anomaly one to a rectangular prism body. *Geophysics*, 31, 97 – 121.

Bhattacharyya, B.K and Leu, L.K. (1975). Spectral analysis of gravity and magnetic anomalies due to two dimensional structures. *Geophysics* 40, 993 – 1013.

Bhattacharyya, B.K. and Leu, L.K. (1977). Spectral analysis of gravity and magnetic anomalies due to rectangular prismatic bodies. *Geophysics*, 42, 41 – 50.

Bibby, H. M., Risk, G. F., Grant-Caldwell, T and Heise, W. (2009). Investigations of deep resistivity structures of the Wairakei geothermal field. *Geothermics*, 38: 98 – 107

Blackely, R. J. (1995). Potential theory in gravity and magnetic application. Cambridge university press, Cambridge. 307 – 308

Burke, K. (1969). Seismic areas of the Guinea Coast where the Atlantic fracture zones reach Africa. *Nature*. 222: 655 – 657

Burke, K; Dessauvagie, J.F.J. and Whiteman, A.J. (1972). Geological history of Benue valley and adjacent areas in T.J.F. Dessauvagie and A.J. Whiteman (Eds). African Geology, Ibadan Univ. Press. 206 – 218.

Burke, K., Dewey, J. and Kidd, W. S. F. (1977). World distribution of sutures – sites of former oceans. *Tectonophysics*. 40: 66 – 99

Byerly, P.E. and Stolt, R.H. (1977). An attempt to define the Curie point isotherm in northern and central Arizona. *Geophysic*s, 42, 1394 – 1400.

Chandrasekharam, D. (2005). Geothermal energy resources of India: Past and the present: proceedings of world geothermal congress 2005, 1 – 9

Chapman, D.S. and Furlong, K.P. (1992). The thermal state of the lower crust. In: Fountain, D.M. Arculus, R.J. and Kay, R.M. (eds). Continental lower crust development in geo-tectonics, 23, 179 – 199.

Chinwuko, A.I; Onwuemesi, A.G; Anakwuba, E.K. and Nwokeabia, N.C. (2012). Interpretation of aeromagnetic anomalies over parts of Upper Benue Trough and southern Chad Basin, Nigeria. *Advances in Applied Science Research*, 3(3) 1757 – 1766.

Chukwu-Ike, I. M. and Norman, J. W. (1977): Mineral crustal show on satellite imagery of Nigeria. *Tran. Int, Min. Met.* 86: 855 – 857.

Cratchley, C. R., Louis, P., Ajakaiye, D. E. (1984). Geophysical and geological evidence for the Benue – Chad Basin Cretaceous rift valley system and its tectonic implications. *Journal of African Earth Sciences*. 2(2): 141 – 150

Davies, J.C. (1973). Statistics and data analysis in Geology, John Wiley and Sons, New York, 193 – 482.

Dobrin, M. B. and Savit, C. N. (1988). Introduction to geophysical prophysical prospecting, 4th Edition, McGraw Hill, Singapore

Dolmaz, M.N; Ustaomer, T; Hisarli, E.M. and Orbay, N. (2005). Curie point depth variations to infer structure of the crust at the African – Eurasian Convergence Zone, SW Turkey. *Earth Planets Space*, 57, 373 – 383.

Doust, H. and Omatsola, E. (1990). Niger Delta in Edwards, J. D. and Santogrossi, P. A. (Eds) Divergent/Passive Margins Basins, *AAPG memoir*. 48: 239 – 248

Downing, R. A. and Gray, D. A. (1986). Geothermal energy - the potential in the United Kingdom. British Geological Survey report 3 – 7.

Duze, M. and Ojo, A. (1977). Senior School Atlas, Macmillan Educational Ltd, Nigeria.

Ekweozor, C. M. and Daukoru, E. M. (1984). Petroleum source bed evaluation of Tertiary Niger Delta. *AAPG Bulletin*. 68: 390 – 394

Eletta, B.E. and Udensi, E.E. (2012). Investigation of the point isotherm from the magnetic fields of the eastern sector of central Nigeria. *Geosciences*, 2(4), 101 – 106.

Elueze, A. A. (1988): Geology of the Precambrian schist belt in Ilesha area Geological Survey of Nigeria report. 77 – 89.

Espinosa – Cardena, J. M. and Campos – Enriquez, J. O. (2008). Curie point depth from spectral analysis of aeromagnetic data from Cerro Prieto geothermal area, Baja California, Mexico. *Journal of Vulcanology and Geothermal Research.* 176: 601 – 609

Garba, I. (2003). Geochemical Characteristics of mesothermal gold mineralization in the Pan – African (600 ± 150Ma) basement of Nigeria. *Applied Earth Science*: 112(3): 319 – 325

Geological Survey of Nigeria (1974). Geological map of Nigeria, Published by Geological Survey division, Federal Ministry of Mines and Power, Lagos

Griscom, A. and Muffler, L. J. P. (1971). Aeromagnetic map and interpretation of the Salton sea geothermal area, California, US Geological Survey. Geophysical investigations report map GP – 754.

Gudmundsson, A., Berge, S. S., Lyslo, K. B. and Skurtveit, E. (2001): Fracture networks and fluid transport in active fault zones. *Journal of Structural Geology.* 23: 343 – 353

Hahn, A; Kind, E.G and Mishra, D.C. (1976). Depth estimation of sources by means of Fourier amplitude spectra, *Geophys. Prospect*; 24: 287 – 308.

Hildenbrand,T. G., Blakely, R. J., Hinze, W. J., Keller, G. R., Langel, R. A., Nabighian, M. and Roest, W. (1996). Aeromagnetic Survey over US to advance geomagnetic research. *American Geophysical Union.* 77 (28): 265 – 268

Hubbard, F. A. (1975). Precambrian crustal development in western Nigeria: Indications from the Iwo Region. *Bulletin of Geological Society of America*. 86: 548 – 554.

Jessop, A. M., Hobart, M. A. and Schlater, J. G. (1976). The world heat flow data collection 1975. Geothermal Services of Canada. *Geotherm Sev.* 50: 55 – 77.

Jiakang, L. and Igor, M. (2005). Potential Field investigation of Williston Basin Basement. Canadian Society of Exploration Geophysicist National Convention, 65 – 66.

Kasidi, S. and Nur, A. (2012). Curie depth isotherm deduced from spectral analysis of magnetic data over Sarti and environs of northeastern Nigeria. *Scholarly Journals of Biotechnology.* 1(3): 49 – 56

Kellog, O. D.(1953). Foundations of potential theory, Dover publications. New York

Kogbe, C.A. (1976). Geology of Nigeria, (2nd rev edition). Rock view Nig Ltd; Jos.

Komolafe, A. A. (2010). Investigations into the tectonic lineaments and thermal Structure of Lake Madadi, southern Kenya rift using integrated geophysical methods. M.Sc unpublished thesis, International Institute for geo–information Science and Earth observation, Enschebe, The Netherlands, 60

Lowrie, W. (1997). Fundamentals of Geophysics, Cambridge University Press, London

Mariita, N. O. (2013). Applications of potential field methods for geothermal exploration – A case for Olkaria and Menengai geothermal fields, Kenya. *Short Course VIII on Exploration for Geothermal Resources*

Mary, H. D. and Mario, F. (2004). What is geothermal Energy? Institution di Geoscienze e Georisorse, Pisa, Italy. 1 – 61

Mayhew, M.A. (1985). Curie isotherm surfaces inferred from high altitude magnetic anomaly data. *Journal of Geophysical Research*, 90(3),

Mbonu, M. O. (1990): The trends and geologic consequences of belts of epeirogeny in Nigeria. Nigerian Mining and Geosciences Society conference, Kaduna. Book of abstract, 14

Mishra, D.C. and Naidu, P.S. (1974). Two dimensional power spectrum and analysis of aeromagnetic fields, *Geophys. Prospect*, 22, 345 – 353.

Mishina, M. (2009). Distribution of crustal fluids in northeast Japan as inferred from resistivity survey: *Goudwana Research.* 16: 563 – 571

Nagata, T. (1961). Rock Magnetism, Maruzen Publishers, Tokyo, 350.

Negi, J. G., Agrawal, P. K. and Rao, K. N. N. (1983). Three dimensional model of the Moyan area of Maharshiatra State, India, based on the spectrum analysis of aeromagnetic data. *Geophysics,* 48 (7): 964 – 974

Nur, A., Ofoegbu, C. O. and Onuoha, K. M. (1999). Estimation of the depth to the Curie point isotherm in the Upper Benue Trough, Nigeria. *Journal of Mining and Geology*. 35 (1): 53 – 60

Nwachukwu, S.O. (1972). The tectonic evolution of southern part of Benue Trough, Nigeria. Geology Magazine, Viva, 414 – 419.

Nwankwo, I. I. and Olasehinde, P.I. and Akoshile, C.O. (2008). Spectral analysis of aeromagnetic anomalies of northern Nupe Basin, central Nigeria. *Global J. Pure Applied Sci*; 14, 247 – 252.

Nwankwo, I. I; Olasehinde, P.I. and Akoshile, C.O. (2009). An Attempt to estimate the curie-point isotherm in the Nupe Basin, central Nigeria. *Global J. Pure Applied Sci*. 15, 427 – 433.

Nwankwo, I. I, Olasehinde, P. I. and Akoshile, C. O. (2011). Heat flow anomalies from the spectra analysis of airborne magnetic data of Nupe Basin Nigeria. *Asian Journal of Earth Sciences*. 4 (1) 46 – 53

Obaje, N. G. J., Wehner, H., Hamza, H., Scheeder, G. (2004). New geochemical data from the Nigerian sector of the Chad Basin: Implications on hydrocarbon prospectivity. *Journal of African Earth Sciences*. 38(5): 477 – 487

Obande, E. G., Lawal, K. M. and Ahmed, A. L. (2013). Geothermal characterization using spectral analysis and apparent magnetization of Wikki warm spring, northern Nigeria. *Journal of Mining and Geology*, 49 (1) 53 – 63

Ofoegbu, C.O. (1985). Long wavelength anomalies and the crustal structures underneath the Benue Trough and the surrounding regions. *Nigeria Journal of Mining and Geology*. 22, 45 – 50.

Ofoegbu, C.O. and Onuoha, K.M. (1989). Analysis of magnetic data over the Abakaliki anticlinorium of the Lower Benue Trough, Nigeria: Petroleum geological implications. *Mar. Petrol. Geol*. 8, 174 – 183.

Ofor, N. P. and Udensi, E. E. (2014). Determination of the heat flow in the Sokoto Basin, Nigeria using spectral analysis of aeromagnetic data. *Jour. Nat. Sci. Res:* 4(6) 2 – 14

Okubo, Y; Graf, J.R; Hansen, R.O; Ogawa, K and Tsu, H. (1985). Curie point depths of the Kyushu and surrounding areas, Japan *Geophysics*, 53, 481 – 494.

Okubo, Y; Tsu, H. and Ogawa, K. (1989). Estimation of Curie point temperature and geothermal structure of island arc of Japan. *Tectonophysics*, 159, 279 – 290.

Okubo, V; Matsushima, J. and Correia, A. (2003). Magnetic Spectral analysis in Portugal and its adjacent seas. *Physics and chemistry of the Earth*, 28, 511 – 519.

Olade, M. A. and Elueze, A. A. (1979). Petrochemistry of Ilesha amphibolites and Precambrian crustal evolution in the Pan – African domain of SW Nigeria, Precambrian Resources: 303 – 318

Olasehinde, P.I. (1991). Spectral evaluation of the aeromagnetic anomaly over part of the Nigeria basement Complex. Ph.D Thesis unpublished, University of Ilorin.

Oluyide, P. O. and Udo, A. N. (1989): Preliminary comments on the fracture systems of Nigeria, In: Proceedings of the national seminar on earthquakes in Nigeria, 97 – 109

Onuoha, K. M. and Ekine, A. S. (1999). Surface temperature variations and heat flow in Anambra Basin, Nigeria. *Journal of African Earth Science.* 28(3): 64 – 65

Onwuemesi, A.G. (1997). One-dimensional Spectral analysis of aeromagnetic anomalies and Curie depth isotherm in the Anambra Basin of Nigeria. *J. Geodynamics,* 23(2) 95 – 107.

Rahaman, N. A. (1989). Review of the Basement Geology of south-western Nigeria. In: Kogbe, C. A. (Ed) Geology of Nigeria, Rock View Limited, Jos, Nigeria, 39 – 56

Reyment, R.A. (1965). Aspects of the Geology of Nigeria, University Press, Ibadan, 145.

Rogers, A. S., Imevbore, A. M. A. and Adegoke, O. S. (1969). Physical and chemical properties of Ikogosi warm spring, western Nigeria, *Nigeria Journal of Mining and Geology.* 4: 1 – 2.

Rybach, L. and Mulffler, L. J. P. (1981). Geothermal Systems: Principles and case histories. John Wiley and Sons, London

Salem, A; Ushijima, K; Elsirafi, A. and Mizunaga, H. (2000). Spectral analysis of aeromagnetic data for geothermal reconnaissance of Quseir Area, northern Red sea, Egypt. proceedings on world geothermal congress, Kyushu – Tohoku, Japan. May -June 10, 2000. 1669 – 1674.

Sheu, A. T., Udensi, E. E., Adeniyi, J. O. and Jonah, S. A. (2004). Spectral analysis of the magnetic residual anomalies over the upper Sokoto Basin, Nigeria. *Zuma Journal of Pure and Applied Sciences.* 6 (2): 213

Short, K.C. and Stauble, A.J. (1967). Outlines of Geology of Niger Delta. *AAPG Bull*. 51, 761 – 799.

Smith, R.B; Shuey, R.T; Freldline, R.O; Otis, R.K. and Alley, L.G. (1974). Yellowstone hotspot: new magnetic and seismic evidence. *Geology* 2, 451 – 455.

Spector, A. and Grant, F.S. (1970). Statistical models for interpreting aeromagnetic data. *Geophysics*, 35, 293 – 302.

Stacey, F. D. (1977). Physics of the Earth (second edition), John Wiley and Sons Inc. New York

Strampolidis, A. and Tsokas, G. (2002). Curie point depths of Macedonia and Thrace, northern Greece. *Pure and Applied Geophysics*, 159: 1 – 13.

Tanaka, A; Okubo, Y. and Matsubayashi, O. (1999). Curie point depth based on spectrum analysis of the magnetic anomaly data in east and southeast Asia. *Tectonophysics*, 306, 461 – 470.

Telford, W.M; Geldart, J.P. and Sheriff, R.F. (1990). Applied geophysics, Cambridge university press, Cambridge. 841.

Trifonova, P., Zhelev, Z. and Petrova, T. (2006). Curie point depths of the Bulgarian territory inferred from geomagnetic observations. *Bulgarian Geophysical Journal* 32: 12 – 22

Tsokas, G; Hansen, R.O. and Fyticas, M. (1998). Curie point depth of the island of Crete (Greece) – *Pure and Applied Geophysics*, 152, 747 – 757.

Vaidya, D., Shah, M., Sircar, A., Sahajpal, S. and Dhale, S. (2015). Geothermal energy: Exploration efforts in India. *International Journal of Latest Research in Science and Technology,* 4 (4): 61 – 69

Wright, J. B., Hastings, D. A., Jones, W. B. and Wiliams, H. R. (1985). Geology and mineral resources of West Africa. George Allen and Erwin, London. 90 – 120